Sustainable automotive components for interior door trims

University of Porto | Faculty of Engineering

Mechanical Engineering Department

Sustainable automotive components for interior door trims

Dissertation submitted to the Faculty of Engineering of the University of Porto for obtaining the degree of Doctor of Philosophy in Leaders for Technological Industries of the MIT-Portugal Program

Nuno Alexandre de Oliveira Calçada Loureiro

Mechanical Engineer | Master in Industrial Design

PORTO, 2013

Supervisor

Professor José Luís Soares Esteves
Assistant Professor | Mechanical Engineering Department Faculty of Engineering | University of Porto | Portugal

Co-Supervisors

Professor Júlio César Machado Viana
Associate Professor | Polymer Engineering Department Engineering School | University of Minho | Portugal

Professor Satyabrata Ghosh
Head of Research and Development | Carborundum Universal Limited| India

This work has been done under the Engineering Design and Advanced Manufacturing (EDAM) focus area of MIT-PORTUGAL Program. This program is an international collaboration of Massachusetts Institute of Technology, Faculty of Engineering of University of Porto, University of Minho and Instituto Superior Técnico.

This work has the financial support of the Portuguese Foundation for Science and Technology (Fundação para a Ciência e Tecnologia) through the PhD Grant SFRH/BD/42978/2008 and through the project MIT-Pt/EDAM-SMS/0030/2008 - Assessment and Development of integrated Systems for Electric Vehicles on the scope of QREN – POPH – Topology 4.1 Advanced Formation Scope. (Co-participated by the European Social Found and by MEC national founds).

Ao meu filho João Dinis,
para que sempre saiba que, com trabalho,
todos os sonhos se concretizam.

To my son, João Dinis,
to always know that, with work,
all dreams come true.

Confitebor tibi Domine
Deus meus in toto corde meo
(Psalms 85.12)

Aknowledgments

To Prof. José Luis Esteves, for his continued support as supervisor and friend, and for the friendship offered me all over these years.

To Prof. Júlio Viana for all the support provided as co-supervisor, particularly for all the support in scientific areas of knowledge that I less dominated and that was vital to the completion of the work.

To Prof. Satyabrata Ghosh for the continuous support, the scientific guidance which contributed to the coherence of this work and also for the friendship that has been given for him.

The Faculty of Engineering of University of Porto , University of Minho and the Engineering School of Polytechnic Institute of Porto by the possibility of using all the resources necessary to realize this work.

To Pole for Innovation in Polymer Engineering (PIEP), especially to technical staff Andreia Vilela, Bruno Silva, Carlos Azevedo, Elizabeth Oliveira, Flora Barbosa and Paula Peixoto for their assistance during the use of the equipment necessary for prosecution of the work .

To Institute of Mechanical Engineering and Industrial Management (INEGI) for allowing the use of the laboratorial equipment need for the material characterization.

To Mr. Serafim Sampaio, Main Specialist Technic of the Polymer Engineering Department of University of Minho, for all the patience had in helping me to establish the injection moulding parameters and to proceed the first injection tests.

To Dr. Carla Monteiro, FEUP's technical assistant, by her rapidity and commitment that led to unlock the bureaucratic and legal situations that I stumbled throughout this time.

To Prof. Luis Durão that always cheered me and encouraged in times of greatest anguish and always invested on me.

To Prof. Francisco Brito a good friend who appeared on the right time and reveal himself a support on UMinho structure and on the MOBI-MPP project.

To all the colleagues, friends and family for the direct or indirect contribution to this work.

To all my students of ISPGaya that often had to have extra lessons on Saturday mornings forcing them to absent themselves from their family due my laboratory work.

And because in the end is the most important one, a special acknowledgment to my wife, Teresa, who during these years was often alone and without the support that I need to provide so I can finish this work. I thank her for the understanding and sacrifice.

Resumo

Os biomateriais têm sido alvo de interesse, ao longo dos últimos anos, ao nível da investigação científica e tecnológica e ao nível industrial. O aumento da preocupação ambiental e o uso excessivo de recursos petrolíferos levou ao aumento do desenvolvimento de novos materiais, os biocompósitos, que terão uma grande importância futura.

É um facto que, aliado à redução de peso, a indústria automóvel poderá beneficiar com a inclusão destes materiais nos automóveis, não só devido ao receio instalado da diminuição e extinção das reservas petrolíferas, mas também devido à forte legislação que obriga a uma incorporação cada vez maior destes materiais nos automóveis.

Este tema apresenta um grande potencial, pois visa encontrar soluções para um desenvolvimento sustentável, com preocupações ambientais, de modo a ser possível obter soluções biodegradáveis para os painéis interiores dos automóveis.

Sendo o principal objectivo deste trabalho a criação de um bio-compósito capaz de poder substituir os actuais painéis interiores dos automóveis, o trabalho centrou-se na obtenção desse bio-compósito, tendo em conta a redução de custos das matérias-primas e a manutenção dos processos de fabrico dos actuais painéis.

Assim, foram estudadas mecânica e morfologicamente as misturas de PLA e PHA de modo a poder definir a melhor matriz para a aplicação em estudo.
Seguidamente foi estudada a incorporação de fibras de celulose para se afinar as propriedades necessárias.

Ao longo deste relatório, é possível encontrar uma descrição das várias tarefas realizadas no desenvolvimento deste projecto. O trabalho desenvolvido iniciou-se com uma análise aprofundada na literatura acerca de materiais biocompósitos.

Em seguida, apresenta-se o trabalho experimental realizado. A escolha da matriz e dos parâmetros de processamento, seguido do estudo da incorporação de fibras. Tendo o compósito definido terminou-se o trabalho com a produção de uma peça para demonstrar a potencialidade destes materiais.

Em termos conclusivos verifica-se que a matriz composta por 70% PLA e 30% PHA (fracção mássica) apresenta as melhores propriedades para a aplicação em estudo. A incorporação de 20% de fibra nesta matriz melhora o comportamento térmico do material, provando assim que é possível substituir os polímeros de origem petrolífera por estes biocompósitos sem comprometer o comportamento mecânico dos painéis interiores de porta.

Abstract

In the last few years, biomaterials have been a target of interest at scientific, technological research and industrial level. The increasing of the environmental concern and the excessive use of petrol resources have conducted to the development of new materials, biocomposites, which will achieve a great importance into the future.

It's a fact that, allied to weight reduction, the automotive industry can benefit from the inclusion of these materials in cars, not only because of the installed fear of decline and extinction of oil reserves, but also because of the strong legislation that forces an increasing incorporation of these materials in automobiles.

This topic presents a big potential because it seeks to find solutions for a sustainable development with environmental concerns in order to be able to obtain biodegradable solutions for the interior door trims.

Since the main purpose of this work is to create a bio-composite that is suitable to replace the existing interior door trims, the work has focused on obtaining that bio-composite, taking account into the raw-materials cost reduction and the maintenance of the manufacturing process of current door trims.

Therefore PLA and PHA blends mechanical and morphological behavior have been studied in order to define the best matrix for use in this study.
Subsequently it was studied the incorporation of cellulosic fiber to adjust the properties to meet the required values.

Throughout this report, it's possible to find a description of the various tasks performed in the development of this project. The work began with a review of the literature about biocomposites materials.

Then it's presented the experimental work. The study of the choice of matrix and processing parameters, followed by the study of the fibers incorporation is presented. Having defined the composite the work ends with the production of an interior door trim made into this bio-composite to demonstrate the potentiality of these materials.

In conclusion it verifies that the matrix containing 70% PLA and 30% PHA (weight fraction) has the best properties for the interior door trims. The incorporation of 20% of fiber improves the thermal behavior of the composite, proving that it is possible to replace the petrol-based polymers for these biocomposites without compromising the mechanical behavior of interior door trims.

Résumé

Les biomatériaux sont devenus un sujet d'intérêt, au cours des dernières années, soit dans la recherche scientifique et technologique, soit dans l'industrie. Les préoccupations croissantes avec l'environnement et l'utilisation excessive des ressources pétrolières sont à l'origine de la recherche et développement des matériaux nouveaux, les bio-composites, très importants pour l'avenir.

L'industrie automobile bénéficiera de l'utilisation de ces matériaux, notamment par la réduction du poids des voitures. En plus, ils pourront être une alternative face à la crainte de diminution et épuisement des réserves de pétrole et répondront favorablement à la forte législation qui oblige à une incorporation progressive de ces matériaux dans les voitures.

Ce sujet présente un grand potentiel, puisque il permet de trouver des solutions pour un développement durable, avec des préoccupations écologiques, afin d'obtenir des solutions biodégradables pour les panneaux intérieures des voitures.

Étant donné que l'objectif de ce travail est la création d'un bio-composite qui permet le remplacement des panneaux de portes des voitures, toutes les démarches ont eu comme objectif l'obtention de ce bio-composite, en tenant compte la réduction des dépenses en matières premières et le maintient du processus de fabrication des panneaux actuels.

Ainsi, on a étudié mécaniquement et morphologiquement les mélanges de PLA e PHA afin de définir la matrice la plus correcte pour l'application désirée. Ensuite, on a étudié l'incorporation des fibres pour l'ajustement des propriétés nécessaires.

Le long du texte, il est possible de trouver la description des différents procédés d'investigation au niveau de ce projet. Le travail a commencé par une analyse attentive de la littérature sur les matériaux bio-composites. Ensuite, on présente le travail expérimental réalisé. Le choix de la matrice et des paramètres du processus, suivi de l'étude de l'incorporation des fibres. Une fois le composite défini, on a terminé le travail par la production d'une pièce pour démontrer le potentiel de ces matériaux.

En conclusion, on vérifie que la matrice composée de 70% PLA et 30% PHA (fraction massique) présente les propriétés idéales pour l'application proposée. L'incorporation de 20% de fibre dans cette matrice permet une amélioration importante du comportement thermique de ce matériel, en prouvant, ainsi, qu'il est possible de remplacer des polymères d'origine pétrolière par ces bio-composites, sans, toutefois, compromettre le comportement mécanique et thermique des panneaux intérieures des portes des voitures.

Abstrakt

Biomaterialen wurden das interessenziel in den letzten Jahren im umfang der wissenschaftlichen und technologischen Forschung und in der Industrie. Steigende umweltbewusstsein und den übermäßigen Einsatz von Öl-Ressourcen führte zu einer erhöhten Entwicklung neuer Materialien, Biocomposites, die eine große Zukunft Bedeutung haben wird.

Es ist eine Tatsache, dass, gepaart mit der Gewichtsreduktion, die Automobilindustrie kann von der Einbindung dieser Stoffe in Autos profitiert, nicht nur wegen der Angst vor Verfall und Auslöschung installiert Ölreserven, sondern auch wegen der starken Rechtsvorschriften, die erfordert eine zunehmende integration dieser Materialien in Autos.

Dieses thema stellt ein großes potenzial, weil es um Lösungen für eine nachhaltige Entwicklung zu finden mit Umweltbelangen, um in der Lage sein, biologisch abbaubare Lösungen für die Innenverkleidung des Autos erhalten soll.

Da der Hauptzweck dieser Suchung auf eine Bio-Composites schaffen die bestehende Macht Autoinnenraum Platten ersetzen kann, hat die Suchung über den Erhalt derartiger bio-Verbund konzentriert, unter Berücksichtigung der Kostenreduktion von Rohstoffen und Wartung von Herstellungsprozess der aktuellen Zellen.

Daher wurden Mischungen aus PLA und PHA morphologisch und mechanisch untersucht, um die besten Matrix zur Verwendung bei der Untersuchung zu definieren.

Anschließend wurde die Einbindung von cellulosefasern untersucht, um die gewünschten Eigenschaften einzustellen.

In diesem Bericht finden Sie eine Beschreibung der verschiedenen Aufgaben bei der Entwicklung dieses Projektes durchgeführt. Die Arbeit begann mit einer gründlichen Analyse der Literatur über Biocomposites Materialien.

Dann stellen wir die experimentelle Arbeit. Die Wahl der Matrix und Verarbeitungsparameter, durch Untersuchung der Einbindung von Fasern folgt. Nach der Definition der Verbund wurde Werkstück Produktion beendet, um die Fähigkeit dieser Materialien zu demonstrieren.

Abschließend, es scheint, dass die Matrix mit 70% PLA und 30% PHA (Gewichtsanteil) die besten Eigenschaften für die Anwendung unter Berücksichtigung hat. Die Einarbeitung von 20% Faser in dieser Matrix verbessert die thermische Leistung des Materials, was beweist, dass es möglich ist, die Polymere aus Erdöl gewonnene für diese Biocomposites ohne die mechanischen Türinnenverkleidungen ersetzen.

Contents

List of Symbols

$		United States Dollar
ΔC_P	[J.ºC.g^{-1}]	Heat Capacity
ΔH_{cc}	[J.g^{-1}]	Enthalpy of Cold Crystallization
ΔH_m^0	[J.g^{-1}]	Enthalpy of melting
ΔH_m	[J.g^{-1}]	Enthalpy of fusion
σ_b	[Pa]	Blend Maximum Stress
σ_c	[Pa]	Composite Maximum Stress
σ_f	[Pa]	Fiber Maximum Stress
σ_m	[Pa]	Matrix Maximum Stress
σ_{max}	[Pa]	Maximum Stress
υ	[ ]	Poisson Coefficient
υ_d	[ ]	Dispersed Phase Poisson Coefficient
υ_m	[ ]	Matrix Poisson Coefficient
Ø	[%]	Weight Fraction
$Ø_{fib}$	[%]	Fiber Weight Fraction
$Ø_d$	[%]	Dispersed Phase Weight Fraction
$Ø_{max}$	[%]	Nielson maximum packaging fraction
ζ	[ ]	Einstein Coefficient
B	[ ]	Béla-Pukásnky Load-bearing capacity
C_P	[kJ.(kg.K)$^{-1}$]	Specific Heat at Constant pressure
E	[Pa]	Young's Modulus
E_c	[Pa]	Composite Young's Modulus
E_b	[Pa]	Blend Young's Modulus
E_d	[Pa]	Dispersed Phase Young's Modulus
E_f	[Pa]	Flexural Young's Modulus
E_{fib}	[Pa]	Fiber Young's Modulus
E_m	[Pa]	Matrix Young's Modulus
H	[kJ.kg^{-1}]	Enthalpy
K	[ ]	Nicolais-Narkis Interaction Constant
Q	[kg.h^{-1}]	Mass flow rate
T_c T_{cc}	[ºC]	Cold Crystallization Temperature
T_g	[ºC]	Glass Transition Temperature
T_m	[ºC]	Melting Temperature
V_f	[%]	Fiber Volume Fraction
x_c	[%]	Crystallinity
wf w_f	[%]	Weight fraction

List of Abbreviations

A

ABS	Acrylonitrile Butadiene Styrene
ASTM	American Society and Testing Materials

B

bbl	barrel
BIW	Body-in-white
BMC	Bulk Molding Compound
BP	Béla-Pukánsky Model
BTU	British Thermal Unit

C

CIM	Compound Injection Moulding
CO_2	Carbon Dioxide

D

DSC	Differential Scanning Calorimetry

E

ELV	End-of-Life Vehicle
EU	European Union

F

FAO	Food and Agriculture Organization of the United Nations
FEUP	Faculty of Engineering of University of Porto
FRP	Fiber Reinforced Plastic

H

HDT	Heat-Deflection Temperature

I

ICm	Ishai and Cohen model
ISEP	School of Engineering of Polytechnic Institute of Porto
ISO	International Organization for Standardization
ISPGaya	Polytechnic Superior Institute Gaya
IUPAC	International Union of Pure and Applied Chemistry

K

KUT	Kerner-Uemura-Takayanagi Model

L

LCA	Life-Cycle Analysis
LFT	Long Fiber Reinforced Thermoplastics

N

NN	Nicolais-Narkis Model

M

MDF	Medium Density Fiberboard
MFI	Melt-Flow Index
mHT	Modified Halpin-Tsai equation
MTm	Mori-Tanaka model

O

OEM	Original Equipment Manufacturer

P

PA6	Polyamide 6 (also known as Nylon 6)
PBA	Poly (butyl acrylate)
PCL	Poly(ε-caprolactone)
PET	Polyethylene Terephthalate
PGA	Polyglycolic Acid
PHA	Polyhydroxyalkanoate
PHB	Polyhydroxybutyrate
PHBO	Poly(hydroxybutyrate-*co*.hydroxuoctanoate)
PHBV	Poly(hydroxybutyrate-*co*-hydroxyvalerate)
PLA	Poly(lactic Acid)
PP	Polypropylene
Prepreg	Pre-impregnated fiber reinforcements

R

ROM	Rule of Mixtures Model

S

SEM	Scanning Electron Microscopy
SMC	Sheet Molding Compound

U

UMinho	University of Minho
USD	United States Dollar

W

WAXD	Wide angle X-Ray Diffraction
WF	Wood Fiber

List of Figures

List of Tables

Chapter 1.

Introduction

1.1 Introduction

The preservation of our environment requires that we stop using materials that will last indefinitely. In the last years the ecological concerns develops a natural interest to the natural materials and eco-solutions.

Into the automotive area, researches are exploring natural fibers, such as flax, hemp and kenaf, [1] as an eco-alternative to glass fibers.

The Kyoto Protocol has pushed the European Union Member States to find ways to reduce emissions.
As expected the transport sector, who in 2004 was responsible for 30% of UK energy-consumption, is one of the first areas to be studied[2].

1.2 Petrol trend

It's easy to understand that petrol price rules all the other prices. Energy, plastics, assembling lines and metallic materials prices are directly or indirectly connected with the petrol price.

It's possible to verify that in 2008 the financial crises originated by the crash of Lehman Brothers drives to a crash of the oil prices.

The financial speculation leads the oil prices to increase and it's expected that it will continues this trend for the next years.

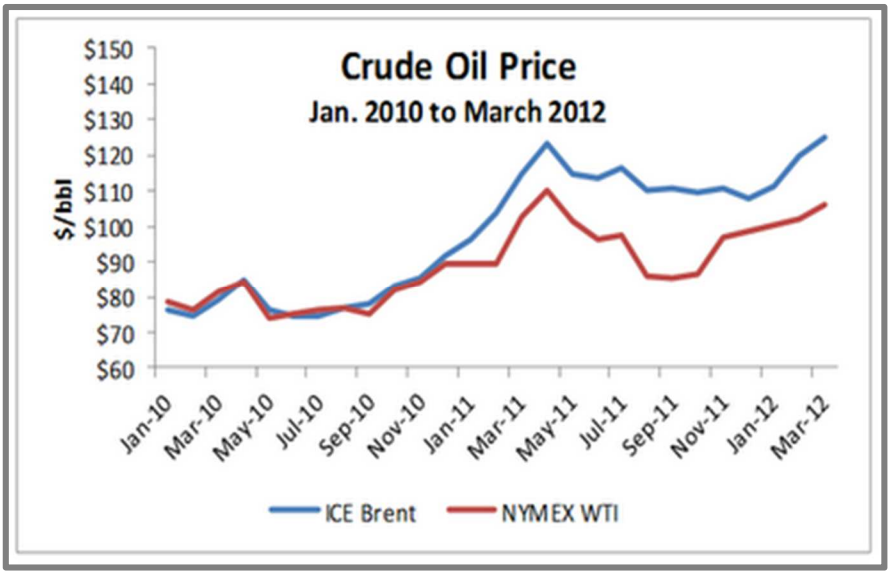

Figure 1.1 – Evolution of Oil Price (source: US Energy Information Administration)

Since the plastics use in automotive parts are manly Polypropylene(PP) or Acrilonitrile-Butadiene-Styrene (ABS) and these are petrol-based polymers it's easy to understand that with the increase of the oil price, the price of PP, ABS and energy will also increase.

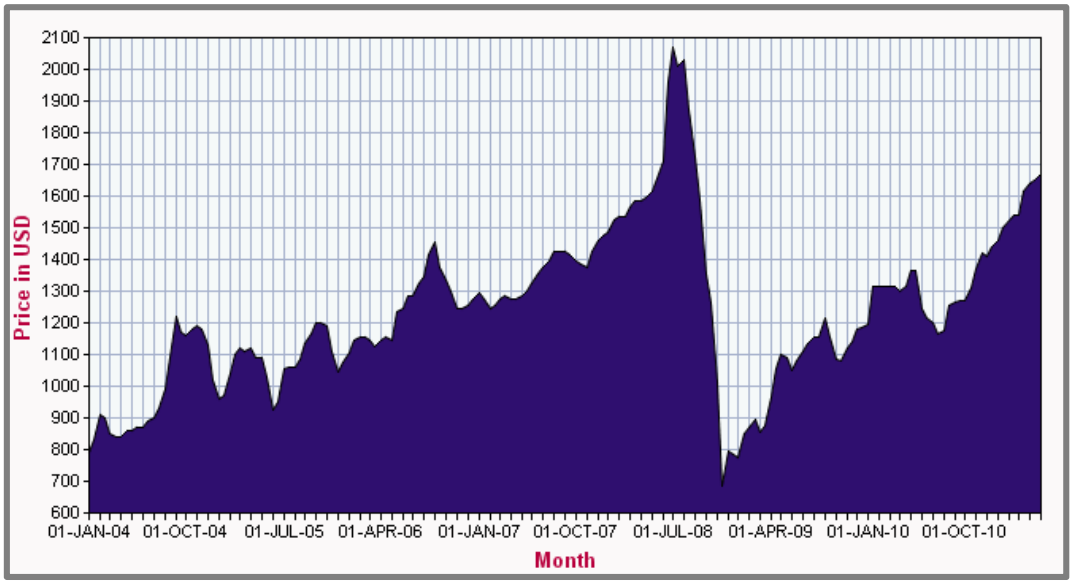

Figure 1.2 – Evolution of PP price per ton (source: www.plastmart.com)

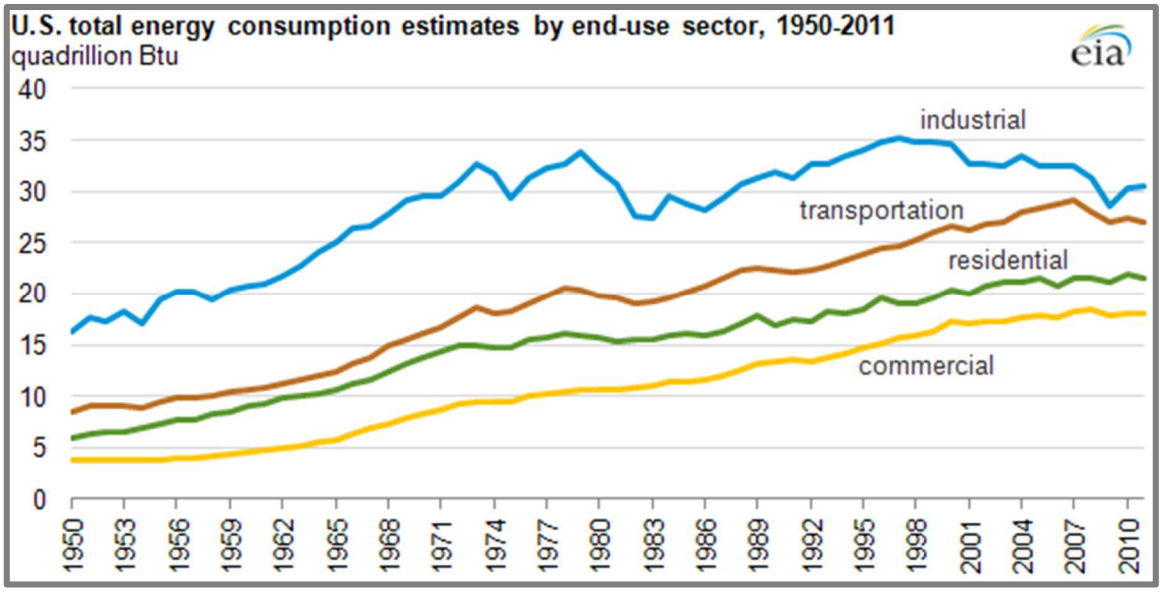

Figure 1.3 – Evolution of energy price (source: US Energy Information Administration)

With all this figures it's easy to achieve that the future of automotive industry goes to create lighter cars that are not dependent of petrol-based polymers and with engines that will spend less fuel.

1.3 Automotive Components

The substitution of automotive components made from glass-fiber composites for the natural fibers composites, in addition to the reduction of the problems due to recycling of the vehicles, drives to a decrease of fuel consumption and gases emission. That means that this substitution contributes for a better life quality.

The natural fiber-filled thermoplastics are 35-40% lighter than the glass fiber analogs[1]. Associating the weight decreasing to a better crash absorbance and sound insulation it's possible to realize the profit achieved when applied to door trims, instrument panels, package trays, glove boxes, arm rests and seat backs.
The first attempt to use "natural" composite materials probably was made by Henry Ford in the early 1930s. Henry Ford walked into his company's research laboratory with a bag of chicken bones, dumped them on the desk and asked his technicians to see what they could make out of them. They responded by experimenting with a variety of natural materials including cantaloupes, carrots, cornstalks, cabbages and onions in a search of materials to build an organic car body. In 1940, Ford scientists discovered that soybean oil could be used to make high-quality paint enamel and could also be molded into a fiber-base plastic.

In 1941, composites, particularly those based on natural fibers reinforcements received increased attention. During the World War II, seats and fuselages into aircrafts were made in those materials due to the shortage of aluminum at that time. An example is the "GORDON-AEROLITE" a composite of unidirectional, unbleached flax yarn impregnated with phenolic resin and hot pressed. This material was used in aircraft fuselages. At that time also appears a cotton-polymer composite, which was reportedly the first fiber-reinforced plastic used by the military, for aircraft radar.

In 1942, Henry Ford developed the first prototype composite car made from hemp fibers. The car didn't go to general production due to economic limitations at the time.

Between 1950 and 1960 in Europe, the body of the East German "Trabant" car was one of the first to be built form materials containing cotton fibers into a polyester matrix.

In 1996, the E-Class vehicle from Mercedes integrates a jute-based door panels.
In the last decade, bio-fiber reinforced polymer composites have been embraced by European car makers for door panels, seat backs, headliners, package trays, dashboards, and trunk liners.

Table 1.1 – Automotive manufactures, models and components using bio-fibers [3-4]

Automotive Manufacturer	Model and Application
Audi	TT, A2, A3, A4, A4 Avant,, A4 Variant (1997), A6, A8 (1997) , Roadster, Coupe: Seat Back, side and back door panel, boot lining, hat rack, spare tire lining.
BMW	Serie 3, Serie 5, Serie 7: Door insert, Door panels, Headliner panel, boot lining, seat back.
Citroen	C4 (2001)
Daimler - Chrysler	Class A, Class C, Class E, Class S: Door panels, windshield, Dashboard, business table, pillar cover panel; Class A, Travego Bus: Exterior underbody protection trim; Class M: Instrumental panel Class S: 27 parts manufactured from bio fibers
Fiat	Punto, Brava, Marea, Alfa Romeo 146 and 156, Sportwagon
Ford	Mondeo CD 162 (1997); Focus; Cougar (1998); Mondeo (2000), : Door inserts, Door panels, B-pillar and cover, Boot liner, parcel tray, motor protection (cover under shield)
MAN	Bus (1997)
Mitsubishi	Space Star: Door panels; Colt: Instrumental panels
Nissan	Miscellaneous models
Opel / Vauxhall	Astra, Vectra, Zafira: Headliner panel, door panels, door inserts, pillar cover panel, instrumental panel, rear shelf panel, column cover;
Peugeot	New 406 model
Renault	Clio, Twingo
Rover	Rover 2000 and others: Insulation, rear storage shelf and panel
Saab	Coupe (1998): door inserts; door panels
SEAT	Door panels, door inserts, seat backs
Toyota	Miscellaneous models
Volkswagen	Golf A4, Passat Variant, Golf A4 Variant (1998), Bora: Door panel, Door inserts, seat back, boot lid finish panel, boot liner, rear flap lining, parcel tray;
Volvo	C70, V70, Coupe (1998): Door inserts, parcel tray;

Nowadays, in the USA more than 1.5 million vehicles are the substrate of choice for biofibers such as kenaf, jute, flax, hemp and sisal and thermoplastic polymers such as polypropylene and polyester.

Bio fibers composites are, nowadays, used also in the exterior components of an automotive.
DaimlerChrysler's innovative application of abaca fibers in exterior under floor protection for passenger cars has been recently recognized.

Figure 1.4 – Automotive door in-liner, instrumental panel made from bio-fiber reinforced composites [4]

Figure 1.5 – Under floor protection trim of Mercedes A Class made from banana fiber [4]

Other exterior parts (front bumper, under floor trim of bus) from flax fiber reinforced composites will follow.

The automotive company Ford is using composites of kenaf fibers and polypropylene for the door panels of the Ford Mondeo.

The Mercedes S-Class has, actually, 27 components manufactured in bio-fibers reinforced composites with a total weight of 43 kg representing an increasing of 73% composite weight.

Figure 1.6 – Mercedes S Class components made from different bio-fiber reinforced composites [4]

Figure 1.7 – Model U Ford Hybrid-Electric Car. Corn based materials are used into the interior roof fabric and floor matting. Soy and corn-derived resins replace carbon black in the tires. Synthetic polyester is use to cover seats [5]

Nowadays approximately 18 million of automobiles and Lorries are manufactured in Europe per year. Each unit possesses between 5 to 10 kg of fiber which indicates a potential market of 90.000 to 100.000 tons per year of fiber.

Taking into account the 37 million of cars and light vans that are manufactured in the rest of the world the global potential market for natural fibers rises to 250.000 to 500.000 tons per year.

Each automobile is about 8% plastics and composites, which can be translated in around 245 lbs(79kg)/vehicle. [6]

The potential of composites materials provide a wide range of parts and components – body panels, suspension, steering and brakes among others.

The assessment of the viability of composites in automotive applications is based on the very limited cost information currently available.

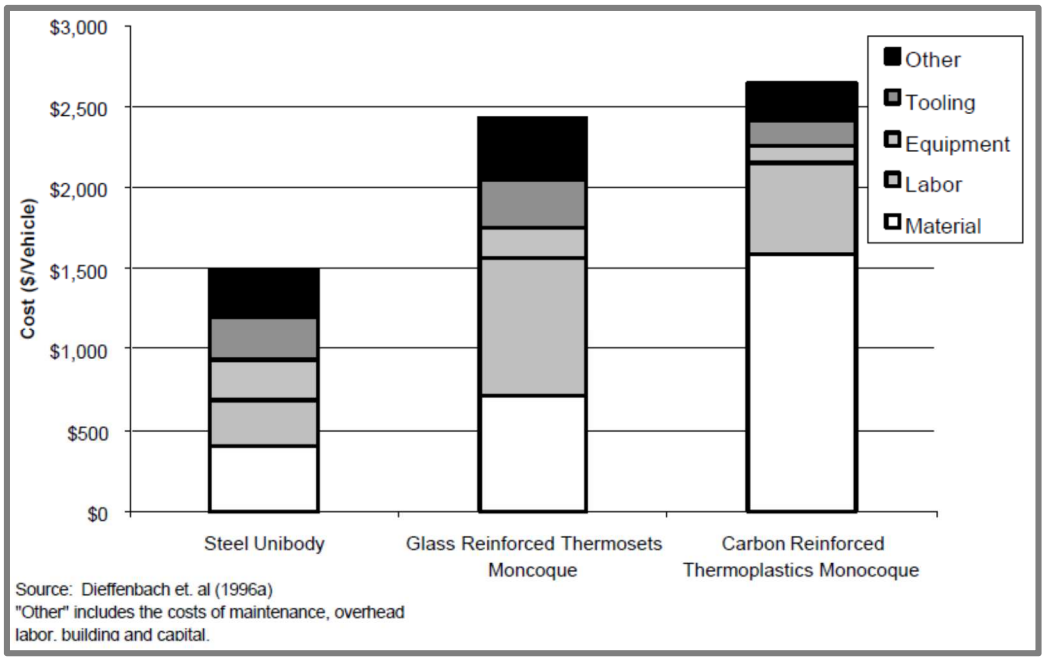

Figure 1.8 – Cost Structure Comparisons of BIW designs [6]

The comparative study, whom some results are presented into figure 1.8, of two composite monocoque Body-in-white (BIW) indicates that the material cost contributes with 60% for the total cost of carbon fiber-reinforced thermoplastics, but contributes only 27% with stell unibody and 29% if used glass fiber-reinforced thermosets. The next table compares the costs of various BIW designs on USD/lb basis.

Table 1.2 – Cost Component comparisons of various BIW designs (USD/lb) [6]

BIW Design	Material	Labor	Eqpt	Tooling	Other	Total
Steel Unibody	0,60	0,42	0,37	0,40	0,45	2,24
Glass-reinforced Thermoset Monocoque	1,38	1,64	0,36	0,57	0,74	4,68
Carbon-reinforced Thermoplastic Monocoque	4,55	1,61	0,30	0,44	0,65	7,55

(source: Dieffenbach et al. (1996a))

The recyclability of thermoplastics shows a great promise but the work should develop the cost-effective means of recycling including the fiber separation.

1.4 The future for Automotive Components

Faced with pressures to produce fuel-efficient, low-pollution vehicles and "green" cars, the automotive industry is looking for eco-friendly composites.

The usual composites present a polluted and intensive energy production. Glass, carbon and aramid fiber reinforced polyester, epoxy or similar resins are difficult to recycle and hard to dispose. [5]
The European Union regulations require that, by 2015, all new vehicles should be 95% recyclable. For that the use of thermoplastics, that can be thermally recycled to produce new products, will be good solution for that.
For reinforce instead using the non-recyclable common fibers, the automotive manufactures are also seeking for new materials. The new generation of fibers, based on agricultural products is already being in with mechanical properties that are suitable for some automotive applications.

Table 1.3 – Comparison of properties of various natural and synthetic fibers [5]

Fiber	Specific Gravity [g.cm^{-3}]	Tensile Strength [GPa]	Specific Strength [GPa/(g.cm^{-3})]	Tensile Modulus [GPa]	Specific Modulus [GPa/(g.cm^{-3})]
Spruce pulp	0,60	0,98-1,77	1,63-2,95	10-80	17-133
Sisal	1,20	0,08-0,50	0,07-0,42	3-98	3-82
Flax	1,20	2,00	1,60	85	71
E-Glass	2,60	3,50	1,35	72	28
Kevlar® 49	1,44	3,90	2,71	131	91
Carbon (standard)	1,75	3,00	1,71	235	134

Lightweight, strong and low-cost the bio-fibers are poised to replace glass and mineral fillers in numerous interior parts. [4]
In the last decade, bio-fiber reinforced polymer composites have been embraced by the European car manufactures for several interior parts (door panels, seat backs, headliners, package trays, dashboards, trunk liners, etc).
This trend reaches actually the North America. In the USA more than 1,5 million vehicles are the substrate of choice for biofibers.

On average each automotive can use around 20 m^2 of fibers or fabrics, woven or non-woven based composites. This is an increasing trend due to the advantages of lightweight, high strength and day-by-day lowering costs of textile products [4].

The European and North American market for bio-fibers reinforced plastics composites reached 685000 ton in 2002 with a value of 775 million USD. The major automotive manufacture European country – Germany – is increasing the consumption of bio-fibers (from 4000 ton into 1996 to 18000 ton into 2003).

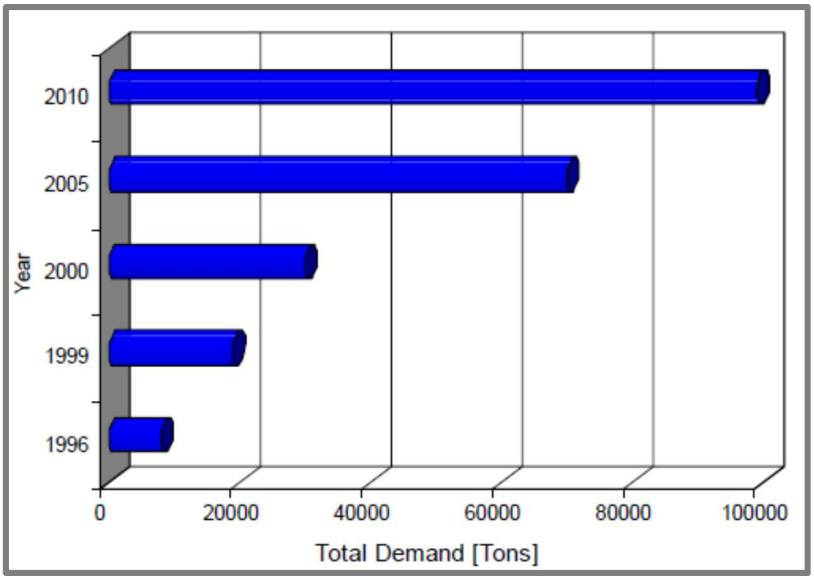

Figure 1.9 – Total consumption of bio-fibers within Western Europe; 2005 and 2010 are predictions [4]

Many automotive components are now made from bio-fiber reinforced composite materials.
However, these composites present a thermoplastic matrix but not a biodegradable one. That drives us to a stage that the automotive part can be reutilized, reprocessed but not decomposed without affecting the environment.

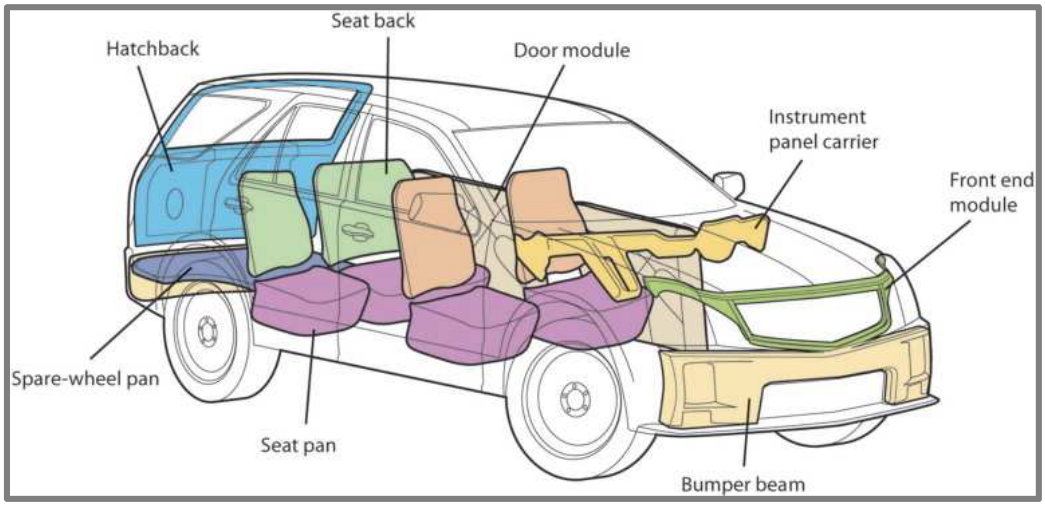

Figure 1.10 – LFTs applications in automotive parts [7]

Long fiber reinforced thermoplastics (LFT), used primarily in automotive applications, continue to show strong growth as they replace metal, short fiber reinforced thermoplastics, and thermoset plastics such as SMC and BMC.

R. Babinsky [7] estimates consumption was 160.000 – 190.000 metric tons of LFTs in 2006. The same study estimates that in North America and Europe, about 80% of the regional volume of LFTs goes into automotive applications.

The automotive industry is increasingly turning to LFTs to reduce both costs and vehicle weight. LFTs significantly reduce weight compared to metal, improving fuel efficiency and reducing emissions. Using LFTs to replace metal allows suppliers to integrate parts, thus greatly reducing assembly costs in parts such as door modules.

On the other hand, the incorporation of LFTs drives to need of setup new machines and production line. That's why for non-structural parts the automotive industry is trying to develop new composite materials that can be processed with the already installed production lines.

References

[1] M. Pervaiz, M.M. Sain, *Sheet-molded Polyolefin Natural fiber Composites for Automotive Applications,* Macromolecular Materials and Engineering, vol. 288, pp. 553-557 (2003)

[2] G.P. Hammond, S. Kaliu, M.C. McManus, *Development of biofuels for the UK automotive market*, Applied Energy, vol. 85¸pp. 506-515 (2008)

[3] R.R. Franck, *Bast and other plant fibres,* edited by Woodhead Publishing, Cambridge (2005)

[4] Andrzej K. Bledzki, O.F., Volker E. Sperber*, Cars from Bio-Fibres.* Macromolecular Materials and Engineering, vol. 5, pp.449.457 (2006)

[5] G. Marsh, *Next step for automotive materials*, Materials Today, April, pp.36-43 (2003)

[6] S. Das, *The cost of automotive polymer composites: A review and assessment of DOE's lightweight materials composites research*, Oak Ridge National Laboratory report for U.S. Department of Energy (2001)

[7] J. Markarian, *Long fibre reinforced thermoplastics continue growth in automotive,* Plastics, Additives and Compounding, vol. 9, pp. 20-24 (2007)

Chapter 2.

Literature Review

2.1 Introduction

The synthetic plastics influence so much the XX Century material culture that this period can be described as "The plastic Age".
Although, in the XV Century, it was possible to find luxury goods made by natural plastics, the development of the first modern plastic is attributed to the chemistry Alexander Parkes (1813 – 1890) who, in the XIX Century, found the nitrocellulose.

Due to the easy manipulation, cheap production, good corrosion resistance and versatility of the production processes, the plastics continue to be one of the most useful and popular materials as showed in fig. 2.1.

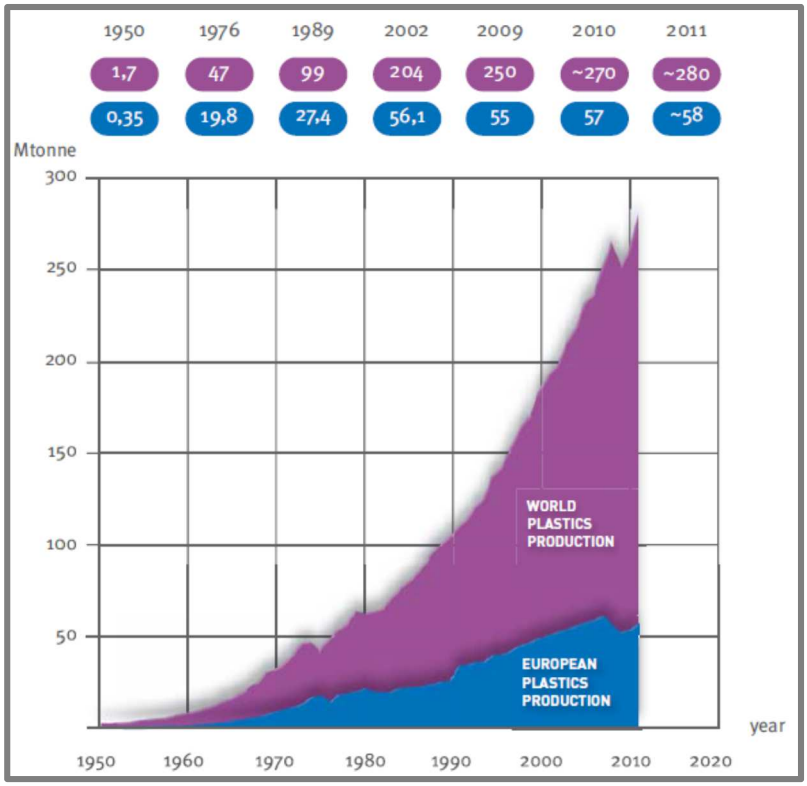

Figure 2.1 – World Plastics production 1950 – 2011 [1]

It's easy to understand that with this production figures, the waste are increasing gradually. Since the most of the plastics are thermosets polymers, these mean that a big percentage of disposable plastics are not degradable and will fill the landfills.

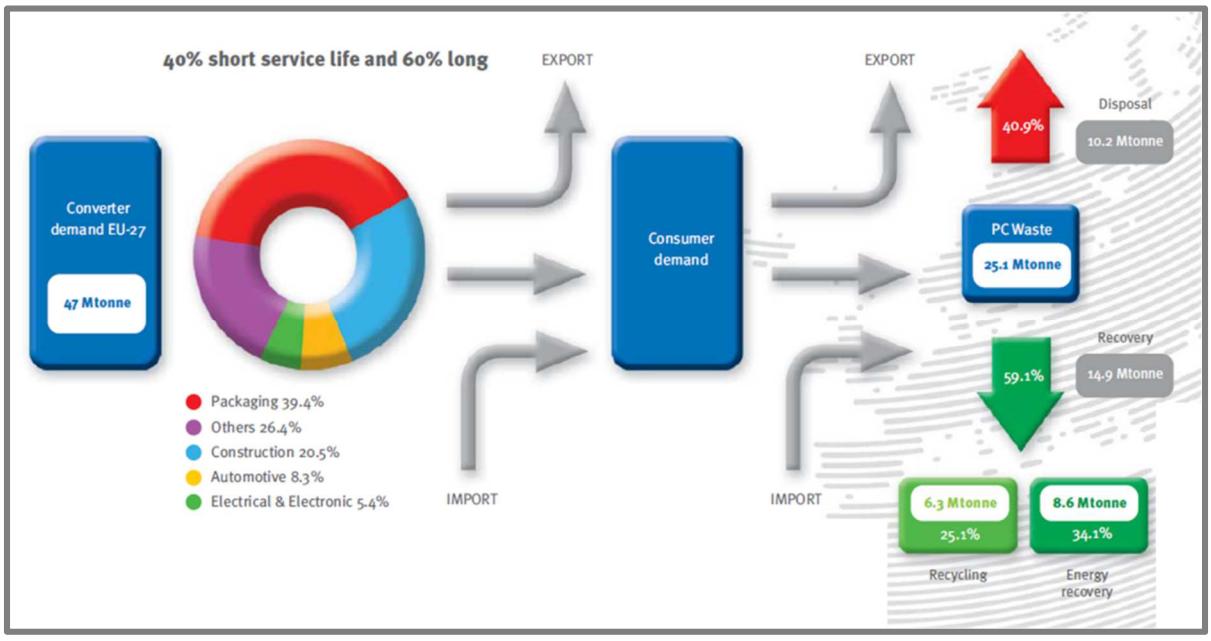

Figure 2.2 – Recovery reached almost 60% in 2011 (EU27+NO/CH 2010) [1]

[1] *Source: PlasticsEurope Market Research Group (PEMRG)*

2.1.1 Engineering Plastics

An Engineering Plastic can be defined as a synthetic organic polymer capable of being formed into load-bearing shapes, made by an artificially process from a carbon-based material with or without additives.
A polymer is a material composed of molecules made up of many (poly-) repeats of some simpler unit, the monomer.
All polymers have in common that they are chemically constructed by the repeats of the basic monomer unit, which is chemically bonded to others of its kind to form one, two or three dimensional molecules, with high molecular weight.

2.2.2 Types of Polymers

The polymer classification is not easy. Any division leads to a discussion.

Normally, the classification that leads minor discussion is the one based not only in the polymer origin (synthetic or natural), but also in some generic properties.

Using this classification it's possible to verify that natural polymers have more complex structures and the elastomers can have natural or synthetic origin.

The engineering plastics are polymers that are made synthetically, and the focus will be set only in the discussion of this group of polymers.

The engineering plastics can be divided into several ways, however the most current division is the one that are described into fig. 2.3.

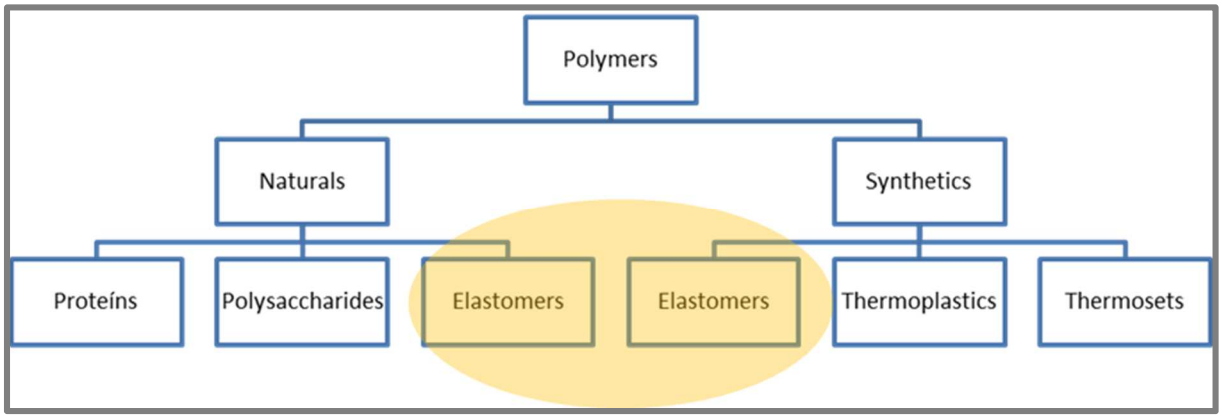

Figure 2.3 - Usual Polymer classification

The sub-groups described in Fig. 2.3 can be described by the generic properties as follow:

- Elastomers – Polymers that possesses a huge rate of elasticity. That means that when these types of polymers are submitted to a stress, even a small one, they deforms significantly. This deformation it's reversible and, when the stress ends, the polymers returns to the original shape;

- Thermosets - These polymers when heated, suffer irreversible chemical reactions that origin intermolecular cross-connections. The result is a reticulated structure which is infusible;

- Thermoplastics – These polymers when heated melts, and they can be heated and cooled anytime. These polymers, due to these characteristic, can be processed by the traditional methods: Injection, extrusion and rolling;

The properties of the engineering plastics are strictly connected with the raw-monomer and the chemical reaction used to produce the polymer.

Nowadays it's possible to process polymers by three chemical processes:

- Polyaddition – The monomers presents a double-connection carbon-carbon. In this process, the formation of sub-products doesn't exist and the final molecular weights can reach a magnitude of 10^5-10^6;

- Polycondensation - In this process, the formation of sub-products exists, and these sub-products must be removed of the reaction environment. The molecular weights reach a magnitude of 10^4;

- Chemical modification – This process consists in the polymers chemical modification. The changes on the molecular weight, the physical and mechanical behavior of the modify polymers allows a hugh diversification of the polymers applications;

As said before theses polymers can be divided into three groups: Elastomers, thermoplastics and thermosets.

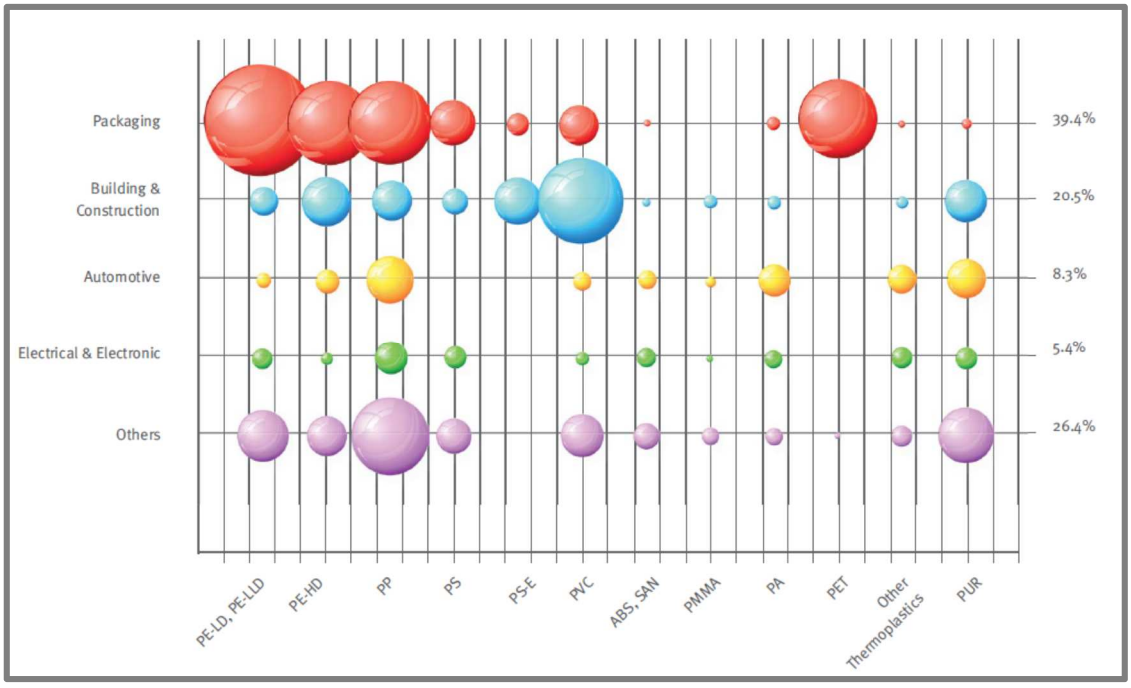

Figure 2.4 - European Plastics Demand by Segment and resin type 2011 [2]

[2] *Source: PlasticsEurope Market Research Group (PEMRG)*

As already related into Chapter 1, the automotive industry is using thermoplastic polymers for the automotive plastic parts. For that reason the focus will be settled on this kind of materials.

2.2 Biodegradable Polymers

Biodegradable polymers (biopolymers) are thermoplastic polymers obtained from renewable resources, synthesized microbially, or synthesized from petroleum-based chemicals. Through blend of two or more biopolymers a new biopolymer may be designed for specific requirements. Thus biodegradability is not only a function of origin but also of chemical structure and degrading environment.

Biodegradable polymers can be define as those polymers that are capable of undergoing decomposition primarily through enzymatic action of microorganisms in to CO_2, methane, inorganic compounds, or biomass, in a specified period of time.

As seen into figure 2.5, it's possible to obtain several biopolymers from different sources, even from petrol.

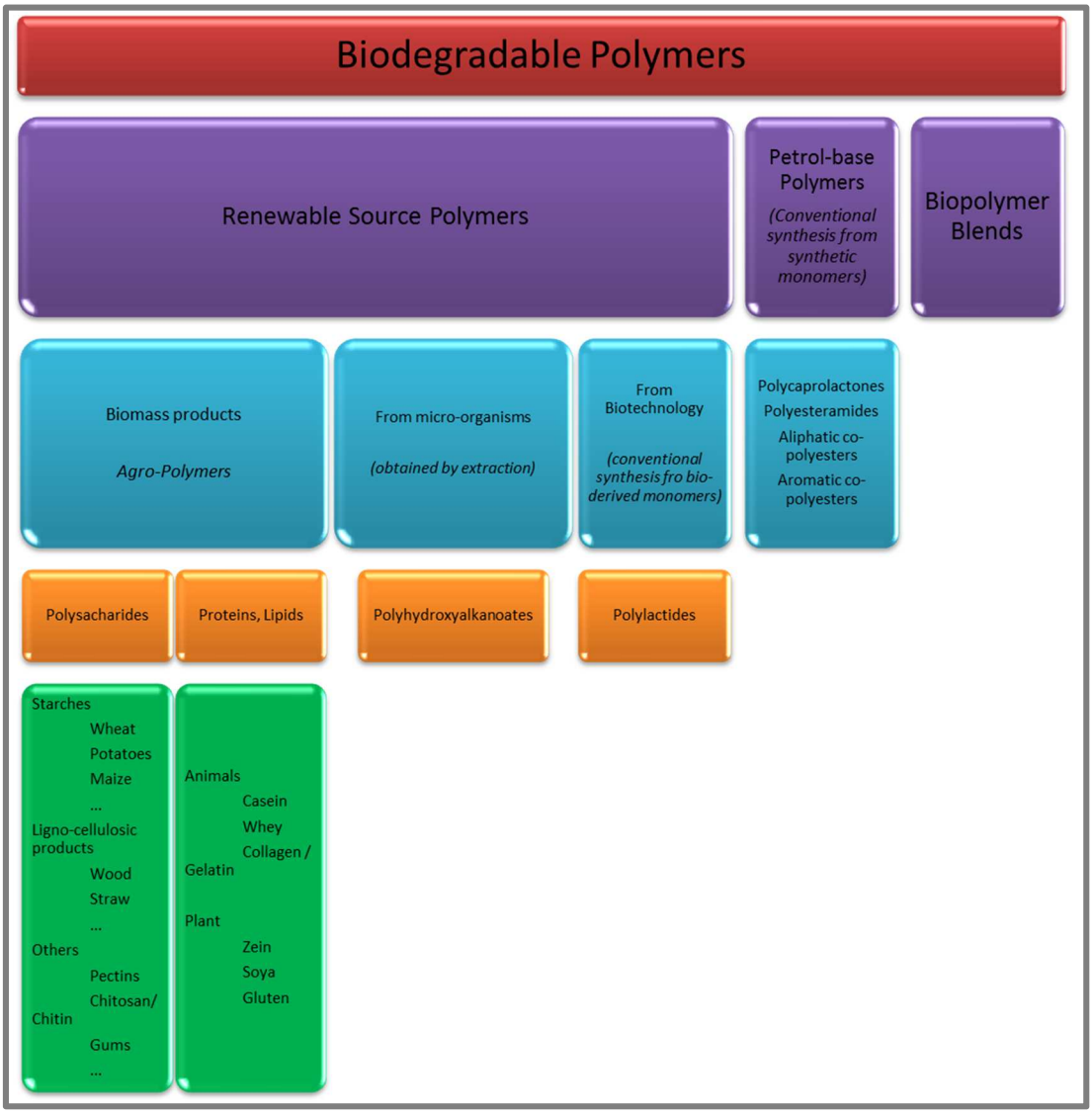

Figure 2.5 - Classification of Biopolymers [1-2]

The automotive industry, as discussed into Chapter 1, is trying to have green parts. For achieving that objective its necessary not only that the polymer presents biodegradable properties but also that the origin is also *green*, reason why the present state-of-art will focus the renewable source polymers only.

Originally, biopolymers were intended to be used in packaging industries, farming, and other applications with minor strength requirements.

The basic idea behind the biopolymers is taken from nature's cycle. Every year 100 billion of tones of organic material are generated by photosynthesis all over the globe. Most of this material is converted back into starting products, carbon dioxide and water by micro-organisms.

This cycle is the role-model for biopolymers, which are made from renewable raw materials obtained from agricultural production or agricultural sub-products or waste.
When the biopolymer parts as reach its end, it can be composted, closing the loop.

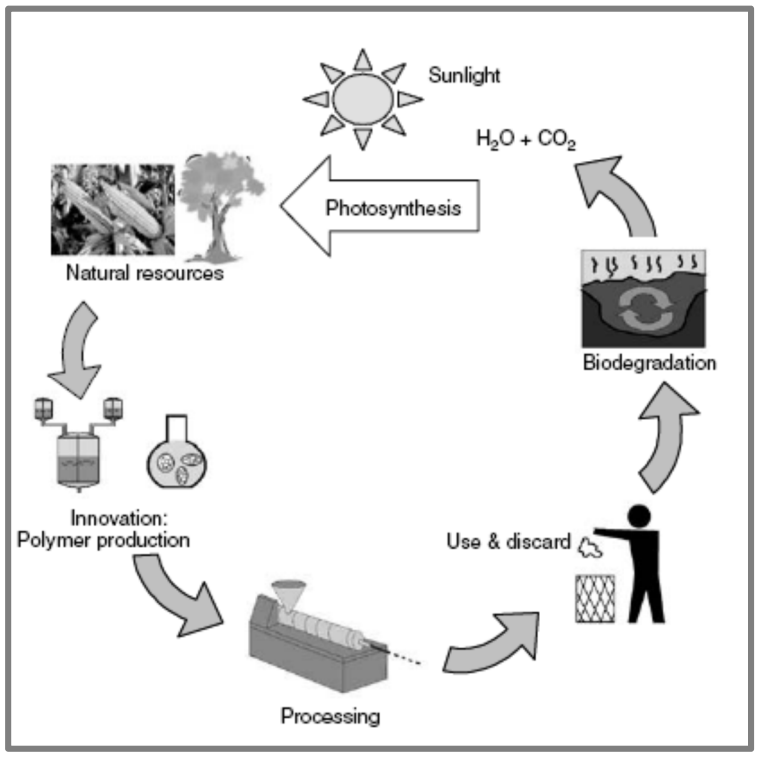

Figure 2.6 - Ideal closed loop life-cycle of biodegradable products [1]

The, yet, high cost of biopolymers and the performance limitations are major barriers for the widespread acceptance as substitute for traditional non-biodegradable polymers by the biodegradable polymers. However the high cost is not due to the raw material but it is mainly attributed to the low volume of production.

2.2.1 Biodegradable Polymers used

The use of biodegradable polymers from renewable resources to replace the petro-source polymers is increasing worldwide. The actual growing of petroleum cost and the overuse of landfills combined with environmental factors and policies are making a swift on the general sense of the use of biopolymers[3]. Several biopolymers and their blends are being used into a large spectrum of utilities. This new type of polymers allied to the life-cycle-analysis is making a turnover in the polymer industry.

However, it's mandatory to find biopolymers blends with properties that fulfill the product´s technical specifications at a low price, decreasing the ratio price/quality.

From the universe of biodegradable polymers from natural resources, the Polyhydroxyalcanoate (PHA) presents mechanical properties that can replace a large spectrum of petro-source polymers, namely in the automotive industry. However, due to its actual price, the solution isn't economically viable for mass consumption. Polylactic acid (PLA) is a lower cost polymer but does not meet fully the requirements of polymers for automotive components, for example, in terms of temperature resistance. To make a competitive solution is necessary to reduce the price of the final polymer. One way is to blend PHA with a less expensive biopolymer, such as PLA.

Most of the biodegradable polymers contain hydrolysable linkages such as amide, ester, urea and urethane along the polymer chains. However, the use of aliphatic polyesters (such as PLA) due to their useful biodegradability and their versatility regarding physical, chemical and biological properties is most attractive.

2.3 Poly(Lactic Acid)

Poly(lactic Acid) (PLA) is a polymer derived from lactic acid (2-hydroxy propionic acid). PLA is a rigid thermoplastic biodegradable polyester polymer that can be semi-crystalline or totally amorphous, depending on the stereopurity of the polymer backbone. PLA is the first commodity polymer produced from annually renewable resources.

The PLA production presents numerous advantages:

1- It can be obtained from a renewable agricultural source – corn, sugarcane, starch;
2- The production consumes carbon dioxide;
3- It provides significant energy savings;
4- The PLA is recyclable and compostable;
5- It can help improve farm economies;
6- The physical an mechanical properties can be manipulated through the polymer architecture;

The next figure presents a life-cycle model of PLA.

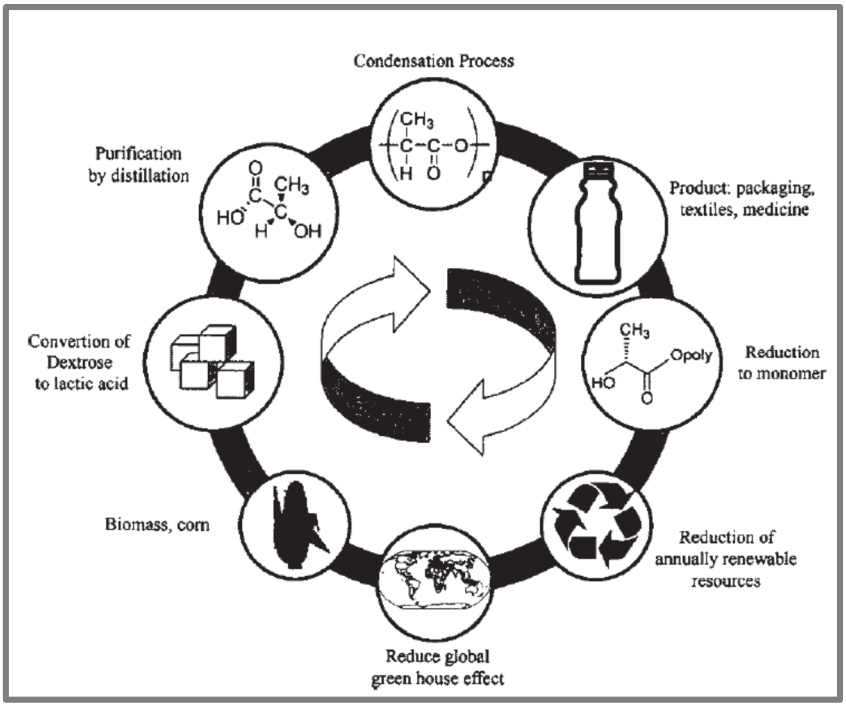

Figure 2.7 - Life-cycle model of PLA [4]

2.3.1 PLA Production

The PLA can be manufactured by carbohydrate fermentation or chemical synthesis.

In 1780 the first building block of PLA that was isolated from sour milk by the Swedish chemist Scheele and the first commercialization has been in 1881. [5]

Lactic acid is the simplest hydroxyl acid with an asymmetric carbon atom and it exists in two optically active configurations, the L (+) and D (-) isomers.

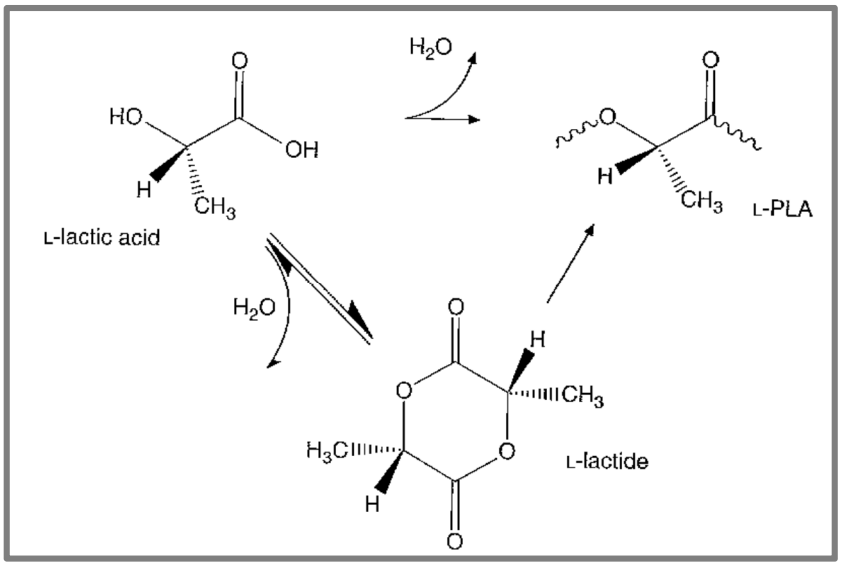

Figure 2.8 - Polymerization of L-Lactic acid to L-PLA by direct condensation or by ring opening via the L-lactide [6]

The L-Lactic Acid (2-hydorxy propionic acid) is the simplest hydroxyl and the natural and most common form of this acid. The asymmetric carbon atom drives to production of two optical isomers: the L-Lactic Acid (+) produced by mammalian and the D-Lactic Acid (-) produced by mammalian and other microorganisms.

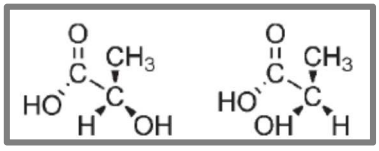

Figure 2.9 - Chemical Structure of L (left) and D (right) Lactic Acid [4]

The lactic acid is made by bacterial fermentation of carbohydrates. The fermentation processes to obtain lactic acid can be classified according to the type of bacteria used.

In the Heterofermentative method less than 1.8 moles of lactic acid per mole of hexose is produced along with significant levels of other metabolites such as acetic acid, ethanol, glycerol, mannitol and carbon dioxide.

In the Homofermentative method an average of 1.8 moles of lactic acid per mole of hexose and minor levels of other metabolites are produced. This conversion yields 90 g lactic acid per 100 g glucose.

Since homofermentative pathways lead to greater yields of lactic acid and lower levels of byproducts, these pathways are mainly used by industry. The majority of the fermentation processes nowadays use a genus of Lactobacilli which yields a high rate of lactic acid. These bacteria are classified as homofermentative, and the general processing conditions include a pH of 5.4 to 6.4, a temperature of 38 to 42 ºC and a low oxygen concentration.

The main sources are, in general, simple sugars such as glucose and maltose from corn or potato, sucrose from cane or beet sugar and lactose from cheese whey.

The production rate depends of the production type. Generally, batch processes produce 1 to 4,5 g /(l.h) of lactic acid while continuous processes produce 3 to 9,0 g/(l.h) . It's possible to reach a rate of near to 76 g/(l.h) if it's use cell recycle reactors.

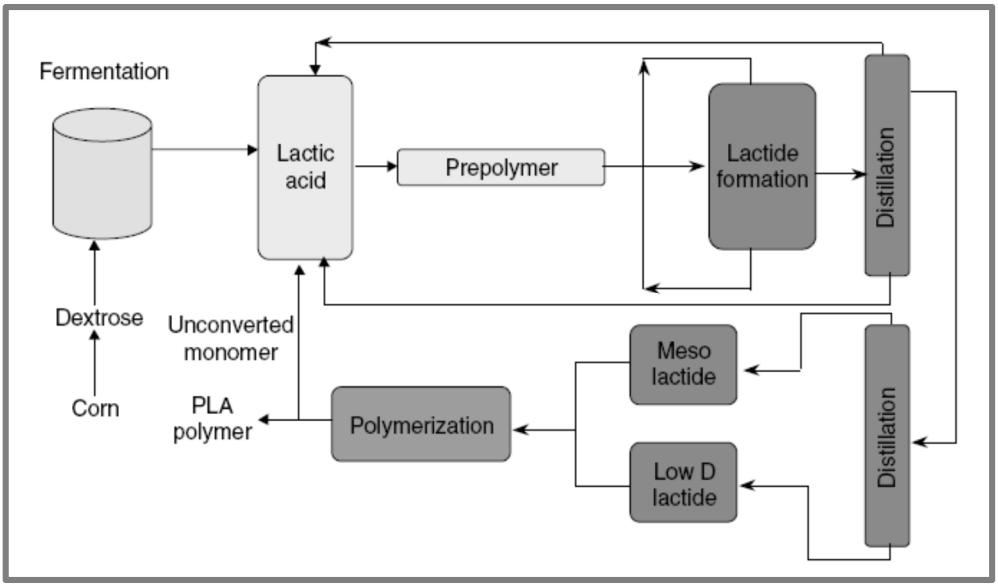

Figure 2.10 – Non-solvent process to prepare Poly(Lactic Acid) [4]

In order to produce PLA for industrial processes is necessary that the polymer possess adequate thermal stability to prevent degradation and maintain the molecular weight and properties. PLA undergoes thermal degradation at temperatures above 200 ºC by hydrolysis, lactide reformation, oxidative main chain scission and intra- or intermolecular transesterification reactions. [5]

The PLA homopolymers presents a T_g around 55ºC and a T_m of 175ºC.

2.3.2 PLA Properties

PLA is a unique polymer that in many ways behaves like PET, but also performs a lot like PP.

The properties of PLA are determined by the polymer architecture (i.e. the stereochemical makeup of the backbone) and the molecular mass, which is controlled by the addition of hydroxylic compounds. The ability to control the stereochemical architecture allows a precise control over the speed of crystallization and the degree of crystallinity.
That ability allows, also, the control of the mechanical properties and the processing temperatures of the material.

It's possible also to control the degradation behavior since it is strongly dependent of the crystallinity of the polymer.

Due to its good strength properties, film transparency, biodegradability, biocompatibility and availability from renewable sources, the PLA is commercially interesting.

The physical characteristics of PLA are very dependent on its transition temperatures for common qualities such as density, heat capacity and mechanical and rheological properties.

In the solid state PLA can be either amorphous or semicrystalline depending on the stereochemistry and thermal history.
For the amorphous PLA the glass transition temperature (T_g) determines the upper use temperature for most commercial applications.

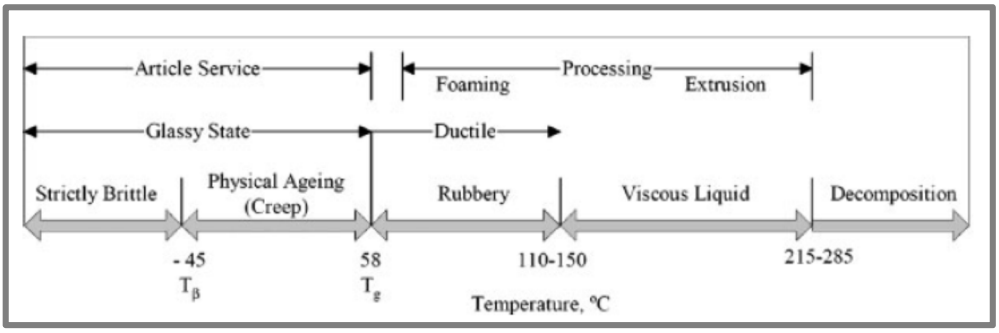

Figure 2.11 – Metastable states of amorphous PLAs [4]

For semicrystalline PLAs, both T_g (aprox. 58 ºC) and melting point (T_m), 130-230 ºC are important for determining the use temperatures across various applications. T_g and T_m are strongly affected by the overall optical composition, primary structure, thermal history and molecular weight.

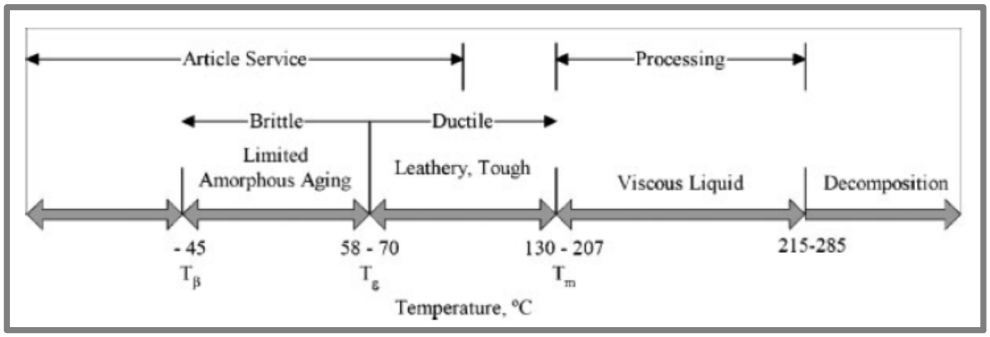

Figure 2.12 – Metastable states of semicrystalline PLAs [4]

2.3.3 PLA Biodegradation

As mentioned earlier, the biopolymers are polymers that are chemically synthesized or biosynthesized during growth cycles of all organisms. Some micro-organism and enzymes, already identified, are capable of degrading them.

Under typical use conditions, PLA is very stable and will retain its molecular weight and physical properties for years.

However under conditions of high temperature and high humidity PLA will degrade quickly and disintegrate within weeks to months.

PLA and its copolymers degrade to non-toxic breakdown products under certain conditions of temperature and moisture content. The degradation occurs initially by a non-enzymatic hydrolytic process. However the mass and the shape of the PLA part can be preserved until extensive degradation has taken place.

The primary mechanism of degradation is hydrolysis and cleavage of the ester linkages in the polymer backbone, followed by bacterial attack on the fragmented residues.

In the initial phase, the high molecular weight polyester chains hydrolyze (to a lower molecular weight oligomers) and after water penetration this molecular weight decrease rapidly due the PLA solubility in water only at very low molecular weight.

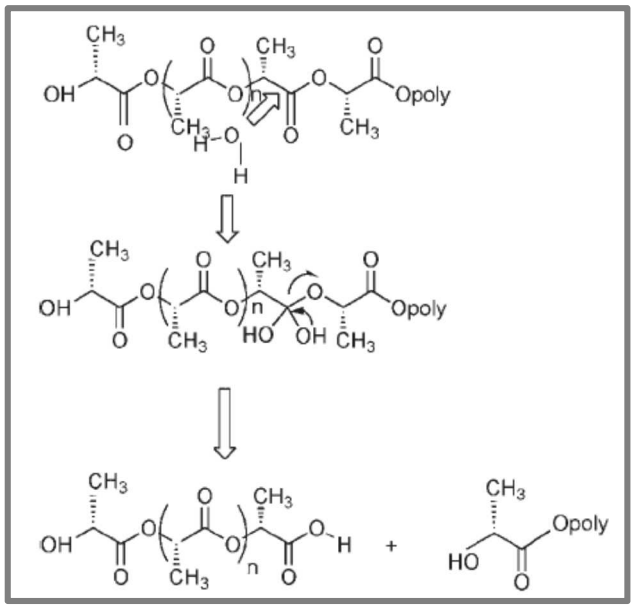

Figure 2.13 – PLA Hydrolysis and molecular weight loss [4]

The rate of hydrolysis is determined by its intrinsic rate constant, water concentration, acid or base catalyst, temperature and morphology. Since PLA is very water permeable this hydrolysis reaction is autocatalytic.

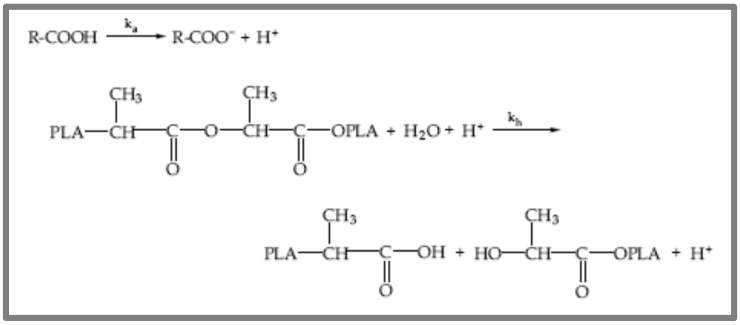

Figure 2.14 – Autocatalytic Hydrolysis reaction [1]

In the next steps of the degradation several enzymes can catalyze PLA hydrolysis. The most common enzymes are the Proteinase K, Pronase and Bromelain.
The enzymes are large molecules and are unable to diffuse through the PLA crystalline regions. Enzymatic involvement can produce pores and fragmentation making more polymer regions accessible to the enzymes.

2.3.4 PLA Based Composites

The PLA composites can be categorized into two different groups: one in which products are mainly used in the field of medical applications and a second group in which applications are in the field of structural plastics intended for other uses.

PLA composites for medical applications have often been reinforced with bioactive mineral fillers like zirconia, magnesium oxide, tricalcium phosphate or hydroxyapatite. The reinforced by carbon fibers is also used.
The main reason for the use of these types of composites is to mimic the mechanical properties and behavior of the bones in surgical applications.

There are several reasons to use PLA as a matrix into natural fiber biocomposites.

- PLA is nowadays the most advanced biopolymer in terms of commercialization;
- PLA has good mechanical properties that are similar to those of the polystyrene;
- PLA can be melt-processed with standard processing equipments at temperatures below those at which natural fibers start to degrade;

There are innumerous studies of PLA composites.

Bledzki and Jaszkiewicz studied the composites of PLA reinforced with Jute, Abaca or Man-made cellulose. [7] They concluded that by adding 30% (wf) of man-made cellulose, an increase in tensile strength of up to 50% can be achieved, and in average it's possible to obtain an improvement of around 30%.

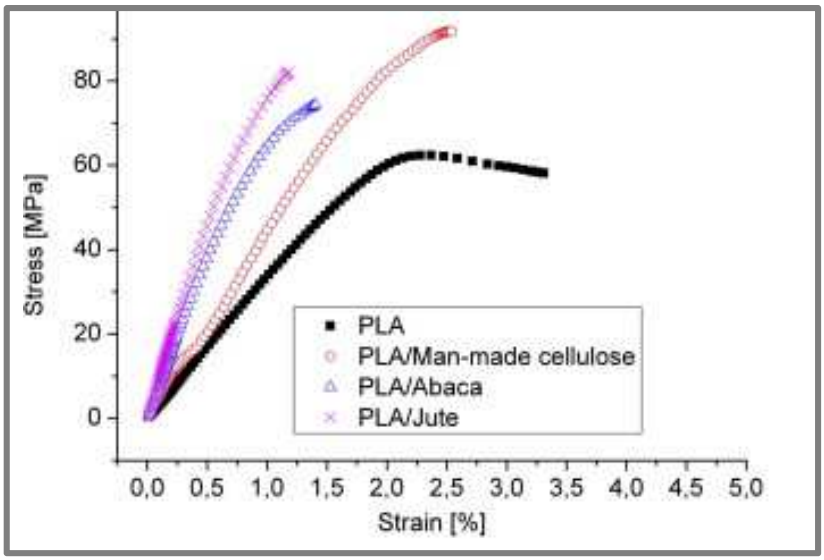

Figure 2.15 – Stress-strain curves of the tested composites [7]

Oksman, Skrifvars and Selin [8] investigates if PLA can be used as matrix in composite systems where natural fibers are used as reinforcements. They concluded that PLA works very well as matrix material for natural fiber composites. The composite strength is about 50% better compared to similar PP/flax fiber composites, which are used today in many industrial applications. The stiffness of PLA is increased from 3.4 to 8.4 GPa with an addition of 30 wf.% flax fibers. Generally these results indicate that PLA natural fiber composites have mechanical properties high enough for use instead of conventional thermoplastic composites.

Huda, Drzal, Misra and Mohanty, [9] studied the mechanical and thermomechanical properties of wood-fiber (WF) reinforced PLA composites and compared them with PP composites. The composites were processed by Compounding Injection Molding. To evaluate the reinforce effect on the mechanical behavior the incorporation rate of the fibers goes from 20 to 40%. The results allow them to conclude that the flexural strength decreases with the increasing the fiber incorporation. The flexural modulus increases significantly with the addiction of fibers. That suggests an efficient stress transference between the polymer and the fiber.

Table 2.1 Flexural properties of the composites [9]

Polymer/ fibers (wt %)	Flexural strength (MPa)	Flexural modulus (GPa)	Improvement in the modulus (%)
Neat PLA	98.8 ± 1.0	3.3 ± 0.1	—
PLA/WF (80/20)	118.3 ± 2.1	7.1 ± 0.2	115
PLA/WF (70/30)	116.6 ± 2.4	8.9 ± 0.8	169
PLA/WF (60/40)	114.3 ± 5.6	10.2 ± 0.9	209
Neat PP	32.9 ± 1.8	1.5 ± 0.2	—
PP/WF (80/20)	43.0 ± 1.2	2.7 ± 0.1	80
PP/WF (70/30)	51.4 ± 4.3	3.4 ± 0.9	126
PP/WF (60/40)	55.1 ± 2.4	4.6 ± 0.3	206

All works shows that the mechanical behavior of PLA composites is better than the mechanical behavior of PP composites when processed with the same conditions. The major synergic effect is obtain for PLA/cellulosic Fibers composites.

2.4 PolyHydroxyAlkanoate (PHA)

In 1923, Lemoigne at the Institut Pasteur demonstrated that aerobic spore-forming bacillus, formed quantities of 3-hydroxybutyric acid in anaerobic suspensions. He proceeded to investigate further and was successful in estimating quantitatively the amount of 3-hydroxybutyric acid formed. Finally, in 1927, he was able to extract a substance from *Bacillus* using chloroform and prove that the material was a polymer of 3-hydroxybutyric acid. However, it was not until the early 1960s that the production of poly(3-hydroxybutyrate) was explored on a commercial scale.

The Polyhydroxyalkanoates (PHAs) represents a range of polyesters produced from renewable resources by bacterial fermentation. The PHAs are semi-crystalline with melting temperatures ranging from 120º to 180ºC depending on the chemical composition.

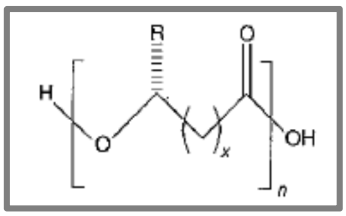

Figure 2.16 – Generic Structure of PHA's (R represents an Hydrogen or a Hydrocarbon chain; X can range 1 to 3 or more) [6]

In addition to biosynthesis, PHAs have attracted much interest due to the biocompatibility and their biodegradability. [10]

The PHA's are truly biodegradable and are enzymatically degraded by a wide range of bacteria, fungi and algae. In fact a wide variety of prokaryotic organisms can accumulate PHA from 30 to 80% of their cellular dry weight. [2] Degradation times depend on the environment and material form and can range from weeks to over a year.

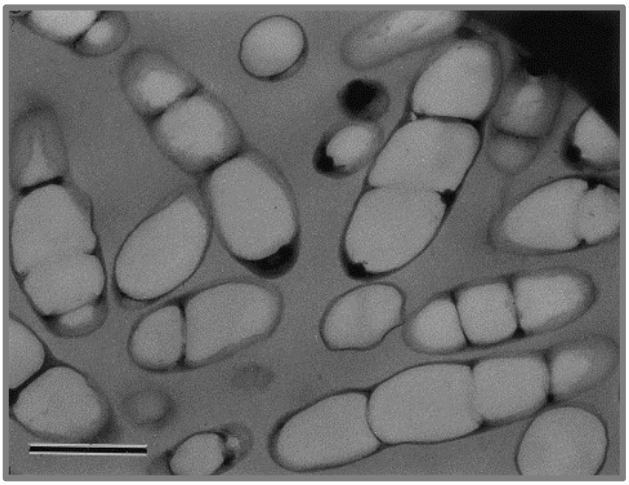

Figure 2.17 SEM of thin sections of recombinant *Ralstonia Eutrophia* cells containing large amounts of P(3HB-*co*- 5mol% 3HHx). Bar represents 0,5 µm [11]

In nature PHAs are microbially synthesized as an energy storage compound. So, the readily degradation by a wide range of bacteria, algae and fungi is not surprising.

Typically, this organism secrete extracellular depolymerises which degrade the polymer into low molecular weight. The degradation products are different according to the degradation environment. Under aerobic conditions the degradation produces carbon dioxide, water and some organic material and under anaerobic conditions the degradation produces methane and carbon dioxide.

The PHA's family is a wide range of polymers that are depending of the carbon substrates and of the metabolism of the micro-organisms that produces the polymers.

Although the PHA's family based polymer is the Polyhydroxybutyrate (PHB), different poly(hidroxybutyrate-co – hidroxyalcanoates) copolymers exists such as poly(hidroxybutyrate-co-hydroxyvalerate) – PHBV – poly(hydroxybutyrate-co-hydroxyhexanoate) – PHBHx – poly(hydroxybutyrate-co-hydroxyoctanoate) – PHBO, among others. [2]
PHB is a highly crystalline polyester with a high melting point when compared with other biodegradable polyesters [2].

PHB homopolymer possesses a narrow window for the processing conditions. To ease the transformation, it's possible to plasticize the PHB with citrate ester, however the PHB copolymer is more adapted for the process.

The production of PHAs is intended to replace synthetic non-degradable polymers for a wide range of applications, packaging, agriculture and medicine [13] once that PHAs are biocompatible.

The PHAs, like the PLAs, are sensitive to the processing conditions. Under extrusion we obtain a rapid diminution of the viscosity and of the molecular weight due to macromolecular chain cleavage by increasing the shear level.

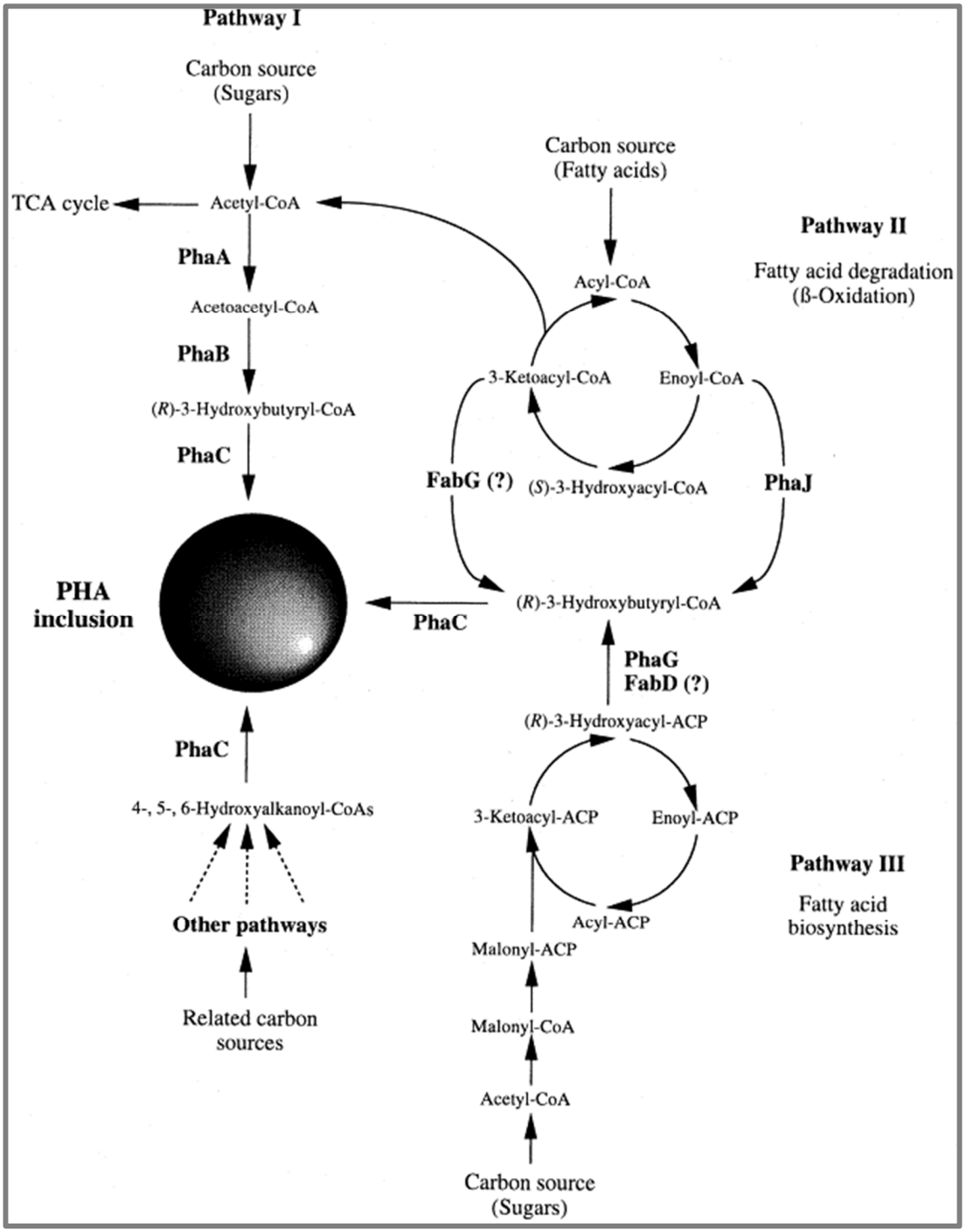

Figure 2.18 – PHA biosynthetic pathways [11-12]

2.4.1 PHA properties

PHB, one of the most popular PHA's is highly crystalline and hence is too rigid and brittle for practical applications. [14] To reduce the crystallinity and increase the flexibility of PHB, co-monomers with long side chains, such as 3-hydroxyvarelate, are copolymerized with the 3-hydroxybutyrate units.
The result is a co-polymer – PHBV – with a relatively high melting temperature, up to 170 ºC, and a relatively high glass transition temperature.

It's possible to tailor the polymer properties by controlling the copolymer composition of the PHA. It's possible to have a PHA hard and crystalline or elastic and rubber. [12]

Table 2.2 – Physical properties of Poly(3-hydroxybutyrate), poly(3-hydroxybutyrate-*co*-3-hydroxyvalerate) and poly(4-Hydroxybutyrate) [12]

Properties	Poly (3HB)	Poly (3HB-3HV)	Poly (4HB)
Melting temperature (°C)	177	150	60
Glass transition temperature (°C)	4	–7.25	–50
Tensile strength (MPa)	40	25	104
Elongation at break (%)	6	20	1000

2.4.2 PHA biodegradation

One of the greatest advantages that PHA's possess over other bio-polymers is the capability to degrade under both aerobic and anaerobic conditions. They can also be degraded by thermal means or by enzymatic hydrolysis. All these type of degradation drives to water and carbon dioxide (or methane under anaerobic conditions) by microorganisms in various environments. [15-16]

The polymer biodegradability is primarily governed by the physical and chemical properties. It has been found [12] that low molecular weight PHAs are more susceptible to biodegradation.

It also been found that, with the increasing of the melting temperature, the biodegradation potential decreases due to the decreasing of the enzymatic degradation capability.

The rate of biodegradation of PHAs depends almost of the environmental conditions like temperature, moisture, pH, nutrient supply, monomer composition, crystallinity, additives and surface area. [17]

As stats before PHAs works as a carbon and energy storage materials in various microorganisms. [16]

Chowdhury [18] reported for the first time the PHA degrading microorganisms from *Bacillus*, *Pseudomonas* and *Streptomyces spp*. Since then, several aerobic and anaerobic PHB-degrading microorganisms have been isolated from different ecosystems.

PHB can be degraded either by the action of intracellular or extracellular depolymerases.

Bibliographic revision appears that there are two modes to biodegrade the PHB [16]:

1. Preferential degradation took place in amorphous regions and crystalline lamellae remained unchanged ;
2. Proliferation of microorganisms on the surface, forming spherical holes without any selection between the amorphous and crystalline part of the polymer (Fig. 2.19);

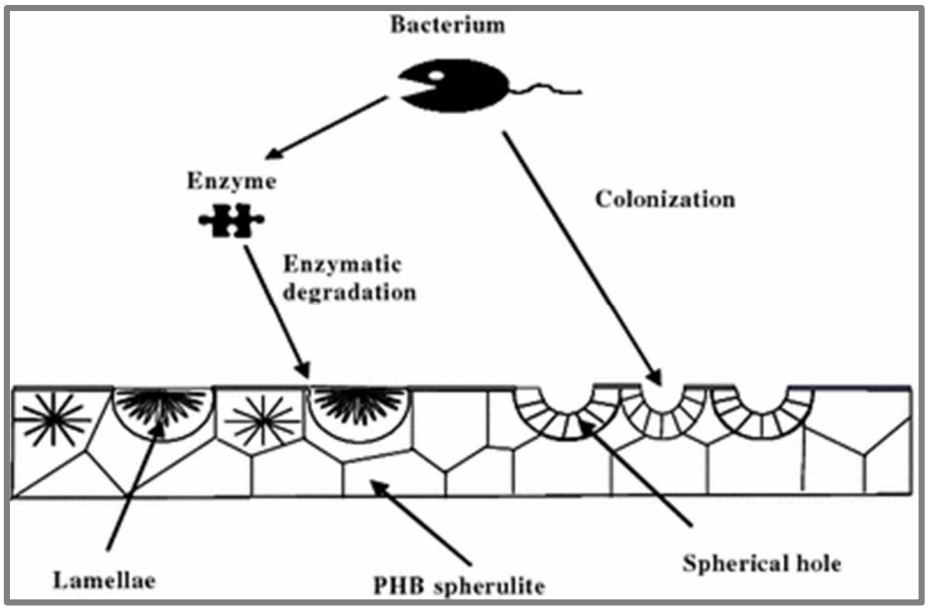

Figure 2.19 – Schematic illustration of two modes involved in the microbial degradation of PHB [16]

The spherical holes were due to the colonization by the degrading bacterium.
If the quenching temperatures increase then the spherulites of PHB become bigger. The PHB crystallinity will also increase driving to a decrease of the microbial degradation.

2.4.3 PHA based Composites

PHAs with natural fibers have been tested to check the reinforce effect on the properties of the final composite.

There are several studies of PHA composites.

P(3HB-3HV) films were reinforced with pineapple leaf fibers (30%wf). This reinforce increases the tensile strength by 100%. [12]

Avella, La Rota, Martuscelli and Raimo [19] studied the composites of PHB and wheat straw and hemp fibers.

Other works, envolving PHAs/natural fibers composites, were summarized by Satyanarayana, Arziaga and Wypych [18] and are presented into the next table:

Table 2.3 – Matrix-reinforcement and characteristics of biodegradable PHAs composites [18]

Matrix system	Reinforcement	Characteristics	Authors
PHB	Flax	No degradation of fiber. The evolution of the tensile properties of the composites as the fiber volume fraction increases	E. Bodros, I. Pillin, N. Montrelay and S. Wong, R. Shanks, A. Hodzic
PHBV	Abaca fibers	Weight loss in degradation burial test was PCL > PHBV > PBS > PLA. PCL losses ca. 45% after 180 days and PLA ca. 10% in 60 days	N. Teramoto, K. Urata, K. Ozawa, M. Shibata
PHB/copolymer PHV	Flax	Adhesion between the fibers and the polyesters was better than for analogous polypropylene composites. Bending modulus was increased. Storage modulus as 4 GPa at 25 °C	R. Shanks, A. Hodzic, S. Wong
PHB [hydroxyvalerate copolymer]	Steam exploded Hemp	Tensile strength of the ductile material was almost doubled by the reinforcement with 27% of fibers to 30 MPa, the *E*-modulus was quadrupled to 3.5 GPa	T. Corbière-Nicollier, B.G. Laban, L. Lundquist, Y. Leterrier, J.A. Manson, O. Jolliet
Biopol® [3]	Jute yarn	Composite enhances 194% the tensile strength, 79% the bending strength, 166% the impact strength and 162% the bending-*E*-modulus comparing with the matrix	A.K. Mohanty, M.A. Khan, S. Sahoo, G. Hinrichesen
PHB-co-PHV	Recycled cellulosic fibers (10%)	Tensile strength of the composite parallel to the fiber direction was 128 ± 12 MPa (10 vol% fiber) up to 278 ± 48 MPa (26.5 vol% fiber), compared to 20 MPa for the PHB/V matrix. Young's modulus was 5.8 ± 0.5 GPa (10 vol% fiber) and reached 11.4 ± 0.14 GPa (26.5 vol% fiber), versus 1 GPa for the matrix	M. Wollerdorfer, H. Bader

2.5 Natural Fibers

The combination of natural fibers with other materials to form composites is not new. For thousand years the Human Kind has been strongly dependent of the natural fibers from vegetable sources[4] for all kind of uses. Those fibroses materials have been common use in construction, although they had been other kind of important applications such as: tools, weapons, energy production, textile products, and paper among others.

Early in the XX Century, the development of synthetic materials causes the substitution of the natural products by these new ones.

Nowadays the World is near a new challenge: Reduce the pollution levels and at the same time increases the industrial output.

[3] BIOPOL ® is a co-polymer of poly(3-hydroxybutyrate –co-3-hydroxyvalerate) produzed by Metabolix (Cambridge, MA, USA)
[4] The natural fibers from vegetable sources will be designated from now on only by : Natural Fibers

This new dilemma drives to the re-born use of natural fibers, not only for the applications from the past, but also to produce new composite materials.

The use of natural fibers from vegetable sources in the production of composite materials has increasing during the last decade, especially into the automotive industry.

Due to the commitment between the resistance, stiffness and weight, the composites reinforce with natural fibers form vegetable sources are competing with the "conventional composites" in particular with the ones that are reinforced with glass-fiber. Natural fibers such as flax, hemp, jute, sisal or cotton are from renewable nature, cheaper, with a minor density, have better specific stiffness and a minor environmental impact since that they are biodegradable and easily recyclable.

Table 2.4 - Mechanical Properties of Natural Fibers [6] [21]

Fiber	Specific Gravity	Tensile Strength (MPa)	Modulus (GPa)	Elongation at break (%)	Specific Modulus
Jute	1,3	393	55	1,16 - 1,5	38
Sisal	1,3	510	28	3 – 7	22
Flax	1,5	344	27	2,7 – 3,2	50
Sunhemp	1,07	389	35	---	32
Pineapple	1,56	170	62	---	40

The natural fibers presents some limitations than need to be resolve so they can effectively compete with glass fibers.
The three major limitations are:

- The weak interfacial adhesion with the synthetic polymers – specially the thermoplastics;
- The high capability of water absorption;
- The low thermal resistance due to its organic nature;

To overcome these limitations, the natural fibers can be submitted to superficial treatments that allows the development of composites with good mechanical properties, bigger durability and reliability due to the operating conditions.

2.5.1 Fibers Classification

Natural fibers are subdivided based on their origins as expressed into figure 2.20:

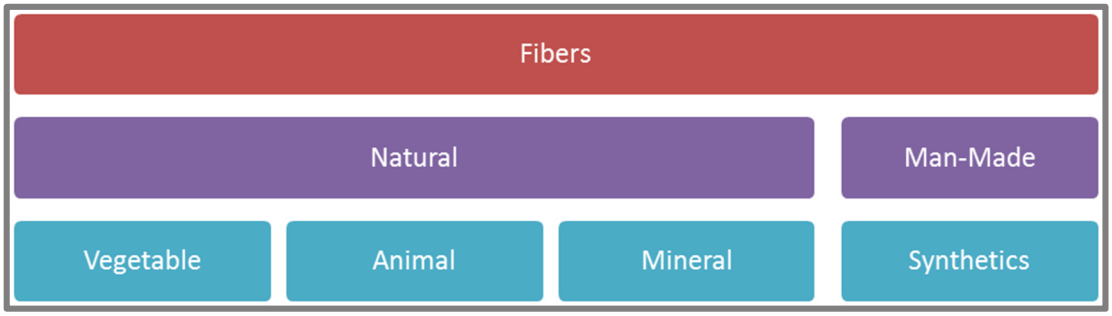

Figure 2.20 - Fibers classification [1] [22]

All plant fibers (vegetable) are composed of cellulose while animal fibers consist of proteins (hair, silk and wool). Plant fibers can include bast (or stem) fibers, leaf or hard fibers, wood, cereal straw and other grass fibers.

Natural fibers can be compared with a composite material consisted by cellulose fibrils embedded in lignin matrix. [17] The cellulose fibrils are aligned along the length of the fiber, and the reinforcing efficiency is related to the nature of cellulose and its crystallinity.

Table 2.5 - Commercially Important Fiber Sources [1]

Fiber	Species	World Production (10^3 ton)	Origin
Wood	(>10,000 species)	1,750,000	Stem
Bamboo	(> 1,250 species)	10,000	Stem
Cotton lint	*Gossypium* sp.	18,450	Fruit
Jute	*Corchorus* sp.	2,300	Stem
Kenaf	*Hibiscus cannabinus*	970	Stem
Flax	*Linum usitatissimum*	830	Stem
Sisal	*Agave sisilana*	378	Leaf
Roselle	*Hibiscus sabdariffa*	250	Stem
Hemp	*Cannabis sativa*	214	Stem
Coir	*Cocos nucifera*	100	Fruit
Ramie	*Boehmeria nivia*	100	Stem
Abaca	Musa textiles	70	Leaf

The vegetable/plant fibers can be further sub-divided into subgroups, as showed in the next figure:

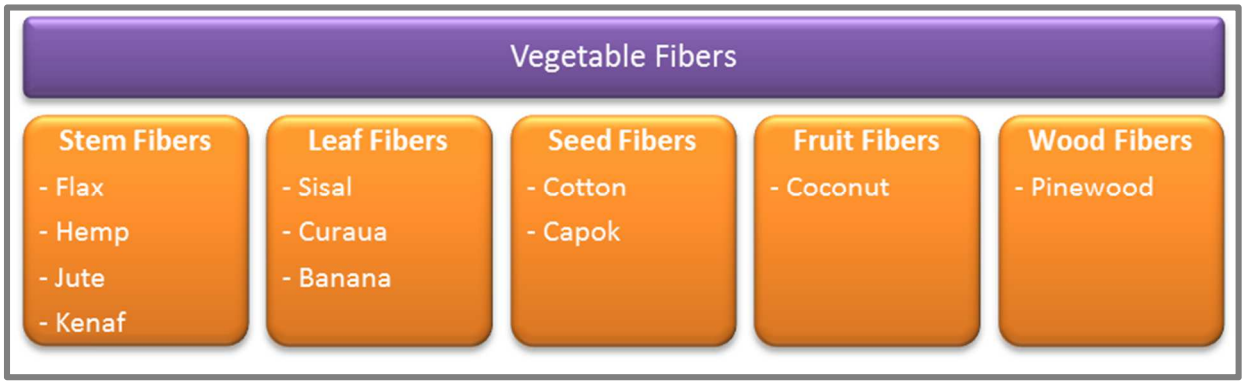

Figure 2.21- Vegetable fiber classification [1]

The most important of the natural fibers in terms of automotive industry are, with no doubt, the stem fibers subgroup.
They are called by that name because their origin is the stem of the plant. The plant stem is composed of an inner woody core surrounded by bundles of long hollow fibers and an outer protective skin.

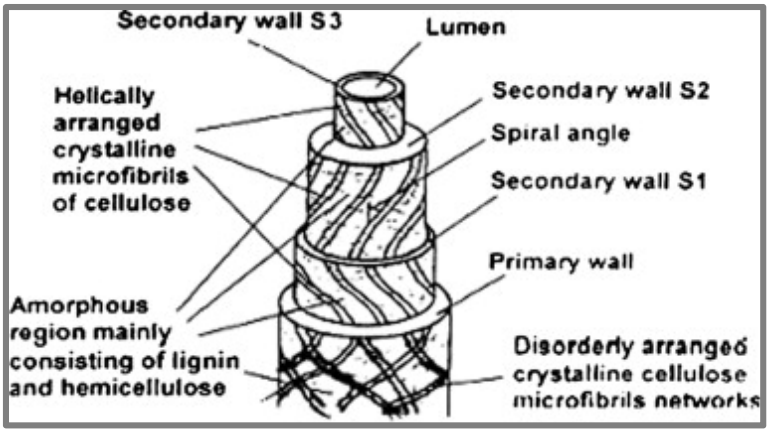

Figure 2.22 – Structure of biofiber [22]

Since the main function of the stem is to stabilize the plant, it's logical that the stem have plant fibers with good mechanical properties. This attribute in conjunction with a low density ensures that stem fibers have the potential to be outstanding reinforcements in lightweight composite parts.

The advantages of using stem fibers in the automotive industry are:

- Renewable and sustainable plant fiber resource;
- Recyclable;
- Weight saving between 10 and 30%;
- Cost savings;
- Abundant supply which is accessible to car manufacturing plants in many regions of the world;

Table 2.6 – Fiber characteristics and growing area of commercially available fibers [4]

Fibre type	Origin	Species	Length (mm)	Width (μm)	Growing area
Cotton	Seed hair	*Gossypium* sp.	12–64	20	Southern parts of North America
Flax	Bast	*Linum usitatissimum* L.	10–36	10–25	EU, Canada, Argentina, USSR, India
Jute	Bast	*Corchorus capsularis* L	3–5	0.017–0.023 mm	India, China, Bangladesh
Hemp	Bast	*Cannabis Sativa* L.	6.5–37.2	0.015–0.46 mm	EU, USSR, Philippines, Central Asia, China
Ramie	Bast	*Boehmeria nivea Gad*	15–25	0.02–0.08	China, Brazil, Thailand, Japan, USA, Malaysia
Kenaf	Bast	*Hibiscus cannabinus* L	2–6	0.014–0.033	Thailand, India North and South America, Iran Southern USSR
Abaca	Leaf	*Musa textilis Louis Nee*	2.2–8.1	0.010–0.033	Philippines and Equador
Sisal	Leaf	*Agave sisalina Perr*	1.2–5.8	0.011–0.30	Central and South America, Africa, Indonesia, West Indies
Esparto	Stem	*Stipa tenacissima* L.	0.25–2.0	0.010–0.015	Spanish plateau
Wheat	Stem	*Triticum aestivum* L.	0.5–3.1	0.008–0.030	Western Asia, USA
Bamboo	Stem		0.21–37	0.005–0.035	Japan, India
Begasse	Stem	*Saccharum officinarum* L.	0.8–2.8	0.010–0.034	India

Nowadays an increasing market is appearing due to the vegetable fibers.

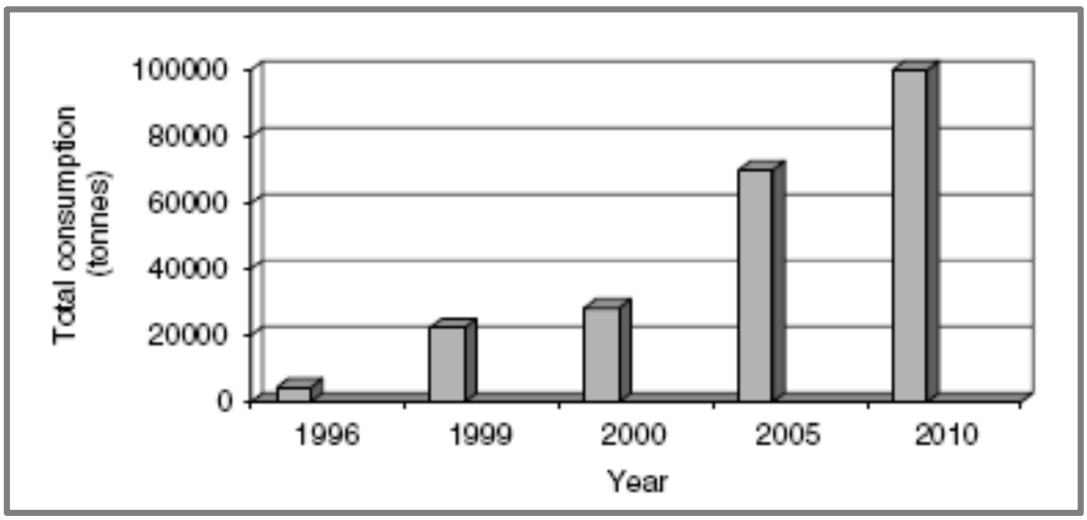

Figure 2.23 - Total consumption for natural fibers in Europe [1]

The world's supply of natural resources is being depleted, the demand for sustainable and renewable materials continues to rise.

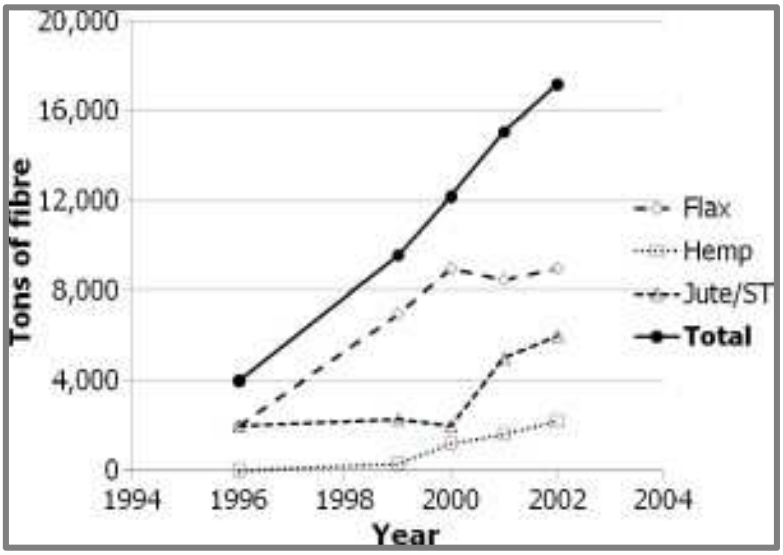

Figure 2.24 - Use of natural fibers in the German automotive industry 1996-2002 (tonnes) [33]

2.5.2 Cellulosic fibers: Advantages and Disadvantages

The biofiber world is full of examples where cells or groups of cells are *designed* for strength and stiffness. Cellulose is a natural polymer with high strength and stiffness per weight, and it's the building material of long fibrous cells.

In general, the fiber consists of a wood core surrounded by a stem.
Within the stem there are a number of fiber bundles, which contain individual fiber cells or filaments. These filaments are made of cellulose and hemicellulos, bonded together by a matrix, normally lignin or pectin. The principal differences between the individual fibers are: fiber qualities, lignin content and odor.

The increasing of interest in lignocellulosic fibers is due mainly to their economical production with few requirements for equipment and low specific weight, which results in a higher specific strength and stiffness when compared to glass reinforced composites.

The biofibers, such as the cellulosic fibers, are nonabrasive to mixing and molding equipment. They have a positive environmental impact and with a production that requires little energy.

However the inherent polar and hydrophilic nature of lignocellulosic fibers and the non-polar characteristics of the common thermoplastics results into a compounding difficulties leading to non-uniform dispersion of the fibers within the matrix which impairs the efficiency of the composite. This is probably the major disadvantage of biocomposites.

Another problem is related to the processing temperatures that for this type of fibers are restricted to 200 ºC once that the vegetable fibers degrade at high temperatures. This will frame the matrix choice.

Another setback is the high moisture absorption of the biofibers leading to swelling and presence of voids at the interface, which leads to a poor mechanical properties and reduces dimensional stability of the composites.

Is clear that the advantages outweigh the disadvantages and most of the shortcomings have remedial measures in the form of chemical treatments.

2.5.3 Cellulosic fibers: Portuguese Market and Extraction Technology

The best way to obtain cellulosic fibers is to use the pulp wastes from the paper plants.
In the north of Portugal and in the Galiza region (Spain) is possible to count 824000 ha of Pine trees and 468000 ha of Eucalyptus trees. [23]

To process and transform the wood in paper this euro-region counts with 9 industrial plants. From these 9 plants, 2 are thermochemical paper pulp plants. The other 7 can be divided in 5 plants to produce MDF and 2 to produce fiberboard.

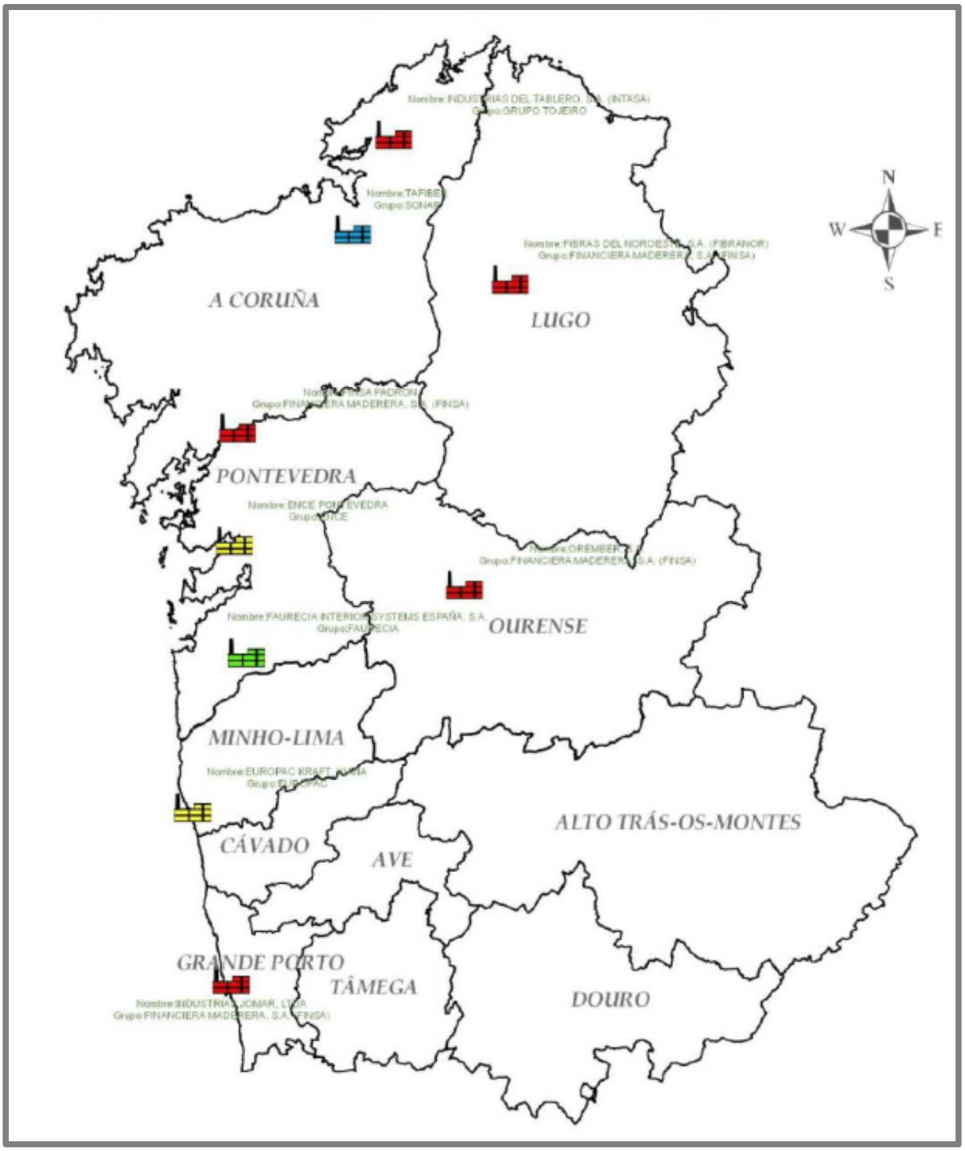

Figure 2.25 – Northern Iberian Peninsula Wood Transformation Plants Geo-localization [23]

The process to extract fibers from the wood is a chemically heavy and requires a parallel system to purify the produced wastes to decrease the environmental impact.

The process is quite similar if we are extracting pine fibers or eucalyptus fibers. The main differences are at the chemical compounds used.

In figure 2.26 it's presented a simplified diagram of a typical pulp and paper process.

For composite applications the fibers don't goes through all process described but after bleaching the pulp goes to the secondary market pulp.

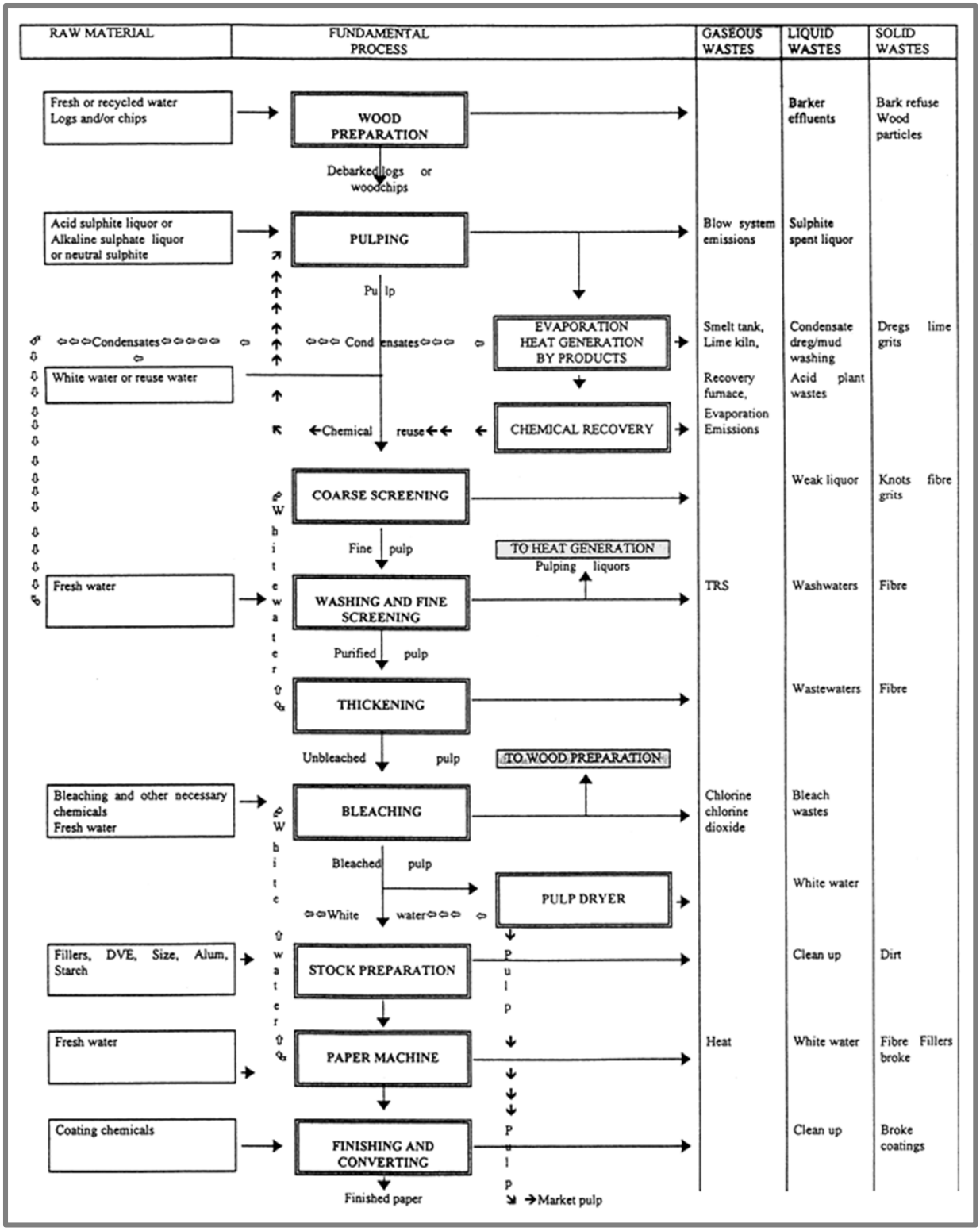

Figure 2.26 – Simplified diagram of a typical pulp and paper process [24]

2.6 Composite Materials

A Composite Material (or composite) can be defined as a micro or macroscopic combination of two or more distinct materials.
The association of these materials aims to create a new material with better properties than the ones who origin it.

The composite materials exist and they are being used for several centuries.
Probably the oldest reference to composite materials appears in the Holly Bible, and describe that the Jewish slaves are forced by the Egyptians to produce bricks from the mixture of straw and mud.[5]

In the VII Century the Japanese sabers were made by steel and iron.

Nowadays it's possible to find composite materials everywhere, starting in the glass of our house windows, passing by the concrete use in construction.

The composite materials are, technically, heterogeneous and anisotropic materials and that means that the mechanical properties are depending of the direction and the place where the solicitation occurs.

Typically, a composite material is constituted by a matrix - a homogeneous resin or polymer material, and reinforcement – a strong material bonded into the matrix to improve its mechanical properties.

2.6.1 Matrices

The purpose of a Composite Matrix is to bind the reinforcement together. This binding is made due to the cohesive and adhesive characteristics of the matrix material.

When under load, resins may microcrack and craze. Due to the coalescence of microcracks, the matrix may form larger cracks. It's also possible to have a debonded of the reinforce fiber. If anyone of these factors occurred it's possible to have a composite with properties far lower than the desired ones.

That's way the matrix is the "weak link" of any composite material.

Nonetheless, the matrix resin provides many essential functions.
The composite matrix is responsible for keep the reinforce into the proper orientation and position, to distribute the load more or less evenly among the fibers, provides resistance to crack propagation and damage, and also provides all of the interlaminar shear strength of the composite.

Furthermore, it's matrix responsibility the overall service temperature limitations.

[5] *Exodus 5,7*

2.6.2 Reinforcements

One of the objectives of the reinforcements is to support most of the load that are applied into the composite material.
Since the reinforcements are, by default, fragile materials they don't contribute to the impact behavior of the composite.

However, the reinforcements are more rigid and stiffener than the matrix material. These characteristics give to the composite a high mechanical behavior.

To a material reinforce effectively a matrix, it must have the following characteristics:

- A Young Modulus higher than the matrix (minimum twice bigger);
- Tensile Stress bigger than the matrix tensile stress;
- A geometry that allows the combination with the matrix and with the final form of the part;
- Have a good adhesion with the matrix;
- Don't react chemically with the matrix;

Normally, the reinforce addition, occurs to improve the mechanical behavior, stiffness, corrosion resistance, thermal conductivity, creep and fatigue resistance.

2.6.3 Thermoplastic Matrix Composites

The composites can be divided into classes in various manners. The first division, and the most common one, is to dived by the matrix material. In this case the division is thermoplastic matrix composites and thermoset matrix composites.

Other division is too dived by the reinforce material. In this case the division is much more complex since it's possible to have an innumerous number of reinforce materials.

Thermoplastic resins are potentially useful as matrices for advanced composites. Thermoplastic resins present three advantages when compared to thermosets resins.

- Processing can be faster since no curing reaction is required. Thermoplastic composites only require heating, shaping and cooling;
- The mechanical properties are attractive, in particular, high delamination resistance and damage tolerance, low moisture absorption and the excellent chemical resistance of semicrystalline polymers;
- Thermoplastic composites offer advantages in terms of environmental aspects. They have very low toxicity since they do not contain reactive chemicals (therefore storage life is infinite). Because it is possible to remelt and dissolve such thermoplastics, their composites are also easily recycled or combined with other recycled materials;

In the automotive industry, thermoplastic composites are used extensively, because they allow fast processing cycles for fairly large components. In the field of injection molded components, the thermoplastic composites, normally, are used with short fibers (5-10mm) in molding pellets.

Thermoplastics resins can have an amorphous or a semi-crystalline structure. If the structure is amorphous, the polymer chains don't present long-range order, which may be viewed as polymer glasses and, in the absence of color pigments, these polymers, are usually transparent.

On the other hand, crystalline polymers have regions of molecular order.

Due to the large size of polymer chains inhibits the perfect crystallization; the crystalline thermoplastics correctly must be described as semi-crystalline, since the degree of crystallinity never reaches 100%. So, the semi-crystalline thermoplastics are really a two-phase materials with a crystalline and an amorphous phase.

Table 2.7 - Characteristic temperatures for thermoplastic resins [25]

Polymer	IUPAC designation	Structure	T_g (ºC)	T_m (ºC)	Processing Temperature (ºC)
Polyamide 6,6	PA6,6	Crystalline	55	265	270-320
Polyamide 12	PA12	Crystalline	35	180	220-260
Polyamide-imide	PAI	Amorphous	275	None	350-400
Polybutylene terephthalate	PBT	Crystalline	20	240	260-290
Polycarbonate	PC	Amorphous	150	None	280-330
Polyether Ether Ketone	PEEK	Crystalline	143	343	380-400
Polyetherimide	PEI	Amorphous	217	None	335-420
Polyether-sulphone	PES	Amorphous	220	None	300-320
Polyethylene terephthalate	PET	Crystalline	70	265	280-310
Polyphenylene Sulfide	PPS	Crystalline	90	280	300-340
Polypropylene	PP	Crystalline	-10	165	200-240
Polysulphone	PSU	Amorphous	190	None	300-350

The use of polymer composites is of great interest in the view of a more intelligent utilization of environmental and financial resources. Several works have being done to create full biodegradable composites by the replacement of the petrol-based polymers and synthetic fiber reinforcement for renewable-source polymers and fibers. These *green* composites, yet, presents some limitations regarding mainly ductility, processability and dimensional stability [26].

It can be stated that the commercial market is still in an opening phase (especially in Europe) for these types of composites. Therefore much can still be done in order finding new applications, improving the properties, the appearance and the marketability of these materials. All of these issues require, and continue to require, significant research efforts in order to:

- find new formulations (virgin or recycled polymers, traditional or biodegradable polymers; type, appearance, quality and amount of the fillers);
- Correctly characterize at all terms the new composites;
- Apply them for the most suitable applications;
- Refine and readjust the processing techniques.

As soon as the market for these composites increases, reduction of costs and improvement of the quality will be achieved.

2.6.4 Composite Production into the automotive industry

The automotive industry seeks for cheap, easy and repetitive methods to produce the parts.
For interior door trims is possible to identify a few processes that allies the thermoplastic matrix properties to the main pillars of the automotive industry production.

In recent years several attempts to reduce the use of glass-fiber and the expensive aramid or carbon fibers into the automotive industry have been observed. These attempts take the advantage of the lower density and cost of some natural fibers. [27]

The incorporation of composites materials has been already discussed into this thesis, however, is important to emphasize that the application of biocomposites in automotive body parts is feasible as far as biocomposites presents comparable mechanical performance with the synthetic ones.

2.6.5 Bulk Moulding Compounding / Sheet Moulding Compounding

The Bulk Moulding Compounding (BMC) and the Sheet Moulding Compounding (SMC) are processes that produce the part by heat deformation.

As the designation indicates the main difference of BMC and SMC is in the form of the raw-materials.

BMC´s reinforcements are usually glass fiber chopped to 6 or 12 mm lengths. The filler content is often higher than SMC and the glass fiber content lower.

Figure 2.27 – BMC raw-material (left) and SMC raw-material (right)

Prepreg SMC is made of glass fibers chopped to lengths of 25 or 50 mm sandwiched between two layers of film.

Under pressure and heat the material flows and fills the mould. Parts of varying thickness can be produced, with ribs and bosses.

Compression moulding is currently the most common method for producing these type of composites.
The press should be capable of delivering a pressure of 50- 70 bar over the projected surface area of the tool.

SMC mats are trimmed according to a template, test-weighted, stripped of carrier film and placed in the tool, to cover 60-80% of the projected surface area of the moulding. A BMC composite, on the other hand, may be weighed and placed directly in the press, which is then closed.

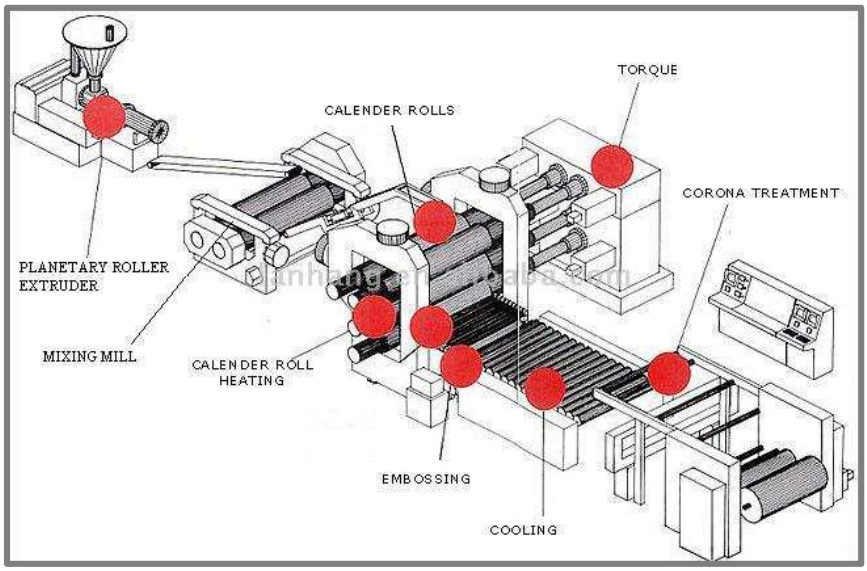

Figure 2.28 – SMC raw-material production line [6]

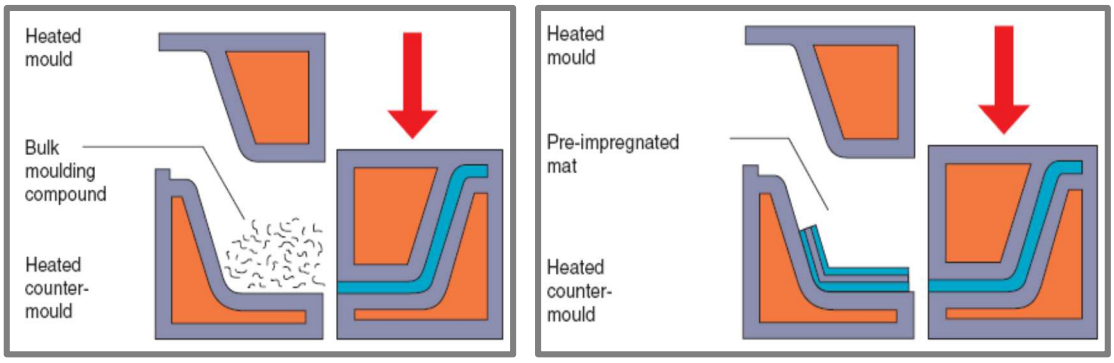

Figure 2.29 - Differences of BMC (left) and SMC (right) compression moulding [28]

One of the main users of compression moulding is the automotive industry, where it is used to produce parts such as body panels.

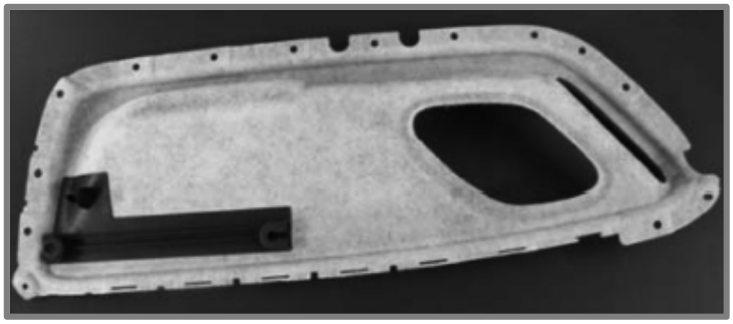

Figure 2.30 – Door inner panel produced by SMC technology [29]

[6] *Courtesy of: Professor Manuel Jorge Dores de Castro, Adjunct Professor at ISEP*

Figure 2.31 – Underbody of a DaimlerChrysler A-Class produced by BMC technology [29]

2.6.6 Injection Moulding

The industry, specially the automotive industry, is always searching for faster productivity allied with safety materials, structural design and economic benefit. In this scenario the plastic materials cannot be ignored.

For structural, or more demanding parts the lower strength and rigidity of the plastic materials [30] turns to a bad handicap.

In order to extend the application area of the plastic materials, polymeric matrix composites are being developed by adding reinforcing materials to the plastic matrix. [30] Due to the fiber strength, the weakness of the net plastic material is overcome.

The FRPs excels in having higher specific strength, higher specific modulus, lower specific gravity and low corrosion, therefore they have become competitive materials in engineering.

The FRP's with thermoplastic matrix can be produce by almost all thermoplastic processes.

Injection moulding presents a set of advantages very attractive to the automotive parts industry, such as, short product cycle, excellent surface of the product and easily molded complicated shapes.

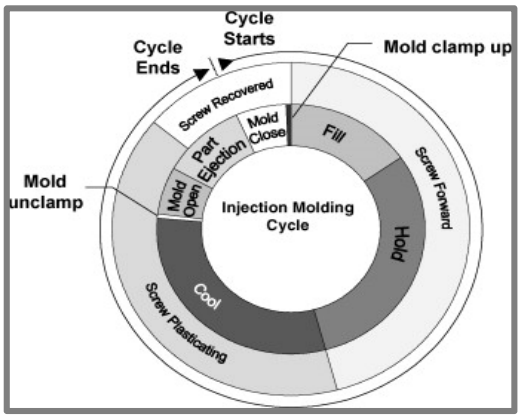

Figure 2.32 – Typical cycle for an injection molding process [31]

Although injection molding is one of the most widely used processes in plastic manufacturing, the characteristics of the product are easily affected by the flow type of the melt, the heat-transfer effect, the material properties and the specific geometry of the mold.

The injection machine is quite simple. All injection molding machines have an extruder for plasticizing the polymer melt. This screw can reciprocate within the barrel to provide enough injection pressure to deliver the polymer melt into the mold cavities.

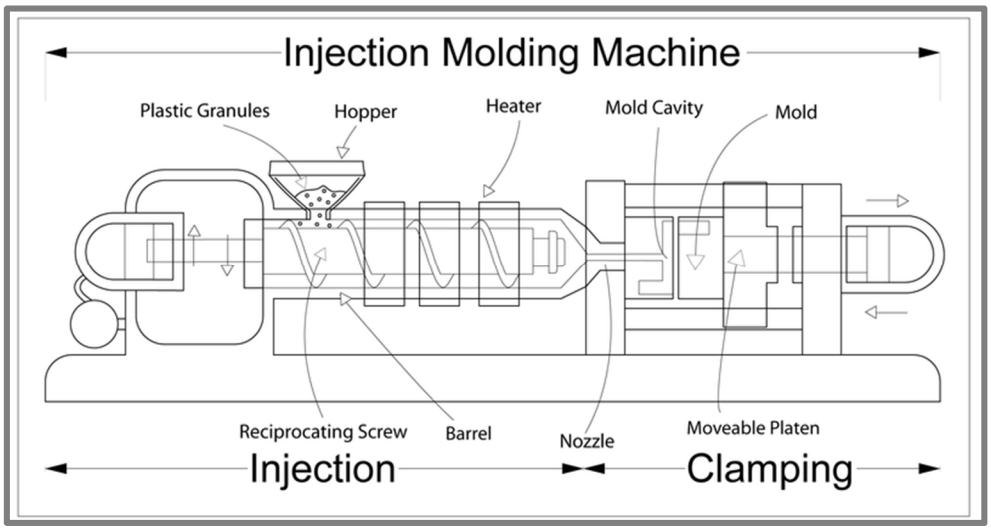

Figure 2.33 - Major components of an injection molding unit [7]

Most injection molding machines for FRPs are based on the reciprocating screw extruder.

Figure 2.34 – Ford Overhead Console produced by injected LFT [32]

[7] *Courtesy of: Professor Manuel Jorge Dores de Castro, Adjunct Professor at ISEP*

References

[1] A.K. Mohanty, M. Misra, and L.T. Drzal, *Natural fibers, biopolymers, and biocomposites*, Boca Raton, FL: Taylor & Francis. (2005)

[2] P. Bordes, E. Pollet, L. Avérous, *Nano-biocomposites: Biodegradable polyester/nanoclay systems*, Progress in Polymer Science, vol. 34, pp. 125-155 (2009)

[3] M.R. Nanda, M. Misra, A.K. Mohanty, *The effects of process engineering on the performance of PLA and PHBV blends*, Macromolecular Materials and Engineering, vol. 296, pp 719-728 (2011)

[4] R. Auras, B. Harte, and S. Selke, *An Overview of Polylactides as Packaging Material,* Macromolecular Bioscience, vol.4, pp. 835-864 (2004)

[5] D. Garlotta, *A literature review of Poly(Lactic Acid)*, Journal of Polymers and the Environment, vol. 9, pp.63-84 (2002)

[6] C. Baillie, *Green composites: polymer composites and the environment*, Boca Raton [etc.] Cambridge: CRC Press Woodhead Publishing. XII, 308 p.-XII, 308 p. (2004)

[7] A.K. Bledzki, A. Jaszkiewicz, *Mechanical performance of biocomposites based on PLA and PHBV reinforced with natural fibres – A comparative study to PP*, Composite Science and Technology, vol. 70, pp. 1687-1696 (2010)

[8] K. Oksman, M. Skrifvars, J.-F. Selin, *Natural fibres as reinforcement in polylactic Acid (PLA) composites*, Composites Science and Technology, vol.63, pp. 1317-1324 (2003)

[9] M.S. Huda, L.T. Drzal, M.Misra, A.K. Mohanty, *Wood-fiber-reinforced Poly(lactic acid) Composites: Evaluation of the Physicomechanical and Morphological Properties*, Journal of Applied Polymer Science, vol. 102, pp. 4856-4869 (2006)

[10] L.M.W.K. Gunaratne, R.A. Shanks, *Multiple melting behavior of poly(3-hidroxybutyrate-co-hydroxyvalerate) using step-scan DSC*, European Polymer Journal, vol.41, pp. 2980-2988 (2005)

[11] K. Sudesh, H. Abe, Y. Doi, *Synthesis, structure and properties of polyhydroxyalkanoates: biological polyesters*, Progress in Polymer Science, vol. 25, pp.1503-1555 (2000)

[12] S. Philip, T. Keshavarz, I. Roy, *Polyhydroxyalkanoates: biodegradable polymers with a range of applications*, Journal of Chemical Technology and Biotechnology, vol. 82, pp. 233-247 (2007)

[13] Y. Xie, D. Kohls, I. Noda, D. Schaefer, Y. Akpale, *Poly(3-hydroxybutyrate-co-3-hydroxyhexanoate) nanocomposites with optimal mechanical properties*, Polymer, vol. 50, pp. 4656-4670, (2009)

[14] H. Sato, Y. Ando, H. Mitomo, Y. Ozaki, *Infrared Spectroscopy and X-ray Diffraction Studies on Thermal Behavior and Lamella Structures of Ploy(3-hidroxybutyrate-co-3-hidroxyvakerate)(P(HB-co-HV)) with PHB-Type Crystal Structure and PHV-Type Crystal Structure*, Macromolecules, vol. 44, pp. 2829-2837 (2011)

[15] A.K. Mohanty, M. Misra, G. Hinrichsen, *Biofibres, biodegradable polymers and biocomposites: An overview*, Macromolecular Materials and Engineering, vol.276/277, pp. 1-24 (2000)

[16] Y. Tokiwa, B. P. Calabia, *Biodegradability and biodegradation of Polyesters*, Journal of Polymers and the Environment, vol. 15, pp.259-267 (2007)

[17] H. Abe, Y. Doi, *Molecular and material design of biodegradable poly(hydroxyalkanoate)s*, Biopolymers 3b, Polyesters II, Wiley-VCH, Weinheim (2002)

[18] K.G. Satyanarayana, G.G.C. Arizaga, F. Wypych, *Biodegradable composites based on lignocellulosic fibers – An overview*, Progress in Polymer Science, vol 34, pp. 982-1021 (2009)

[19] S.S. Cwodhurry, *Poly-β-hydroxybuttersäure abbauende Bakterien und Exoenzym*, Archives of Microbiology. Vol.47, pp.167-200 (1963)

[20] M. Avella, G. La Rota, E. Martuscelli, M. Raimo, *Poly(3-Hydroxybutyrate-co-3-hydroxyvalerate) and wheat straw fibre-composites: termal, mechanical properties and biodegradation behaviour*, Journal of Materials Science, vol. 35, pp. 829-836 (2000)

[21] D.N. Saheb, J.P. Jog, *Natural fiber polymer composites: A review,* Advances in Polymer Technology, vol. 18, pp. 351-363 (1999)

[22] M.J. John, S. Thomas, *Biofibers and biocomposites*, Carbohydrate Polymers, vol.71, pp. 343-364 (2008)

[23] A.R. Campos, G*reenMotion – Transfer of Ecological Materials for the Automotive Industry,* 2nd Journeys of GreenMotion Project, Guimarães, Portugal (2012)

[24] FAO Forestry Paper, *Environmental impact assessment and environmental auditing in the pulp and paper industry*, FAO edition, Rome, Italy (1996)

[25] G. Lubin, S.T. Peters, *Handbook of composites,* Chapman & Hall, London (1998)

[26] F.P. La Mantia, M. Morreale, *Green composite: A brief review*, Composites: Part A, vol.42, pp.579-588 (2011)

[27] G. Koronis, A. Silva, M. Fontul, *Green composites: A review of adequate materials for automotive applications*, Composites: Part B, vol. 44, pp.120-127 (2013)

[28] *Technology update: Compression Moulding*, Reinforced Plastics, vol.47, pp.20-21 (2003)

[29] J. Holbery, D. Houston, *Natural-Fiber-Reinforced Polymer Composites in Automotive Applications*, Journal of the Minerals, Metals and Materials Society, Vol. 58, pp.80-86 (2006)

[30] S. Chang, J. Hwang, J. Doong, *Optimization of the injection molding process of short glass fiber reinforced polycarbonate composites using grey relational analysis*, Journal of Materials Processing Technology, vol. 97, pp. 186-193 (2000)

[31] L.-T. Lim, R. Auras, M. Rubino, *Processing technologies for poly(lactic Acid)*, Progress in Polymer Science, vol. 33, pp. 820-852 (2008)

[32] H. Ramathal, *Unpaited, visible-surface LFT parts for auto interiors*, 10th Annual Automotive Composites Conference & Exhibition, Society of Plastics Engineers-Automotive & Composites Divisions, Michigan, Unites States of America (2010)

[33] J. Summerscales, N. Dissanayake, A. Virk, W. Hall, *A review of blast fibres and their composites. Part 2 - Composites*, Composites Part A: Applied Science and Manufacturing, vol. 41, pp. 1336-1344 (2010)

Chapter 3.

Motivation, Objectives and Research Approach

3.1 Motivation and objectives

The motivation of this work arises the fact that all the OEM's are trying to input more eco-friendly materials into the cars. Although the research on this area is hugh it is focus on natural fibers composites or petrol-based thermoplastics so they can achieved the legal imposed environmental indexes without using the petrol-based polymers.

The use of only one renewable-source polymer will drive us to a much more expensive polymer.

The main objectives of this work are easy to state. It's necessary to develop a new composite material that possesses the minimal properties to replace the petrol-based polymers used into the interior door trims. That new composite must be processed by the usual technological process for manufacturing these type of pieces – injection molding. Allied to that, this new composite material must be biodegradable and must have a renewable-source origin.

3.2 Research Approach

This section describes the research approach used to achieve the goal of this thesis.
As already describe into chapter 2, the PLA is the cheaper biodegradable polymer. However the neat PLA doesn't fulfill all the interior door trims requirements. The blending with PHA tries to reach the mechanical requirements. The PLA/PHA blends have the mechanical capability to replace the used petrol-base polymers but in terms of service temperature stays lower than the required value.
The incorporation of cellulosic fibers will try to improve the service temperature and mechanical behavior.

Once that the idea is to optimize a three material composite, the combinations of the three components can be translated into an enormous sets of samples, tests and data analysis that can take too much time to analyses.

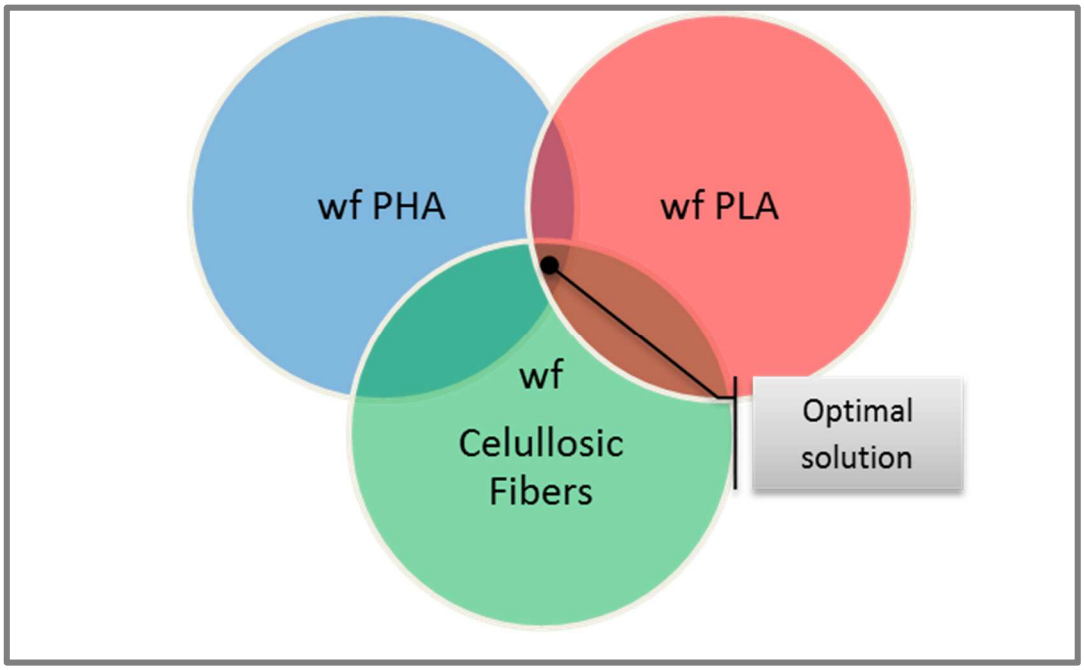

Figure 3.1– Variable interaction for reaching the optimal solution

As possible to conclude by analysis the figure 3.1, to reach to a good substitute of the petrol-based polymers actually in use for interior door trims, it's necessary to make a composite with a polymer blend as a matrix and the correct weight fraction of cellulosic fibers.

The approach that is been chosen starts with a two variable model, and with that the matrix polymer blend will be optimize. After that the weight fraction of fibers will be determined based into a one variable model.

Since the matrix is responsible for the mechanical behavior of the composite the blended polymer matrix will be optimized comparing the mechanical behavior with the mechanical behavior of the actual polymers used into interior door trims.

After that, the thermal behavior will be optimized by the addiction of the fibers.

All the tests were performed taking account the ASTM or ISO standards.

For the matrix, eleven different samples were prepared, with intervals of 10% of variation of the phases, starting in pure PHA samples and ended in the pure PLA samples (PHA/PLA ratios of [100:0] to [0:100]). The values between the ratios were extrapolated from the nearby data.

After chosen the best PHA/PLA ratio, the introduction of the fibers starts with the best PLA/Fiber ratio described in the literature (20% wf) [1] and, after that, a ± 10% fiber weight fiber were tested.

The data extrapolation will give us the best matrix/fiber ratio.

The research approach can be summarized into the next figure.

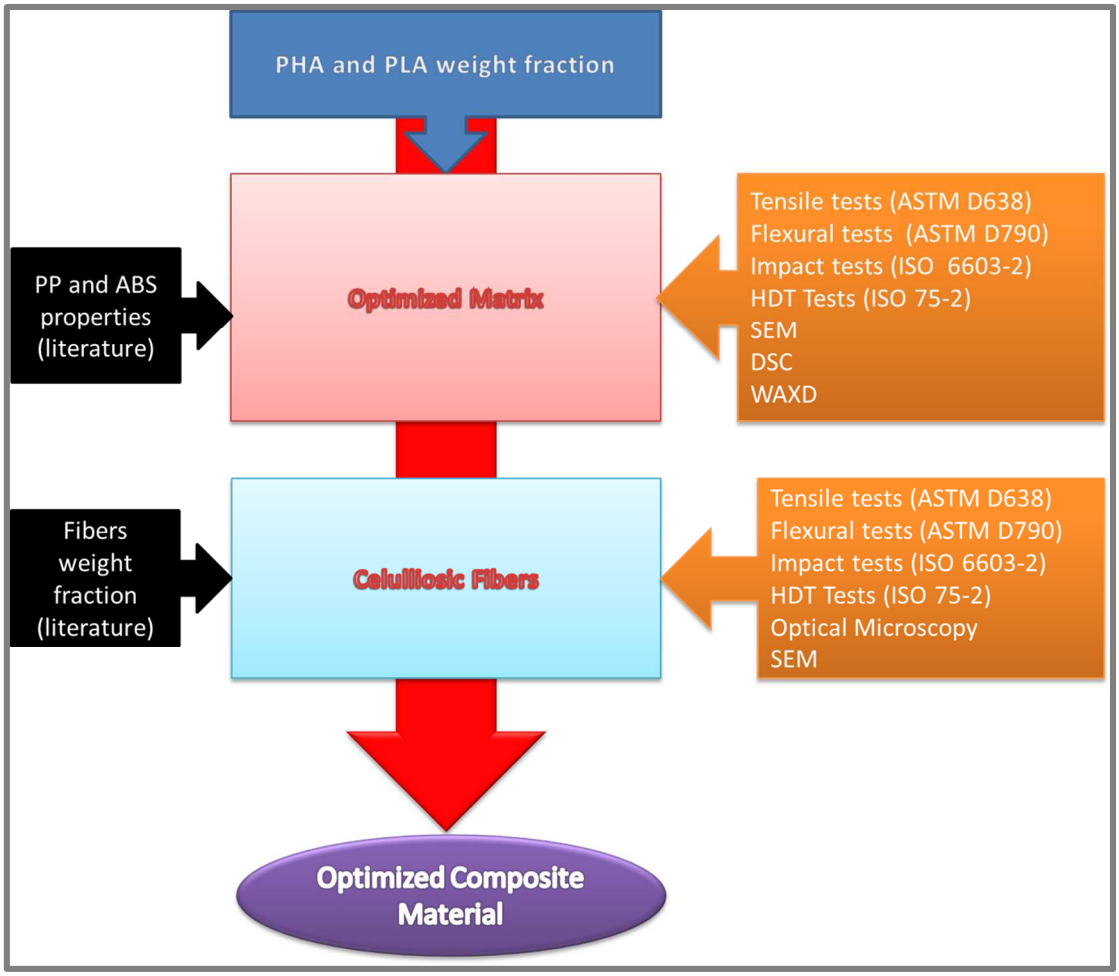

Figure 3.2 – Scheme of thesis research strategy

3.3 Thesis Structure

To reflect all this research work, this thesis starts, in chapter 1, to explain the motivation that energizes all the work.

In chapter 2 it's presented the literature review of all topics that are related with this work and in chapter 3 it is presented the path to reach the final objective.

The used materials and the performed tests and specifications are presented into chapter 4.

Chapter 5 and chapter 6 presents, respectively, the mechanical and morphological characterization of PHA/PLA blends that drives to the selection of the best composite matrix.

Chapter 7 presents the study of the fiber incorporation and the selection of the best matrix/fiber relation.

On chapter 8 the production of a demonstration part is related.

This work ends in, chapter 9, with the final remarks and the indication of some future works that might be done.

References

[1] D. Guimarães, *Efeito das condições de injecção nas propriedades de PLA reforçado com fibras celulósicas*, Master Thesis in Polymer Engineering, University of Minho, Portugal (2009)

Chapter 4.

Materials and Methods

This chapter describes the materials, experimental protocols and characterization techniques used in this thesis.

4.1 Materials

4.1.1 Polyhidroxyalkanoate – PHA

The Polyhydroxyalkanoate used is produced by Natureplast® (France) under the trade name PHI002.

PHI002 is a thermoplastic resin of PHA made from bacterial fermentation and is specifically developed for injection molding. The detailed datasheet can be found in the *Appendix A.1*.

However, the main properties are transcribed into table 4.1

Table 4.1 – PHA Technical data

Melt temperature (ºC)	145 - 155
Degradation temperature (ºC)	200
Tensile Strength at break (MPa)	35
Tensile elongation at break (%)	2
Tensile Modulus (MPa)	2950
HDT A (1,8 MPa) (ºC)	72,5
Density	1,25 (±0,05)
MFI (190 ºC/2.16 kg) (g/600 s)	15-30

4.1.2 Poly(Lactic Acid) – PLA

The Poly(Lactic Acid) used is produced by NatureWorks LLC® (USA) under the trade name INGEO biopolymer 3251D.

INGEO 3251D is designed for injection molding applications. This grade presents a higher melt flow capability and a higher flow capability. The detailed datasheet can be found in the *Appendix A.2*.

However, the main properties are transcribed into table 4.2

Table 4.2 – PLA Technical data

Melt temperature (ºC)	188 - 210
Tensile Strength at break (MPa)	48
Tensile elongation at break (%)	2,5
Density	1,24
MFI (190 ºC/2.16 kg) (g/600 s)	30-40

4.1.3 Cellulosic Fibers

The cellulose fibers used in this work come from the Portucel Kraft paper factory, located in Viana do Castelo and it origin is the *Eucalyptus Globulus* trees.
They have been removed of the production line after the final chemical treatment and before enter in the paper production line, which means that the fibers were bleached and disintegrated.
The bulk fibers are composed essentially of cellulose (~85%) and glucuronoxylan (~15%). The main properties are expressed into table 4.3

Table 4.3 – *Eucalyptus Globulus* fiber general properties [1-2]

Average fiber diameter (µm)	10,9
Average fiber length (mm)	0,66
Tensile Strength at break (MPa)	160
Tensile elongation at break (%)	5,2
Tensile Modulus (GPa)	17,4
Flexural Modulus (GPa)	16
Flexural Strengh at break (MPa)	130
Density	1,6

4.1.4 Preparation of the Blends

The polymers were dried into an oven ate 60ºC for 24 hours before processing and kept into separate Ziploc bags. Just before the injection, the polymers are weighed and then mix into a rotational chamber. When the mixture period ends the blend is injected into a Ferromatik Milacron K85 injection machine, being produced tensile test specimens.

The mold temperature was 20 ºC and the injection temperature profile is described in figure 4.1.

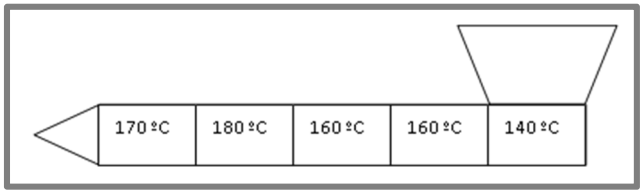

Figure 4.1 – Injection Temperature profile

The temperature profile was established by combining the melting temperature of the polymers, the degradation temperature and the injection molding conditions suggested by the supplier´s datasheets. The other injection parameters were the following: injection velocity: 20 mm/s (corresponding to an injection flow rate of 6,3 cm3/s). Eleven different samples were prepared with intervals of 10wt% of variation of the material´s ratios: PHA/PLA ratio of: [100:0] (pure PHA), [90:10], [80:20, [70:30], [60:40], [50:50], [40:60], [30:70], [20:80], [10:90] and [0:100] (pure PLA).

The blends were injection molded in the form of specimens with dimensions according to the respective standard.

Figure 4.2 – Used tensile specimen injection mold

4.1.5 Preparation of the Composite Material

To prepare the Bio-composite the process used was the same of the preparation of blends.

However before injection it was necessary to extrude the bio-composite and palletize it.

The extrusion takes place into a twin screw Coperion Extruder (Werner & Pfleiderer).

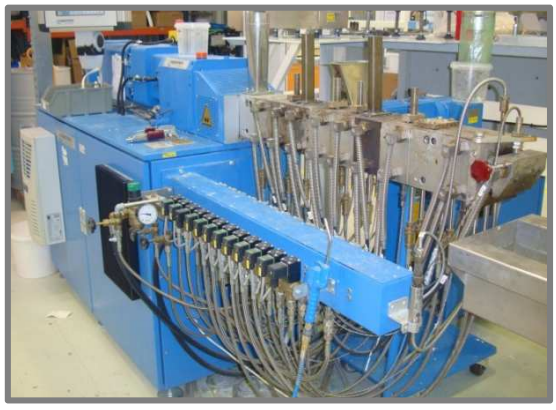

Figure 4.3 – Coperion Extruder

The extruder temperature profile used is expressed into figure 4.4.

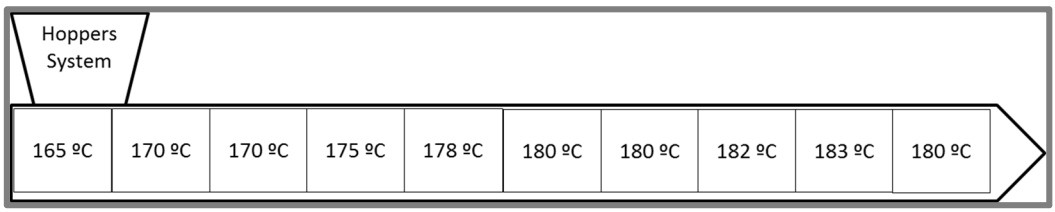

Figure 4.4 – Extruder Temperature Profile

This particular equipment possesses three independent hoppers, one for each component.

Figure 4.5 – Hoppers System

Adjusting the feeding throat of each hopper it's possible to adjust the weight fraction of the extruded composite. The used mass flow rate is expressed into table 4.4.

Table 4.4 – Extrusion flow rates

	Q_{total}	Q_{PHA}	Q_{PLA}	Q_{Fiber}
90% Matrix / 10% Fiber	4 kg/h	1,08 kg/h	2,52 kg/h	0,4 kg/h
80% Matrix / 20% Fiber	4 kg/h	0,96 kg/h	2,24 kg/h	0,8 kg/h
70% Matrix / 30% Fiber	1 kg/h	0,21 kg/h	0,49 kg/h	0,3 kg/h

After the composite extrusion, material goes to extruder incorporated palletizer to be catted and the keep it into Ziploc bags until starts the injection preparation procedure.

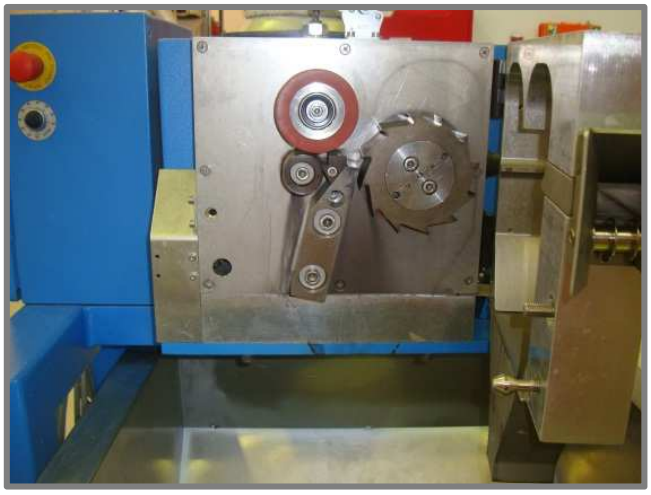

Figure 4.6 – Palletizer cutting System

4.2 Determination of Mechanical Properties

4.2.1 Tensile Test

The measurement of the tensile properties was made according to ASTM D638. For that it has been used a Shimadzu AG-X 10 kN universal testing machine, equipped with a 50 mm extensometer.

Figure 4.7 – Tensile test Apparatus

According to the standard the sample geometry was a type III, with a grip distance of 150 mm. The crosshead velocity was of 5 mm/min and the tests were performed in a standard laboratory atmosphere of 23±2ºC and 50±5% relative humidity.

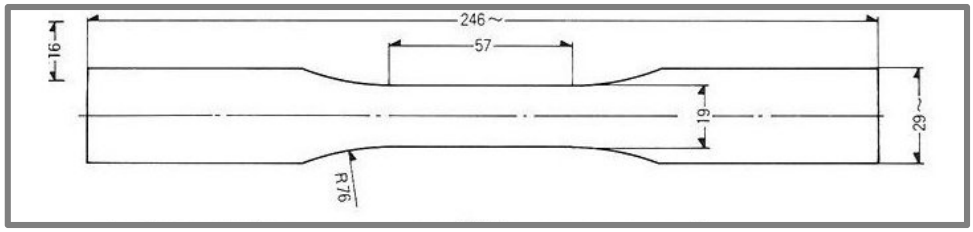

Figure 4.8 – Type III sample dimension [3]

The envisaged tensile properties assessed were the initial modulus, maximum/yield stress and the strain at break.

Also as described into the standard, for each blend composition, at least eleven specimens had been tested.

4.2.2 Flexural Test

The flexural properties were measure according to ASTM D790 standard on a Universal Tiratest 2705 5kN machine. It has been used a 3-point flexural test, with a cross-head velocity of 2,56 mm/min and a spam of 96 mm.

Figure 4.9 – Flexural test apparatus

The specimens have the geometry of a bar with 12x150x6 [mm] [4]. The tests were performed in a standard laboratory atmosphere of 23±2ºC and 50±5% relative humidity, and the envisage flexural properties assessed were the initial modulus, the maximum stress and the strain at maximum stress.

As indicated into the standard, for each blend composition, at least eleven specimens had been tested.

4.2.3 Impact Test

For analyzed the impact behavior, and instrumented impact test, according to ISO 6603-2 standard, were performed into a CEAST fractovis plus impact machine. The drop velocity was 1 m/s wich corresponds to an

impact energy of 12,52 J. All performed tests were carried out in a standard laboratory atmosphere of 23±2 ºC and a 50±5% relative humidity. For each blend 7 specimens, with disc geometry with Ø60x2 [mm] [5], were tested.

Figure 4.10 - impact test apparatus

From the force-displacement curve, the impact toughness was calculated.

4.3 Determination of Thermal Properties

4.3.1 Heat-Deflection Temperature

To measure the Heat-Deflection Temperature, according to ISO 75-2 [6], a RAY-RAN HDT apparatus has been used.

Figure 4.11 - HDT test apparatus

According to the standard, the specimens have the geometry of a bar with 12x150x6 [mm] [6]. The specimens has been submitted to a permanently 3-point stress state of 1,8 MPa while the temperature increases with a velocity of 120ºC/h.

For each blend 5 specimens had been tested.

4.3.2 Differential Scanning Calorimetry

To determine the Glass Transition Temperature and all thermodynamical variables a DSC test were performed, according to ASTM standard. [7]

Figure 4.12 – DSC-SC Diamond Pyris Equipment

It had been use a Perkin-Elmer DSC-SC Diamond Pyris with a thermal cycle represented into the figure 4.13.

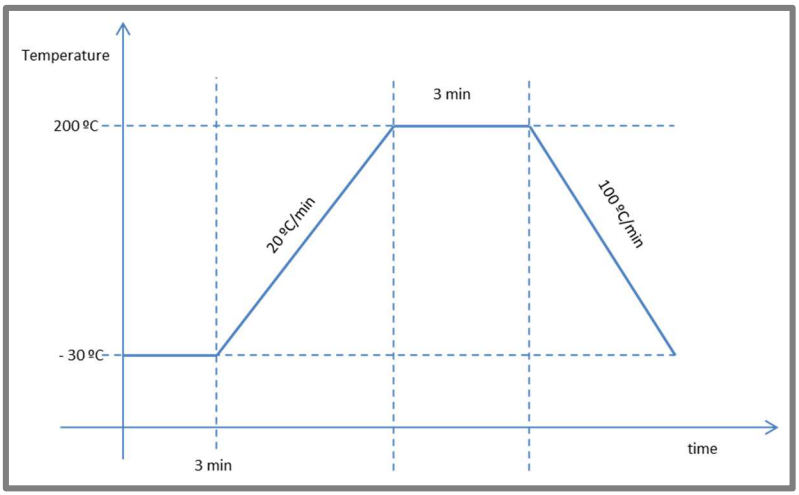

Figure 4.13 - DSC Thermal cycle.

It was tested a sample of about 10 mg of each blend. The samples were sealed into an aluminum pan and all scans were carried out under inert nitrogen.

4.4 Determination of Morphological Properties

4.4.1 Optical Microscopy

To investigate the fiber distribution on the matrix it was used a Axiophot optical microscope from Zeiss equipped with an AxioCam ICc 3.

Figure 4.14 –Optical microscope Axiophot from Zeiss

4.4.2 Wide-Angle X-Ray Diffraction

To investigate the crystal forms of the blends and wide angle X-ray diffraction analysis were carried out into a Bruker D8 Discover X-Ray diffraction, using CuK_{β} radiation operated at 40kV and 40mA. The scattering angle (2Θ) covered was from 5º to 35º ate step of 0,04º and sampling interval of 1 s.

Figure 4.15 –Bruckner D8 Discover WAXD

4.4.3 Scanning Electron Microscopy

An EDAX-Pegasus X4M electronic microscope to observe the different surfaces, which were coated with a thin layer of gold using a Quorum/Polaron E6700 high vacuum evaporator, was used.

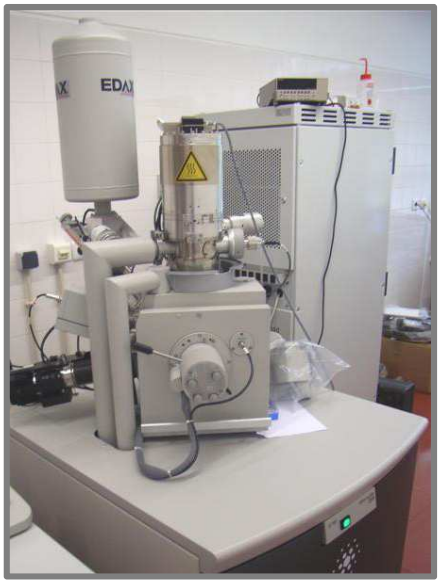

Figure 4.16 –EDAX-Pegasus X4M Electronic Microscope

References

[1] H. Savastano Jr., P.G. Warden, R.S.P. Coutts, *Brazilian waste fibres as reinforcement for cemente-based composites*, Cement & Concrete Composites, vol.22, pp. 379-384 (2000)

[2] V. Agopyan, H. Savastano Jr., V.M. John, M.A. Cincotto, *Developments on vegetable fibre-cement based materials in São Paulo, Brazil: an overview*, Cement & Concrete Composites, vol.27 , pp. 527-536 (2005)

[3] ASTM standard D 638 – 03 *Standard Test Method for Tensile Properties of Plastics* (2010)

[4] ASTM standard D 790 – 10 *Standard Test Method for Flexural Properties of Unreinforced and Reinforced Plastics and Electrical Insulating Materials* (2010)

[5] ISO standard 6603 – 2 *Determination of multiaxial impact behavior of rigid plastics - Part 2: Instrumented puncture test* (2000)

[6] ISO standard 75 - 2 *Determination of temperature of deflection under load - Part 2: Plastics and ebonite* (2004)

[7] ASTM D7426-08 – *Standard Test Method for assignment of the DSC procedure for determining T_g of a polymer or an elastomeric compound* (2008)

Chapter 5.

Mechanical Characterization of PHA/PLA Blends[8]

This chapter presents an investigation about the mechanical behavior of PHA/PLA blends.

The blend mechanical properties can be optimized trough the variation of the PHA contents on the blend. The flexural and tensile properties were estimated by different models: Rule of Mixtures, Kerner–Uemura–Takayanagi model, Nicolai-Narkis model and Béla-Pukánsky model. This aimed at investigating the adhesion between the two material phases. The results anticipate a good adhesion between both polymeric phases when PHA is the disperse phase. For tensile modulus, a linear relationship is found, following the rules of mixtures (or a KUT model with perfect adhesion between phases) denoting a good adhesion between the

[8] *Adapted from N.C. Loureiro, J.L. Esteves, J.C. Viana, S. Ghosh: "Mechanical Characterization of Polyhydroxyalkanoate and Poly(Lactic Acid) Blends", Journal of Thermoplastic Composite Materials (accepted)*

phases over the composition range. The incorporation of PHA in the blend leads to a decrease of the flexural modulus but, at the same time, increases the tensile modulus.

The impact energy varies over 157% over the entire blend composition. For blends with PHA weight fraction lower than 50% the impact strength of the blend is higher than the pure base polymers. The highest synergetic effect is found when the PLA is the matrix and PHA the disperse phase for the blend PHA/PLA of 30/70. The second maximum is found for the inverse composition of 70/30.

PLA has a Heat Deflection Temperature substantially lower than PHA. For the blends, the HDT increases with the increment upon the % of incorporation of PHA. Up to 50% PHA (PLA as matrix), the HDT is practically constant and equal to PLA value. Over this point (PHA matrix), the HDT of the polymer blends increases linearly with % of addition of PHA.

5.1 Mechanical properties prediction models

The mechanical properties of the blends (indicated by subscript b) can be predicted by usual models assuming different interfacial behaviors:

- Well disperse phases with perfect adhesion (rules of mixtures)
- spherical inclusions of one polymer in a continuous polymer matrix with perfect adhesion or no adhesion (KUT model)
- spherical inclusions with variable interphase interactions, ranging from poor to good adhesion (NN model);

These models will be described in the following. They will be used to interpret the adhesion between the polymers phases within the blend.

5.1.1 Rule of Mixtures

The rule of mixtures (ROM) considers perfect adhesion between the matrix (indicated by subscript m) and the dispersed phase (indicated by subscript d) and a perfect dispersion of the spherical inclusions in the matrix. This model can be used to predict the initial modulus and the tensile stress, respectively.

$$E_b = \left(\left[\frac{E_d}{E_m} - 1\right] \times \emptyset_d + 1\right) \times E_m \quad (5.1)$$

$$\sigma_b = \left(\left[\frac{\sigma_d}{\sigma_m} - 1\right] \times \emptyset_d + 1\right) \times \sigma_m \quad (5.2)$$

where E_b is the initial modulus of the blend, E_d is the initial modulus of the disperse phase, E_m is the initial modulus of the matrix, $\emptyset_d$ is the volume fraction of the disperse phase, σ_b is the maximum stress of the blend, σ_d is the maximum stress of the disperse phase, and σ_m is the maximum stress of the matrix.

5.1.2 Kerner-Uemura-Takayanagi model

The Kerner-Uemura-Takayanagi (KUT) model treats the blends as spherical inclusions of one polymer, having an initial module of Ed, in a continuous matrix of another polymer having Em. The Poisson's ratio of the matrix (υm) is taken to be 0,49 [1]. This model has two variations. One assumes perfect adhesion (eq.5. 3) at the blend interface and the other assumes no adhesion. (eq.5.4).

$$E_b = E_m \left(\frac{(7-5\upsilon_m)E_m + (8-10\upsilon_m)E_d - (7-5\upsilon_m)(E_m - E_d)\emptyset_d}{(7-5\upsilon_m)E_m + (8-10\upsilon_m)E_d + (8-10\upsilon_m)(E_m - E_d)\emptyset_d} \right) \quad (5.3)$$

$$E_b = E_m \left(\frac{(7-5\upsilon_m)E_m - (7-5\upsilon_m)(E_m)\emptyset_d}{(7-5\upsilon_m)E_m + (8-10\upsilon_m)(E_m)\emptyset_d} \right) \quad (5.4)$$

5.1.3 Nicolais-Narkis model

In the Nicolais-Narkis (NN) model, the interphase interaction constant – K - is a function of the blend structure. For spherical inclusions, K= 1.21 stands for the extreme case of poor adhesion; interphase adhesion takes place for values of K < 1.21. When K=0, the adhesion is sufficient so that the polymer matrix strength will not decrease, that is, $\sigma_b = \sigma_m$ That means that the better adhesion appears when K is low[1].

The NN model assumes that both phases are of a no-adherent type and the maximum stress is a function of either the area fraction or the volume fraction of the dispersed phase. The NN model is given by:

$$\sigma_b = \left(1 - K\emptyset_d^{2/3}\right) \times \sigma_m \quad (5.5)$$

In this work, the calculation of K values by adjustment of equation 5.5 to the experimental data gives a measure of the adhesion between both phases.

5.1.4 Béla-Pukánsky model

In the Béla-Pukánsky (BP) model, the maximum tensile stress of the blend is determined by the maximum stress of the matrix, the volume fraction of the dispersed phase and the effective load-bearing cross section:

$$\boldsymbol{\sigma_b = \sigma_m \left(\frac{1 - \emptyset_d}{1 + 2.5\emptyset_d} \right) e^{(B\emptyset_d)}} \quad (5.6)$$

B is a parameter that relates the load-bearing capacity of the disperse phase and depends on the size of the contact surface between the polymer and the disperse phase and on the properties of the interphase that is formed. The lower the B parameter the lower is the phase´s adhesion (i.e., no-adhesion case). The highest B is, the better is the adhesion between phases. The aggregation decreases the surface available for the polymer, and therefore drives a decreasing of the value of B. [1]

The calculation of this factor allows the estimation of the load-bearing capacity of the dispersed phase in the blend.

Table 5.1 resumes the models adopted in this work and the information that they give for the interpretation of the blend structure.

Table 5.1 – Models used in this work to interpret blend structure.

Model	Eq.	Blend structure	Interpretation	Use
ROM	(5.1) (5.2)	Spherical polymer inclusions in a continuous polymer matrix with perfect adhesion	perfect adhesion and dispersion	Fit to the model for E and σ
KUT	(5.3) (5.4)	Spherical polymer inclusions in a continuous polymer matrix with perfect adhesion or no adhesion	a) perfect adhesion b) no adhesion	Fit to the model for E
NN	(5.5)	Spherical inclusions with variable interphase interactions, ranging from poor to good adhesion	K - interphase interaction constant, function of the blend structure	K adjustment for σ values: K= 1.21 – no adhesion K < 1.21 – phase´s adhesion K=0 – no property decrement
BP	(5.6)	Blend stress determined by the matrix stress, dispersed phase volume fraction and the effective load-bearing cross section	B - load-bearing capacity of the disperse phase. It depends on the size of the contact surface and interphase properties	B adjustment (for σ values): Lowest B means lower adhesion Highest B means better adhesion

5.2 Mechanical Testing

5.2.1 Flexural Properties

A Universal Tiratest 2705 5kN Machine was used to measure the flexural properties according to ASTM D790 standard. It has been used a 3-point flexural test, with a crosshead speed of 2,56 mm/min and a spam of 96 mm. Tests were performed at room temperature (23 ºC). The envisaged flexural properties assessed were the initial modulus, the maximum stress and the strain at maxim stress. At least 11 specimens were tested for each blend composition.

5.2.2 Tensile Properties

To measure the tensile properties according to ASTM D638, a universal mechanical testing machine Shamidzu AG-X 100kN, equipped with a 50 mm Shamidzu extensometer, was used. The crosshead velocity used was of 5

mm/min and the testes were performed at room temperature (23 ºC). A grip distance of 150 mm was used. The envisaged tensile properties assessed were the initial modulus, the maximum/yield stress and the strain at break. At least 11 specimens were tested for each blend composition.

5.2.3 Instrumented Properties

Instrumented impact tests are performed according ISO 6603-2 standard in a CEAST Fractovis plus pendulum impact machine (velocity of 1 m/s). All performed tests were carried out in a standard laboratory atmosphere of 23±2ºC and 50±5% relative humidity. From the force-displacement curve, the impact toughness was calculated. The impact data presented are the average of 7 measurements.

5.2.4 Heat Deflection Temperature (HDT) Measurements

To measure the Heat Deflection Temperature, HDT, according to ISO 75-2, RAY-RAN HDT apparatus was used. This test used the method HDT A with a stress state of 1,8 MPa and an increasing temperature speed of 120ºC/h. The tests were carried out in a standard laboratory atmosphere of 23±2 ºC and 50±5 % relative humidity. The presented HDT results are the average values of three measurements.

5.3 Results and Discussion

The results of the tensile tests of the PHA/PLA blends are given in Table 5.2.

Table 5.2 – Tensile properties of PHA/PLA blends

PHA/PLA Blend [Mass Fraction]	Tensile Modulus [GPa]	Maximum Stress [MPa]	Strain at maximum Stress [%]
[0:100]	3,62 ± 0,03	59,17 ± 0,7	2,5 ± 0,03
[10:90]	3,15 ± 0,21	51,35 ± 1,0	2,4 ± 0,07
[20:80]	3,32 ± 0,06	43,61 ± 0,6	2,0 ± 0,13
[30:70]	3,36 ± 0,07	46,02 ± 1,5	2,0 ± 0,06
[40:60]	3,63 ± 0,05	43,19 ± 0,6	1,9 ±0,10
[50:50]	3,55 ± 0,05	40,36 ± 4,1	1,7 ± 0,39
[60:40]	3,62 ± 0,06	43,02 ± 0,4	1,9 ± 0,02
[70:30]	3,69 ± 0,08	39,21 ± 0,4	1,8 ± 0,06
[80:20]	3,73 ± 0,25	35,99 ± 5,6	1,6 ± 0,26
[90:10]	3,74 ± 0,11	28,04 ± 3,7	1,3 ± 0,14
[100:0]	3,81 ± 0,12	29,19 ± 0,2	1,6 ± 0,19

Based on the predictive models, the estimated mechanical properties are presented in Table 5.3.

Table 5.3 – Predicted Tensile Modulus

PHA/PLA Blend [Mass Fraction]	Tensile Modulus [GPa]		
	ROM	KUT perfect adhesion	KUT no adhesion
[0:100]	3,62	3,62	3,62
[10:90]	3,64	3,64	3,06
[20:80]	3,66	3,66	2,56
[30:70]	3,68	3,68	2,11

[40:60]	3,70	3,70	1,72
[50:50]	3,72	3,72	1,43
[60:40]	3,73	3,73	1,80
[70:30]	3,75	3,75	2,22
[80:20]	3,77	3,77	2,69
[90:10]	3,79	3,79	3,21
[100:0]	3,81	3,81	3,81

Fig.5.1 shows the evolution of the initial modulus with the PHA weight fraction, based on the data from tables 5.2 and 5.3.

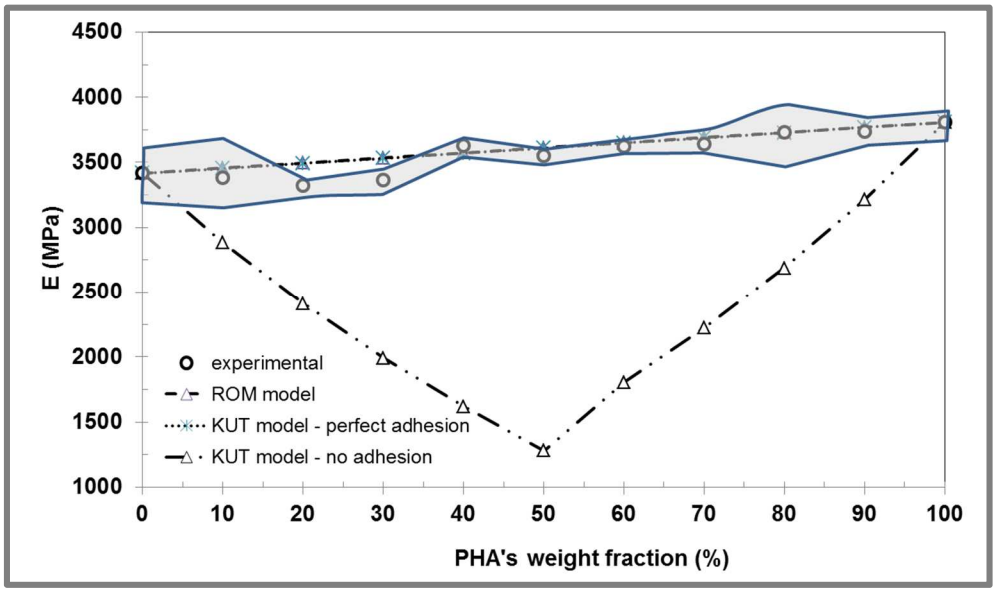

Figure 5.1 –Tensile initial modulus results and predicted values from models

The increase of PHA on the blend results in a general increase of the initial tensile modulus. This is expected since the initial modulus of PHA is slightly higher than PLA. In Figure 5.1 are also presented the predictions of E based on the abovementioned models: ROM and KUT models with perfect and no adhesion between phases. Two main issues can be withdrawn**:** i) the KUT model with no adhesion does not give good predictions of E; ii) the ROM and KUT model with perfect adhesion both give good predictions of the variation of E with the weight faction of PLA in the blend. The maximum deviation between the KUT perfect adhesion prediction and the experimental value is about 5 %. These results anticipate a good adhesion between both phases in the PHA/PLA blends. Nevertheless, for low levels of incorporation of PHA (up to 30%), where PLA is expectantly the matrix, the experimental data seems to deviate from the perfect adhesion models, suggesting a decrease on the adhesion between both polymeric phases when PHA is the disperse phase.

The maximum stress of the blends can be estimated from the above presented prediction models. From the NN and BP models, the parameters K and B can be calculated giving estimations of the interphase interaction and of the load-bearing capacity of the disperse phase, respectively. The calculated values are expressed in Table 5.4 for each blend.

Table 5.4 – Calculated Values for K and B for PLA/PHA blends

PHA/PLA Blend [Mass Fraction]	K (NN model)	B (BP model)
[10:90]	0,55	2,0

[20:80]	0,74	1,7
[30:70]	0,47	2,3
[40:60]	0,48	2,3
[50:50]	0,49	2,3
[60:40]	0,37	4,0
[70:30]	0,42	4,0
[80:20]	0,44	4,2
[90:10]	0,56	2,9
AVERAGE	0,50	2,1 (PLA Matrix) 3,8 (PHA Matrix)

Figure 5.2 shows the variation of K and B with the weight fraction of PHA. K values are always lower than 1.21, meaning that a good adhesion between both phases is achieved. The values of B parameter are also relatively high, indicating a good adhesion between phases. Furthermore, in the PLA fraction 50-60% the values of K show a drop and that of B a sudden increment, which can be attributed to phase inversion in the blends. Again, for the low levels of incorporation of PHA (PHA as disperse phase) the K values are higher indicating a lower adhesion between both phases when PLA is the matrix. For this dilution regime, the B values are lower, indicating a lower load-bearing capacity of the PHA disperse phase, also due to the low tensile strength of this phase.

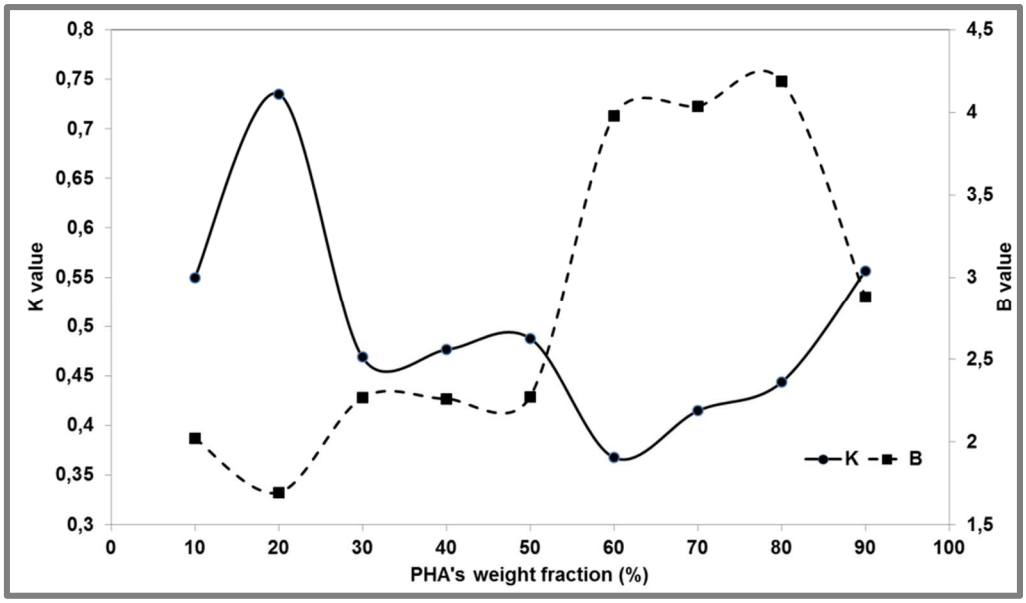

Figure 5.2 –Variations of K and B parameters of NN and BP models with weight fraction of PHA

In Table 5.5 are presented the predictions of the tensile stress for ROM, NN (with different K values) and BP (with average B value) models for the various PHA/PLA mass fractions. For percentages of incorporation of PHA higher than 60% (PLA as matrix), the NN and BP models do not give good agreement with experimental data.

Table 5.5 – Models predictions of Maximum Stress

PHA/PLA Blend [Mass Fraction]	Maximum Stress [MPa]				
	ROM	NN			BP
		K=0	K=0,5	K=1,21	B=2,3
[0:100]	59,17	58,26	58,26	58,26	58,26
[10:90]	56,17	58,26	51,98	43,07	52,79
[20:80]	53,17	58,26	48,29	34,15	49,22

[30:70]	50,18	58,26	45,20	26,67	46,46
[40:60]	47,18	58,26	42,44	19,99	43,85
[50:50]	44,18	58,26	39,91	13,85	40,89
[60:40]	41,18				
[70:30]	38,19				
[80:20]	35,19				
[90:10]	32,19				
[100:0]	29,19				

Fig. 5.3 shows the variations of the tensile maximum stress with % of PHA and respective models predictions.

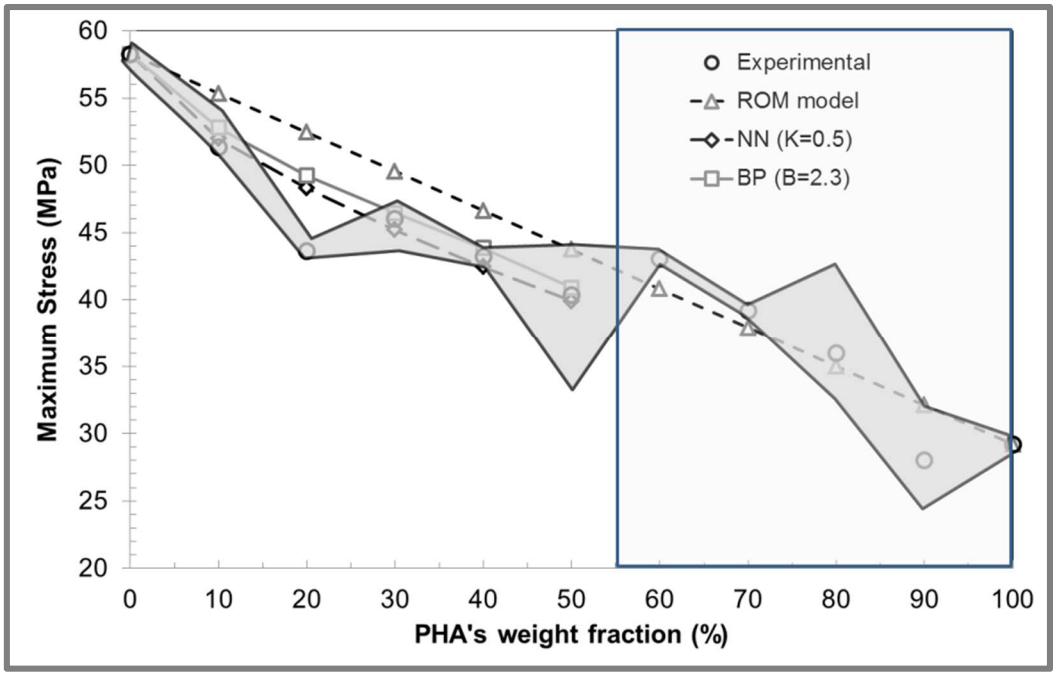

Figure 5.3 – Tensile Maximum Stress Results and Predicted Values

The increase of PHA on the blends drives to a general decreasing of the Maximum Stress. The ROM fits well with the experimental data for the larger amounts of incorporation of PHA, suggesting a very good adhesion between PHA matrix and the PLA disperse phase. For low % of PHA the phase adhesion is small, the experimental data deviates from ROM. In this regime, the values of K and B were adjusted in order to fit better the models predictions. Values of K = 0,5 and B=2,3 were found up to %PHA of 50% (above this value, a best fit is obtained for K=-1,2 and B=4,0). These values regarding both NN and BP models corroborate that the interphase adhesion is promoted when PLA is the disperse phase.

The flexural test results of the blends are given in Table 5.6.
The experimental variation of the flexural module as function of the PHA fraction is small, of 3,52%.

Table 5.6 – Flexural Properties of PHA/PLA blends

PHA/PLA Blend [Mass Fraction]	Flexural Modulus [GPa]	Maximum Stress [MPa]	Strain at maximum Stress [%]
[0:100]	3,59± 0,06	80,52 ± 2,6	2,3 ± 0,1
[10:90]	3,41 ± 0,08	57,36 ± 3,1	2,2 ± 0,1
[20:80]	3,46 ± 0,06	70,87 ± 4,7	2,6 ± 0,2
[30:70]	3,53 ± 0,02	62,30 ± 7,1	2,1 ± 0,4

[40:60]	3,79 ± 0,01	55,31 ± 2,6	1,6 ± 0,1
[50:50]	3,61 ± 0,08	79,93 ± 2,4	3,1 ± 0,1
[60:40]	3,56 ± 0,11	46,49 ± 3,0	1,3 ± 0,1
[70:30]	3,42 ± 0,03	66,10 ± 0,6	2,4 ± 0,1
[80:20]	3,42 ± 0,10	47,32 ± 2,9	1,5 ± 0,1
[90:10]	3,44 ± 0,22	53,94 ± 3,5	2,2 ± 0,4
[100:0]	3,40 ± 0,10	53,97 ± 0,6	2,2 ± 0,1

Fig.5.4 shows the variations of E_f with % of PHA and respective models predictions. Conversely, to the tensile modulus, here for the flexural modulus the ROM does not applies over the full range of compositions. Only for high % of incorporation of PHA (as matrix), the ROM is valid. In the case of PHA as disperse phase, the variations of E_f with PHA fraction are not conclusive. The E_f of the blends seems to be more sensitive to the morphology of the low fraction component (e.g., dispersion, size, aspect ratio).
Also, ROM and KUT-adhesion models give the same predictions of E_f as function of PHA fraction, with maximum error of 7.9% (an average of 2.1%).

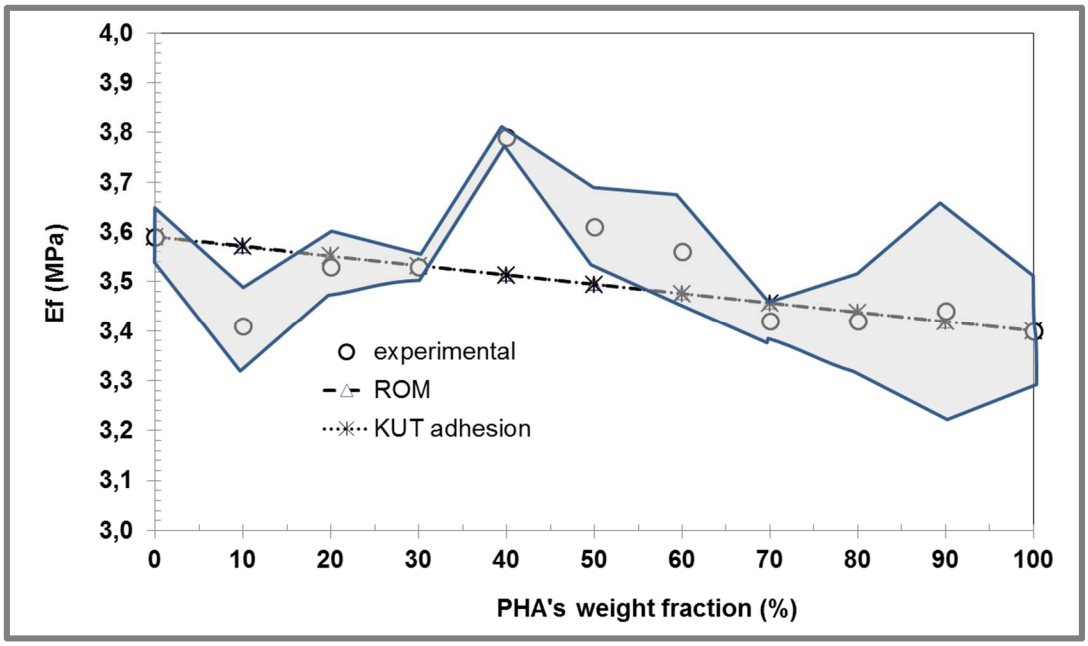

Figure 5.4 - Flexural Young's Modulus Results and Predicted Values.

Fig. 5.5 shows the variations of maximum flexural stress with % of PHA and respective models predictions. Again, the increase of PHA on the blends drives to a general decreasing of the Maximum Stress. As for the flexural modulus, the variations of σ_{max} with % of PHA are subjected to high fluctuations. In general, the ROM does not give satisfactory predictions, even for larger amounts of incorporation of PHA. For low % of PHA the experimental values are always smaller than the ones predicted by ROM, this evidencing a low level of adhesion between both phases. This also happened in the tensile response: when PHA is the disperse phase, the adhesion is small. In this regime, the values of K and B were also adjusted in order to fit better the models predictions. Values of K = 0,48 and B=2,2 were found up to %PHA of 50% for both NN and BP models, respectively. These values are very close to the obtained on the tensile tests (K = 0,45 and B=2,3). Adjustments for the case of PLA as disperse phase, gives K= 0,22 and B=2,6. The K value is reduced substantially when compared with PHA as disperse phase, this meaning a better adhesion between phases; B slightly increases as a reflex of this better adhesion, but the load-bearing capacity of the disperse phase seems to remain

unchanged. When comparing with the tensile test results of k=-1.2 and B=4.0, it seems that under flexural loading the adhesion and load-bearing capacity of the PLA disperse phase are much smaller than for the case of tensile loading.

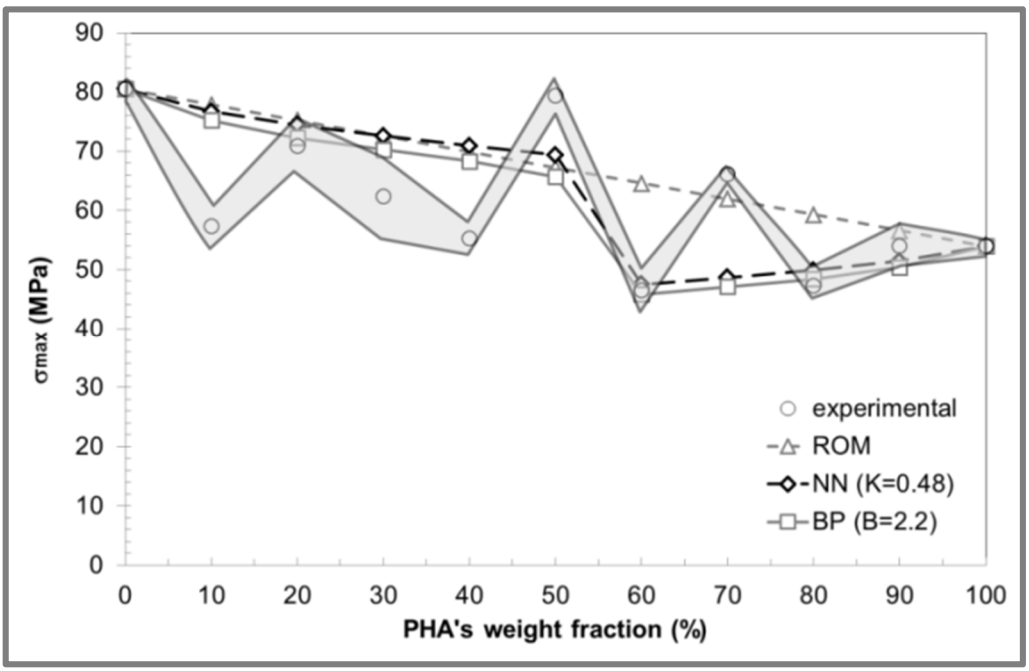

Figure 5.5 - Flexural Maximum Stress Results and Predicted Values.

The impact results of the tested blends are given in Table 5.7. As an example figure 5.6 presents the Impact Force during time for the blends 70:30 and 30:70 [PHA:PLA]. The latter blend shows higher impact force levels, but lower deformation capability.

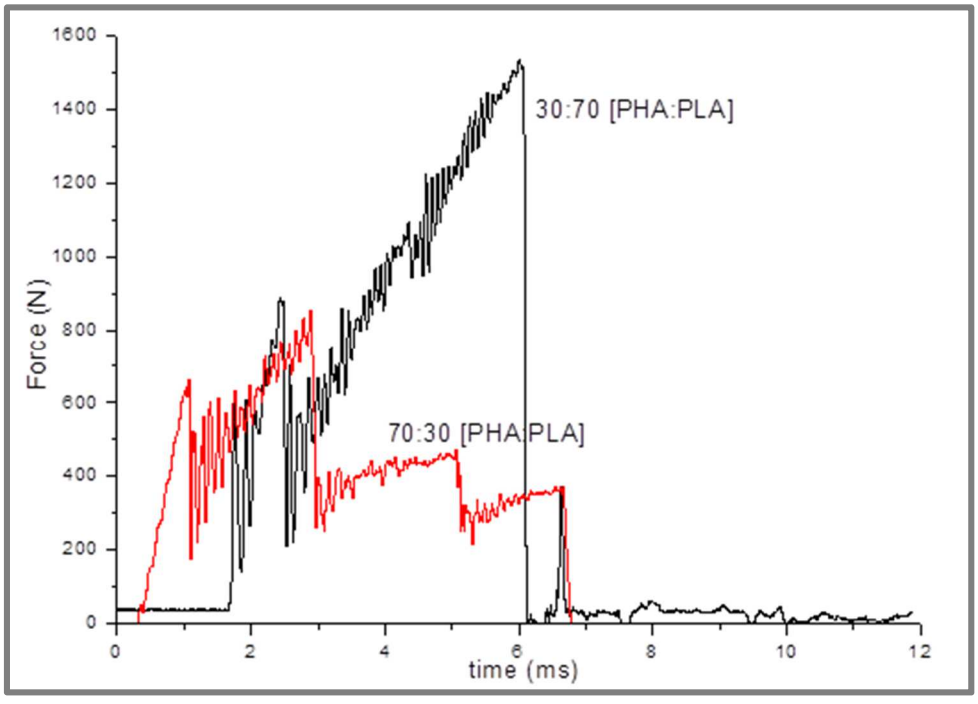

Figure 5.6 – Impact results of the 30:70 and 70:30 [PHA:PLA] blends.

The impact energy establishes the amount of energy that the material can absorbed until it breaks. In the same table 5.7 are also shown the deflection at break.

Table 5.7- Impact Properties of PHA/PLA blends.

PHA/PLA Blend [Mass Fraction]	Impact Energy [J]	Elongation at break [mm]
[0:100]	3,8 ± 0,1	3,6 ± 0,1
[10:90]	4,7 ± 0,2	6,5 ± 1,4
[20:80]	6,1 ± 0,1	6,8 ± 0,7
[30:70]	6,7 ± 0,3	7,9 ± 1,4
[40:60]	6,1 ± 0,2	7,3 ± 1,3
[50:50]	4,9 ± 0,0	6,7 ± 1,6
[60:40]	2,6 ± 0,3	2,7 ± 1,0
[70:30]	3,0 ± 0,1	4,3 ± 1,0
[80:20]	4,2 ± 0,5	3,8 ± 0,9
[90:10]	3,2 ± 0,3	1,9 ± 0,0
[100:0]	3,4 ± 0,1	2,8 ± 0,4

The impact energy varies over 157.7% over the entire blend composition. This is quite surprisingly has both neat polymers show quite similar impact energies (PLA has a higher value of c.a. 12%). Fig. 5.7 shows the variations of the impact energy with blend composition. Two local maximum can be found corresponding to different types of matrices. Phase inversion appears to occur for 50-60% of PHA, as already mentioned. But under impact conditions this is more evident. It is also interesting to observe that for blends with PHA weight fraction lower that 50% (i.e., PLA matrix and PHA as disperse phase) the impact strength of the blends is substantially higher than the pure base polymers. The highest synergetic effect is found when the PLA is the matrix and PHA the disperse phase for the blend PHA/PLA of 30/70. The second maximum is found for the inverse composition of 70/30.

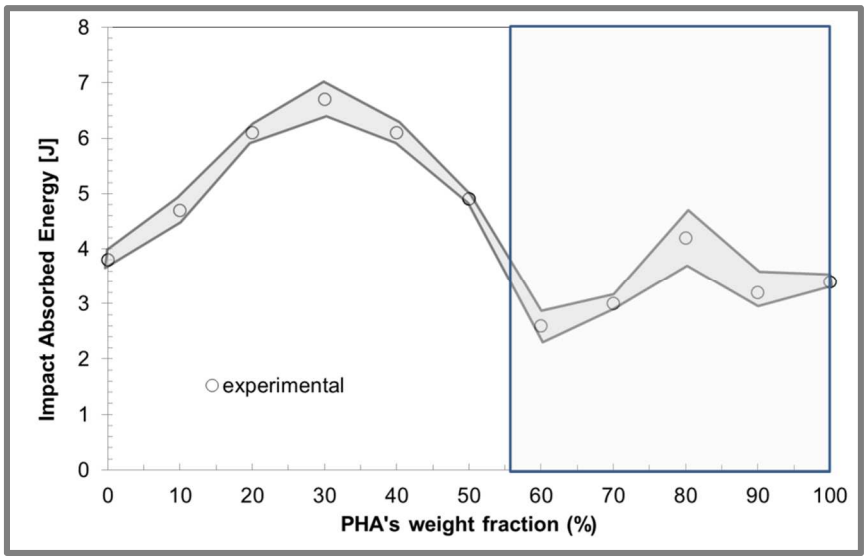

Figure 5.7 – Impact Strength (Experimental)

The toughening of polymer blends has been related to the ligament thickness, i.e., the distance between the disperse phase particles. This ligament thickness is dependent upon the amount of disperse phase and the diameter of the filled particles.

The variations of the elongation at break with blend composition shows a similar evolution as the impact energy, as depicted in Fig. 5.8.

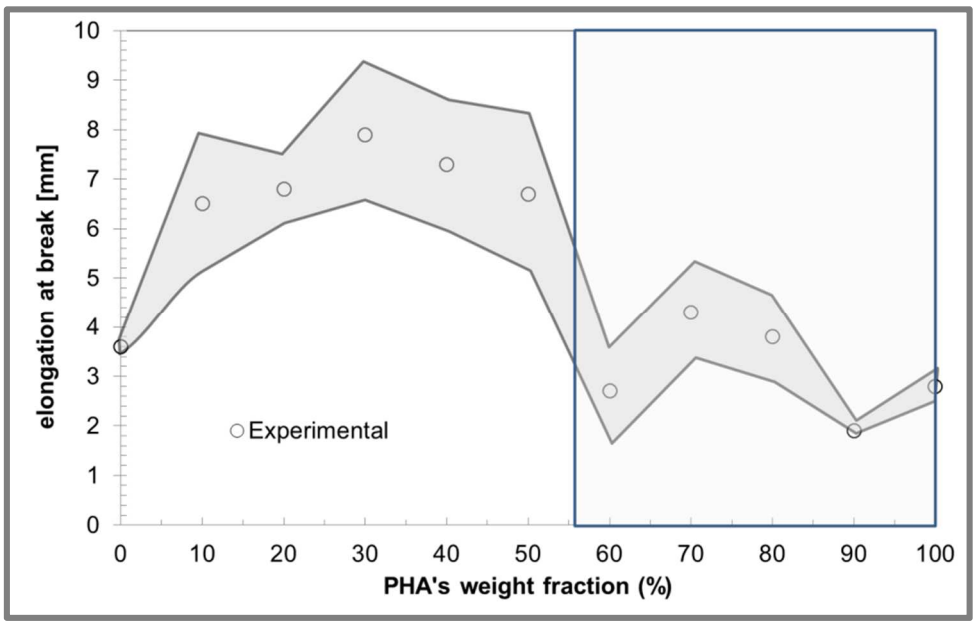

Figure 5.8 – Impact elongation at break (Experimental).

The impact elongation at break varies over 315.8% over the entire blend composition. Again, this is quite surprisingly, as PLA shows an elongation at break only 28,6% higher than PHA**.** Noda et al.[2] have reported a similar effect of the addition of PHA to PLA and observed that when 10% PHA was added to PLA, the percent elongation of the blends improved significantly. This was attributed to the increase of the amorphous phase of the blend. The maximum elongation was observed for the [PHA:PLA] 70:30 weight fraction, where the elongation was 119 and 182% higher than that of neat PLA and PHA, respectively.

The Heat Deflection Temperature (HDT) results are given in Table 5.8 and Fig. 5.9 for all blend compositions.

Table 5.8- Heat Deflection Temperature of PHA/PLA blends.

PHA/PLA Blend [Mass Fraction]	HDT [ºC]
[0:100]	61,4 ± 0,7
[10:90]	60,8 ± 0,5
[20:80]	60,1 ± 0,6
[30:70]	62,1 ± 0.3
[40:60]	61,3 ± 1,0
[50:50]	64,0 ± 0,6
[60:40]	71,2 ± 1,7
[70:30]	74,0 ± 0,5
[80:20]	80,1 ± 1,1
[90:10]	89,6 ± 0,4
[100:0]	92,0 ± 1,8

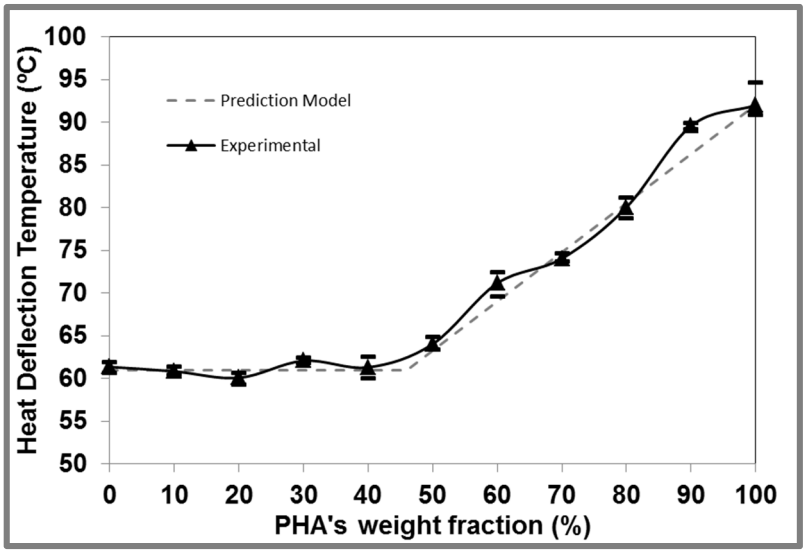

Figure 5.9 – Experimental and predicted HDT Evolution

PLA (61,4 ºC) has a HDT substantially lower than PHA (92,0 ºC). For the PHA/PLA blends, the HDT increases with the increment upon the % of incorporation of PHA. Up to 50% PHA (PLA as matrix), the HDT is practically constant and equal to PLA value. Over this point (PHA matrix), the HDT of the polymer blends increases linearly with % of addition of PHA.

This behavior is dependent upon the amount of disperse phase. It's possible to verify, as seen in the other tests, that around 50%PHA a phase inversion occurs and the thermal behavior changes. For weight fractions of PHA lower than 50% the PLA is the matrix and dictates the HDT value. When the PHA becomes the matrix of the blend (above 50% wf) the HDT increases near to the neat PHA value.
Composition determines the behavior of the PHA/PLA blends, as expected. It also affects the morphology development of both phases with consequences upon the response of the blends. Next work will report the effect of composition upon the developed morphologies of the blends.

5.4 Conclusions

The properties of biodegradable polymers such as PHA and PLA can be tailored to achieve a given performance. PHA/PLA blends over the full ratio of compositions were investigated in this work. The blends were injection molded and their mechanical (tensile, flexural and impact) and thermal (HDT) behavior was assessed. The increment of PHA fraction decreases both the tensile and flexural moduli of the blends. For the tensile modulus, a linear relationship is found, following the rules of mixtures (or a KUT model with perfect adhesion between phases) denoting a good adhesion between the phases over the composition range. Conversely, for the flexural modulus, the ROM does not apply over the full range of compositions, and only for high % of PHA the ROM models become valid and evidencing good phase adhesion. E_f of the blends seems to be more sensitive to the morphology of the low fraction component (e.g., dispersion, size, aspect ratio) than the tensile one.
The incorporation of PHA in the blend leads to a decrease of the flexural modulus but, at the same time, increases the tensile modulus. The maximum stress of the blends can be estimated from the presented prediction models.

Prediction models and material property characterization allowed unambiguous detection of the interfacial behavior of the polymer blends.

PHA/PLA blends can have good impact properties. The best impact properties are achieved with a [PHA:PLA] 70:30 weight fraction ratio blend. The highest synergetic effect on impact is found when PLA is the matrix and PHA the disperse phase.

Up to 50% PHA (PLA as matrix) the HDT is practically constant and equal to PLA value. Over this point (PHA matrix), the HDT of the polymer blends increases linearly with % of addition of PHA.

References

[1] C.L. Simões, J.C. Viana, A.M. Cunha*, Mechanical Properties of Poly(e-caprolactone) and Poly(lactic acid) Blends*, Journal of Applied Polymer Science, vol. 112, pp. 345-352 (2009)

[2] I. Noda, M. M. Satkowski, A. E. Dowrey, C. Marcott, *Polymer Alloys of Nodax Copolymers and Poly(lactic acid),*Macromolecular Bioscience,vol.4, pp.269-275 (2004)

[3] M.R. Nanda, M. Misra, A.K. Mohanty, *The effects of process engineering on the Performance of PLA and PHBV Blends,* Macromolecular Materials and Engineering, vol. 296, pp. 719-728 (2011)

[4] R. Auras, B. Harte, S. Selke, *An Overview of Polylactides as Packaging Materials*, Macromolecular Bioscience, vol.4, pp.835-864 (2004)

[5] N.C. Loureiro, J.L. Esteves, J.C. Viana, *Caracterização Mecânica de Misturas PLA/ABS*, Proceedings of ENMEC'2010 – Encontro Nacional de Materiais e Estruturas Compósitas (2010)

[6] C. Baillie, *Green composites: Polymer composites and the environment*, edited by Woodhead Publishing (2004)

[7] N.C. Loureiro, J.L. Esteves, J.C. Viana, *Mechanical Characterization of PLA/PHA Blends,* Proceedings of ICCS'16 – 16th Internacional Conference on Composite Structures (2011)

[8] Z. Bartczak, A.S. Argona, R.E. Cohena, M. Weinberg, *Toughness Mechanism in Semi-Crystalline polymer blends: II. High-density polyethylene toughened with calcium carbonate filler particles,* Polymer, vol.40,pp.2347-2365 (1999)

[9] T. Gérard, T. Budtova, *PLA-PHA Blends: Morphology, thermal and mechanical properties,* Proceedings of BIOPOL'2011 – International Conference on Biodegradable Polymers (2011)

[10] P.K. Bajpai, I. Singh, J. Madaan, *Characterization of PLA based 'Green' Composites: A review*, Journal of Thermoplastic Composite Materials (2012)

[11] P.K. Bajpai, I. Singh, J. Madaan, *Comparative Studies of Mechanical and Morphological Properties of PLA and PP-based Natural Fibers Composites*¸ Journal of Reinforced Plastics and Composites, vol. 31, pp. 1712-1724 (2012)

[12] J. P. Mofokeng, A.S. Luyt, T. Tábi, J. Kovács, *Comparison of injection moulded natural fibre-reinforced composites wuth PP and PLA as matrices*, Journal of Thermoplastic Composite Materials, vol.25, pp. 927-948 (2012)

[13] M. Avella, A. Buzarovska, M.E. Errico, G. Gentile, A. Grozdanov, *Eco-challenges of bio-based Polymer Composites,* Materials, vol.2, pp.911-925 (2009)

Chapter 6.

Morphological Characterization of PHA/PLA Blends[9]

6.1 Introduction

Poly (lactic acid), PLA, is a polymer produced by the fermentation of simple sugars, such as glucose and maltose from corn or potato, sucrose from cane or beet sugar and lactose from cheese [1]. It's a linear aliphatic polyester thermoplastic used as packaging materials and in production of cloths, carpet tiles, surgical and biomedical devices among others. The PLA has a melting temperature ranging from 188º a 210 ºC, and the glass transition temperature, Tg, of 55-60 ºC (these temperatures are dependent upon the optical composition, the primary structure, the molecular weight, and the thermomechanical history upon cooling). PLA has been blended with other polymers in order to obtain better mechanical properties and/or cost reduction. Several studies have been made on blends of PLA with poly(ε-caprolactone), PCL[2], poly(butylacrylate), PBA [3], and acrylonitrile butadiene styrene, ABS[4].

Polyhydroxyalkanoate, PHA, is a generic designation of polyester polymers produced by the bacterial fermentation of sugars and lipids. These polyesters are a carbon storage and energy reserves in bacteria, such as Ralstonia Eutropha, Bacillus Megaterium, Azotobacterchroococum. By controlling the copolymers composition is possible to tailor most of the mechanical properties of PHA [5].The PHAs are highly crystalline polyesters (above 50%) with melting temperatures ranging from 120º to 180ºC, depending on the chemical composition [6]. The Tg is around 5ºC.

The blending of these two polymers, PHA/PLA, allows obtaining materials with improved properties, being less costly than chemical modifications or synthesis of tailor-made copolymers. The properties of the PHA/PLA

[9] *Adapted from N.C. Loureiro, J.L. Esteves, J.C. Viana, S. Ghosh, Morphological study on Polyhydroxyalkanoates and Poly(Lactic Acid) blends obtained by injection moulding, Journal of Macromolecular Science, Part B - Physics (submitted)*

blends can be easily modified by changing the polymers or co-polymers molecular weight or by varying the blend composition. [7-8]

In this chapter, the morphology development during injection molding of blends of PHA/PLA has been investigated.

6.2 Morphological Calculations based on DSC results

From the DSC thermograms several parameters were evaluated. The degrees of crystallinity (x_c^0) of the pure polymers were estimated using eq.6.1

$$x_c^0 = \frac{\Delta H_m - \Delta H_{cc}}{\Delta H_m^0} \quad (6.1)$$

where, ΔH_m^o is the enthalpy of 100 % crystalline PHA as 146 J.g-1 [3], and PLA had 93 J.g-1, respectively [10]. ΔH_m is the enthalpy of fusion. For the PHA/PLA blends a different approach was followed. In this case, since the cold crystallization is due to PLA and the crystallization to PHA and PLA, it's necessary to take into account not only the crystallization behavior of the base polymers alone, but also the interaction of the two polymers into the blend. For that, in a first approach, the degree of crystallinity of the blends is given by:

$$x_c = \frac{\Delta H_m - \Delta H_{cc}}{\Delta H_{m,PLA}^0 \cdot \emptyset_{PLA} + \Delta H_{m,PHA}^0 \cdot \emptyset_{PHA}} \quad (6.2)$$

This equation relates the enthalpy of fusion of the blend (ΔH_m) and the enthalpy of cold crystallization (ΔH_{cc}) with the enthalpy of melting of the neat polymers ($\Delta H_{m,PLA}^0$ and $\Delta H_{m,PHA}^0$) and their weight fraction ($\emptyset_{PLA}$ and $\emptyset_{PHA}$). The weighting of the enthalpy of melting of the base polymers through the weight fraction of both polymers will give a more realistic value for the enthalpy of melting of the considered blend.

6.3 Results and Discussion

6.3.1 WAXD Measurements

Figure 6.1 reveals the diffractogram of the as-molded injection molded samples of neat PLA, neat PHA, and PHA/PLA blends. The scan shows no peak for neat PLA samples, suggesting that PLA is amorphous under the thermomechanical conditions of injection molding. On the contrary, PHA crystallized to a significant extent, with diffraction peaks at 2θ values at 13.52º and 16.88º [11-12]. The most intense peak for PHA is at 2θ values at 13.52º, originating from 020 plane. The weak reflection peaks at 2Θ=16.88º are originating 110 plane.

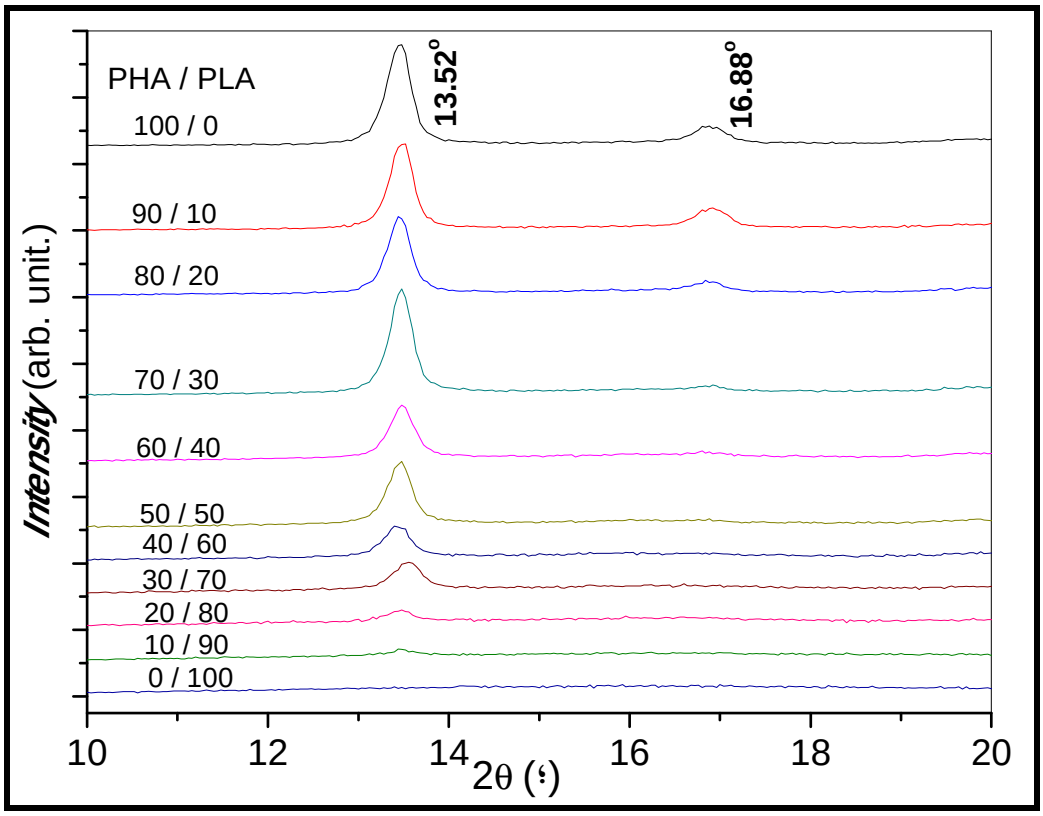

Figure 6.1 - WAXD traces of injection molded PHA/PLA blends.

For blends, the scans can be divided into two different regimes: (i) the increasing fraction of PLA in PHA, (ii) the other is increasing fraction of PHA in PLA. The addition of PLA in PHA revealed that the intensity of reflection at 2θ =13.52º remained relatively same or more intense up to 70/30 PHA / PLA composition, compared to neat PHA. However, the intensity of the peak at 2θ =13.52º decreases monotonically with increasing fraction PLA, and the peak almost disappears with 40/60 PHA/PLA composition.

It is worth to mention here that PLA is a semicrystalline polymer with a slow rate of crystallization. PLA crystallizes significantly from miscible polymer blends with the most intense Bragg peak of 2θ=16.88º [13-14], however is possible to note that neat PLA does not crystallize during standard operating conditions of injection molding. The reason for "the apparent increase peak intensity at 2θ=13.52º, and gradual decrease in peak intensity at 2θ=16.88º" requires further structural experimentation to establish. From 40 / 60 to 90 /10 PHA/PLA composition, the only reflection peak is at 2Θ=13.52º. The suppression of peak at 2θ=16.88º, which is the most peak of crystalline PLA and a less intense of PHA suggests the following: (a) there is a strong interaction between PLA and PHA crystals, and (b) PLA do not crystallize from PHA/PLA blends, under the present thermomechanical environment of injection molding.

6.3.2 DSC of Injection Molded PHA/PLA blends

The first heating of PLA revealed the typical thermal transitions along the temperature axis: (i) a glass transition, (ii) an exothermic cold crystallization, and (iii) an endothermic melting – see Fig. 6.2. The degree of crystallinity of PLA was 1.5 %, estimated from Eq. 1. This low degree of crystallinity of injection molded PLA is fairly in good agreement with the results reported elsewhere [10].

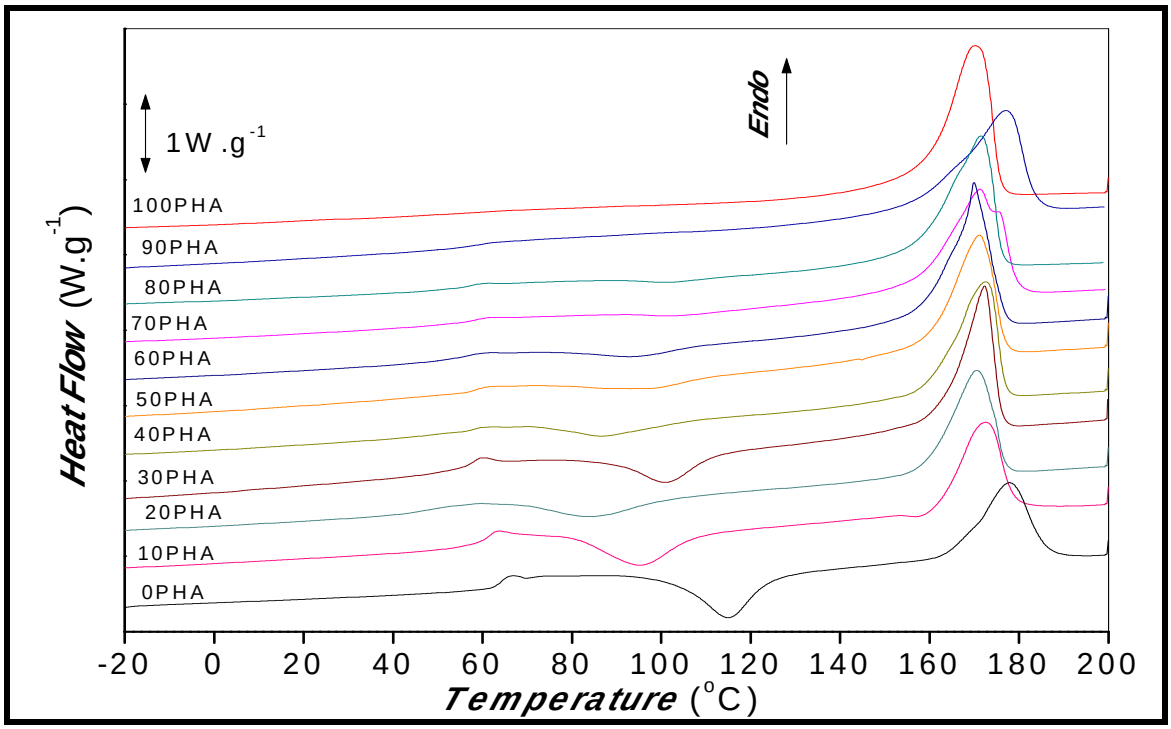

Figure 6.2 – DSC thermograms of the PHA/PLA blends in the heating run.
(from top to bottom the weight fraction of PLA increases and the weight fraction of PHA decreases)

Table 6.1 – DSC data of PHA, PLA and PHA/PLA blends.

PHA wt (%)	PLA wt (%)	T_g (ºC)			ΔC_P (J.g^{-1}.ºC)		T_{cc} (ºC)	ΔH_{cc} (J.g^{-1})	T_m (ºC)	ΔH_m (J.g^{-1})	x_c (%)
		PHA	PLA	Fox eq.	PLA	PHA	PLA				
0	100	-	63.7	63.7	0.575		97.9	29.5	177.7	30.9	1.5
10	90	7.5	61	33.0	0.229	0.254	--	27.6	172.5	40.7	13.8
20	80	7.5	45.8	22.3	0.204	0.255	102.2	15.5	170.5	46.2	31.7
30	70	6.5	55.2	16.8	0.215	0.307	105.8	18.9	172.3	45.4	27.0
40	60	-	58.9	13.5	0.129	0.215	112.1	10.1	172.5	51.3	41.3
50	50	-	54.6	11.3	0.095	0.19	97.4	13.8	171.2	53.9	39.6
60	40	7.0	53.7	9.7	0.404	1.01	72.5	15.9	169.9	62.6	45.4
70	30	6.5	57.5	8.5	0.366	1.22	90	10.4	171.2	69.7	56.8
80	20	6.2	56.2	7.6	0.34	1.7	88	1.8	171.5	66.2	60.8
90	10	-	58.6	6.8	0.329	3.29	100	--	177	67	62.3
100	0	6.2	-	6.2	--	--	--	--	170.3	65.5	60.1

Within the scan range, the injection molded PHA showed only an endothermic melting peak at 170.3 ºC. It is worth to mention that the T_g of PHA was detected in the scan at 6.2 ºC. The degree of crystallinity of injection molded PHA was 60.1 %. The mold temperature, 20 ºC i.e. well above the T_g allowed the highly flexible PHA segments to crystallize significantly.

Figure 6.3 reveals that the Tg of PLA shows a trend to decrease with increasing fraction of PHA. Similarly, the Tg of PHA shows an upward trend with increasing fraction of PLA. The blend T_g between the $T_{g,\,PHA}$ (6.2 ºC) and the $T_{g,\,PLA}$ (63.7 ºC) indicate that PLA and PHA were partially miscible in the processed blends.

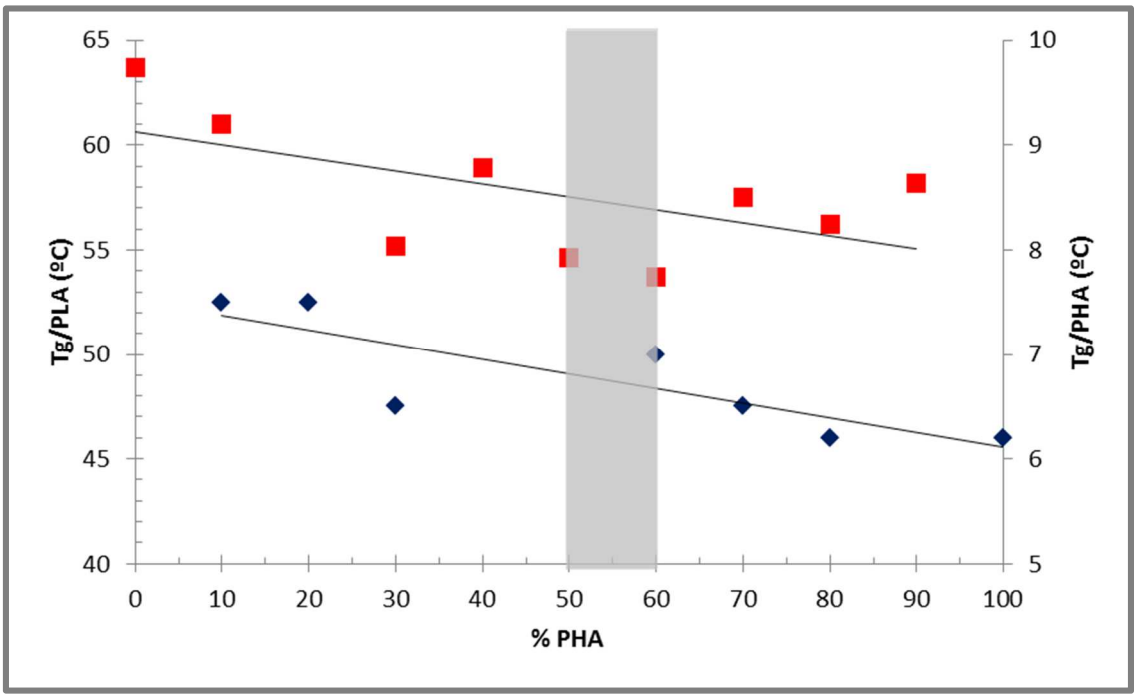

Figure 6.3 – Variation of the two glass transition temperatures with the weight fraction of PHA in the blend.

The blend miscibility can be derived from the comparison of measured T_g values with those predicted by the Fox equation [16], given by:

$$\frac{1}{T_{g,blend}} = \frac{\emptyset_{PLA}}{T_{g,PLA}} + \frac{\emptyset_{PHA}}{T_{g,PHA}} \tag{6.3}$$

Where T_g, $T_{g,PHA}$ and $T_{g,PLA}$ are the glass transition temperatures of the blend, PHA and PLA respectively. For $T_{g,PHA}$ and $T_{g,PLA}$ the values are obtain experimentally and are, respectively, 6,2ºC and 63,7 ºC. The weight fractions of the base polymers in the blend are given by $\emptyset_{PLA}$ and $\emptyset_{PHA}$, respectively. The Fox equation calculates the T_g of the blend assuming that the base polymers are completely miscible one in the other. When comparing the experimental data with the theoretical Fox model (Table 2) is possible to observe that when PHA is the matrix polymer (%PHA>60%) the blend presents some miscibility. This miscibility is confirmed by the shifting of the T_g from the neat polymer value. The phase inversion of the blends is not easy to identify in Fig. 6.3.

Fig. 6.4 shows the effect of increasing the PHA weight fraction in the heat capacity at the PLA glass transition, ΔC_p. Pure PLA shows the highest heat capacity, ΔC_p = 0,575 ($J.g^{-1}.ºC$). The heat capacity at the glass transition is a measure of the fraction of the amorphous phase (of PLA in this case) that relaxes at T_g. Interestingly, two regimes can be found in Figure 6, depending upon the type of matrix in the blend. For low percentages of incorporation of PHA, PHA is the dispersed phase and PLA is the matrix. Adding a small amount of PHA to the blend (10PHA/90PLA) is enough to reduce its heat capacity by 60%, indicating that the amorphous phase of PLA becomes less mobile. Increasing the amount of PHA further reduces ΔC_P of the blend. For the 50PHA/50PLA blend the lowest ΔC_P is obtained, being reduced by 84%. Then, between 50-60% fraction of PHA, PLA becomes the dispersed phase and PHA the matrix. This corresponds to a change on the heat capacity of PLA in the blend that suddenly increases, but still being lower than that of pure PLA (reduction of 30% for the 60PHA/40PLA). Phase inversion is clearly identified by changes on ΔC_P of this PHA/PLA blend. Furthermore, the

amount of mobile PLA amorphous phase at T_g is reduced when PLA is the disperse phase, but not as much when it is the matrix. Increasing more the amount of PHA, further reduces ΔC_P, but not reaching the same decrement as PLA as matrix (reducing more than 43% for 90PHA/10PLA). It's possible to assume that, since ΔC_P is directly connected with the mobility of the chains of the blend, the PLA matrix blends are more flexible that the PHA matrix blends.

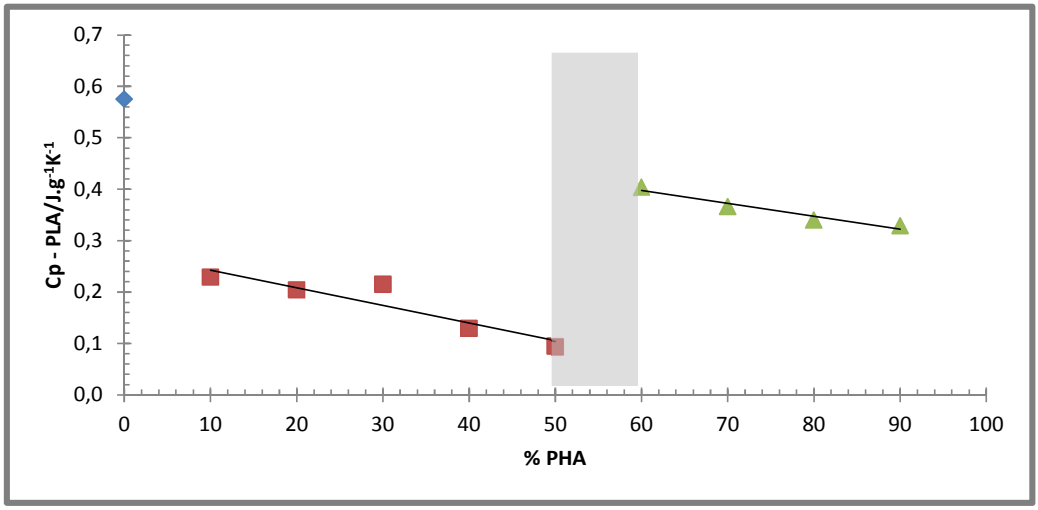

Figure 6.4 – Variation of the heat capacity at the glass transition of PLA with the weight fraction of PHA in the blend.

Figure 6.5 shows the variation of the cold crystallization temperature of PLA with the percentage of incorporation of PHA. Again two distinct evolutions are evident. When PLA is the matrix, T_{cc} increases with %PHA, starting from pure PLA T_{cc}. This increment on T_{cc} means a delay on the cold crystallization of PLA and an expectant reduction on its degree of crystallinity with increasing of %PHA. At 50-60% PHA, phase inversion occurs with a high decrement upon T_{cc} of PLA. PHA becomes the matrix and the cold crystallization of the PLA dispersed phase occurs at a lower temperature, inducing the crystallization. As the %PHA still increases, T_{cc} increases again.

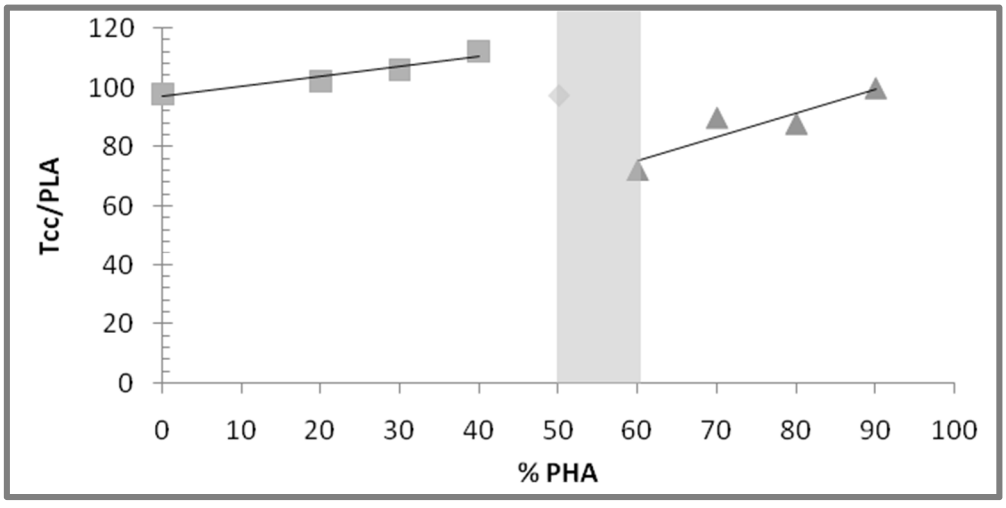

Figure 6.5 – Variation of the cold crystallization temperature of PLA with the weight fraction of PHA in the blend.

The variation of the cold crystallization enthalpy of PLA, ΔH_{cc} with %PHA is shown in Figure 6.6 (ΔH_{cc} data was been weighted by the amount of PLA in the blend). Generally, ΔH_{cc} decreases with %PHA increment. This

decrement means that PLA crystallizes more during the processing stages as PHA is added to the blend. The variations are higher when the PLA is the matrix (from 30 to 7 J/g).

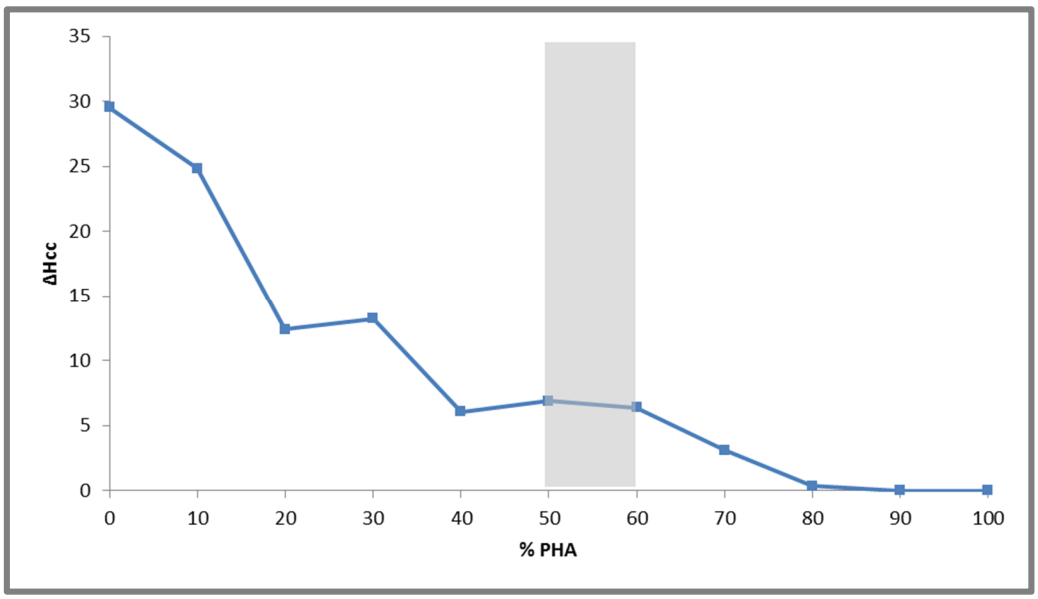

Figure 6.6 – Variation of the cold crystallization enthalpy of PLA with the weight fraction of PHA in the blend.

Considering the melting peak, T_m of the blends does not change significantly over the blend's compositions (between 170.3-172.5 ºC), close to the melting temperature of PHA of 170.3 ºC. Note that the melting temperature of PLA is around 175-180 ºC and this peak should be overlapped by the melting peak of PHA. It can be concluded that the blend composition does not have an effect on thickness of crystalline structures of PHA (i.e., T_m is constant).

As expected, the pure PHA presents a higher degree of crystallinity, X_C=60.1%, than PLA, X_C =1.5%, which is essentially amorphous. Figure 6.7 shows the variations of the degree of crystallinity of the blends with the %PHA (weighted by the composition according to equation 2) and considering only the contribution of PHA for the melting peak. In both cases, X_C increases with %PHA. The degree of crystallinity of PLA is lower when it is the dispersed phase, which can be explained by the nucleating action of PHA in the PLA matrix or by the different cooling conditions that PLA experiences when cold down from the blended melt.

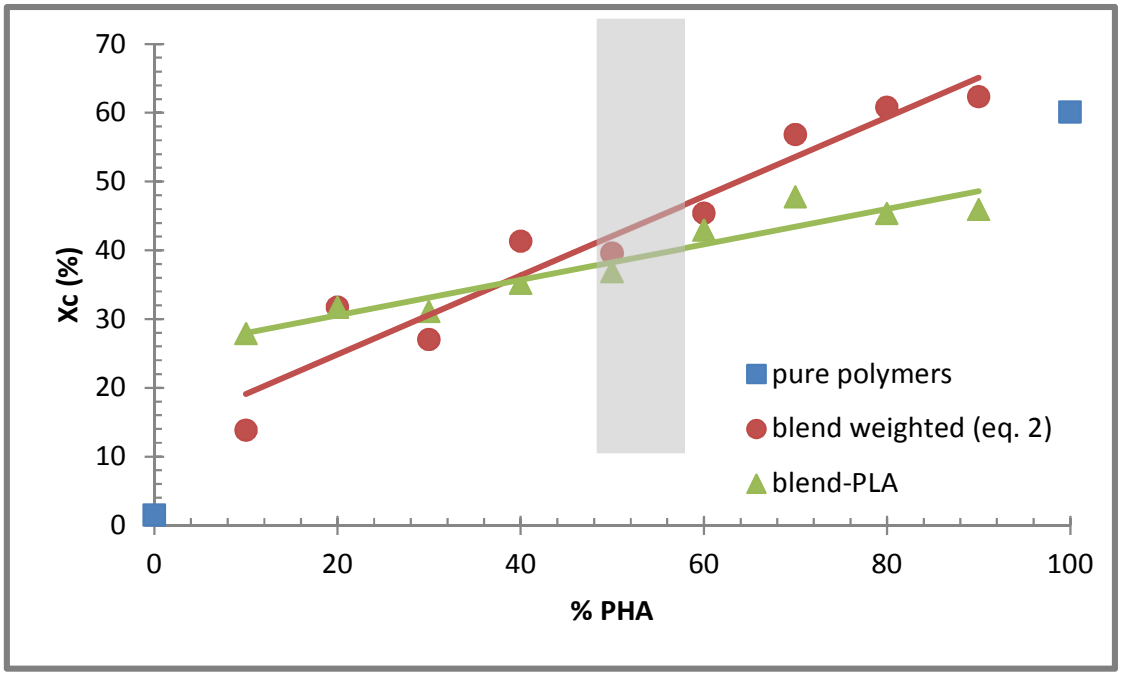

Figure 6.7 – Variations of the degree of crystallinity of the blend with the weight fraction of PHA. χ_c was calculated assuming a weighted contribution of the two polymers and single contribution of PHA for the melting peak.

Figure 6.8 presents the fracture surfaces of neat polymers and their blends. The SEM images show interestingly a clear change on the blend morphology at the phase inversion (c.a. 50%PHA) where a lamellar morphology is developed. This morphology develops in the blends only when PHA is the matrix and becomes more evident as the amount of PLA increases, and a result of the thermomechanical environment applied during processing, with a preferential orientation in the flow direction. On the other hand, a more fine structure of the PHA dispersed phase is revealed in the PLA matrix blends.

It is also evident the more brittle character of the neat PLA, which feature a highly smooth fracture surface, when compared with the rough one of the neat PHA. This is also shown by the blends: when PHA is the matrix the fracture surfaces are rougher. It is expected a different toughness of the blends.

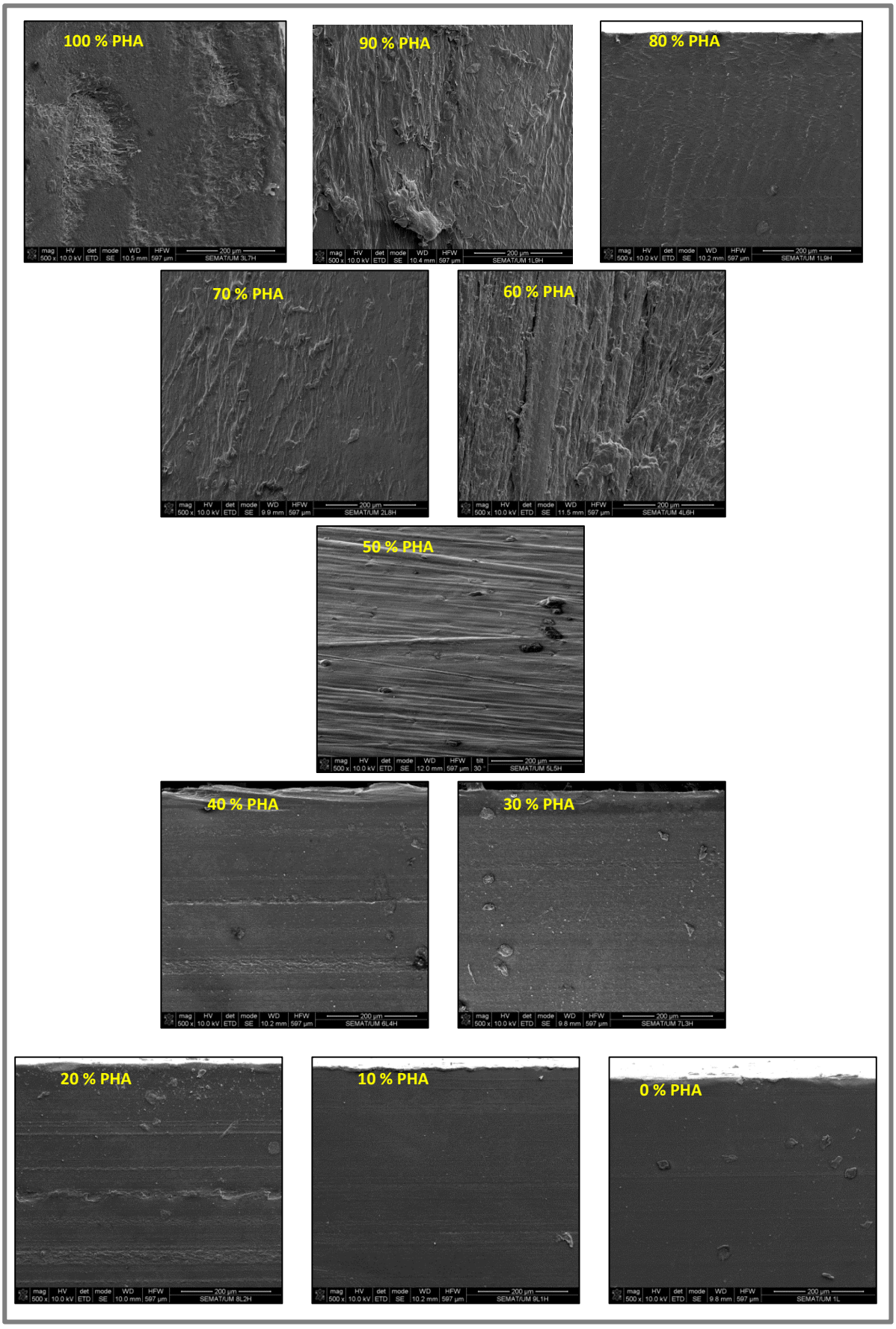

Figure 6.8 – SEM images of fracture surfaces of PHA/PLA blends (magnification of 500x).

6.4 Conclusions

The properties of biodegradable polymers such as PHA and PLA can be tailored to achieve a given performance. PHA/PLA blends over the full ratio of compositions were investigated in this work. The blends were injection molded and their morphology was assessed. The increment of PHA fraction increases the degree of crystallinity of the blend. The WAXD analysis showed that the presence of PHA stops the PLA crystallization. The preferential PHA crystallization plane is the (020) since that is in this plane that the PHA crystallizes even in lower amounts of incorporation. The evolution of the crystallization parameters (e.g., ΔCp, Tcc) trough PHA wt induces a phase inversion around 50-60%.

SEM analyses confirm that the miscibility of PHA/PLA blends increases with the incorporation of PHA and becomes perfect for values of PHA wt higher that 50%.

References

[1] R. Auras, B. Harte, and S. Selke, *An Overview of Polylactides as Packaging Material,* Macromolecular Bioscience, vol.4, pp. 835-864 (2004)

[2] C.L. Simões, J.C. Viana, A.M. Cunha*, Mechanical Properties of Poly(ε-caprolactone) and Poly(lactic acid) Blends*, Journal of Applied Polymer Science, vol. 112, pp. 345-352 (2009)

[3] B. Meng, J. Deng, Q. Lin, Z. Wu, W. Yang, *Transparent and ductile poly(lactic acid)/poly(butyl acrylate)(PBA) blends: Structure and properties*, European Polymer Journal, vol. 48, pp. 127-135 (2012)

[4] N.C. Loureiro, J.L. Esteves, J.C. Viana, *Caracterização Mecânica de Misturas PLA/ABS*, Proceedings of ENMEC'2010 – Encontro Nacional de Materiais e Estruturas Compósitas, Porto, Portugal (2010)

[5] S. Philip, T. Keshavarz, I. Roy, *Polyhydroxyalkanoates: biodegradable polymers with a range of applications*, Journal of Chemical Technology and Biotechnology, vol. 82, pp. 233-247 (2007)

[6] P. Bordes, E. Pollet, L. Avérous, *Nano-biocomposites: Biodegradable polyester/nanoclay systems*, Progress in Polymer Science, vol. 34, pp. 125-155 (2009)

[7] T. Gérard, T. Budtova, *PLA-PHA Blends: Morphology,thermal and mechanical Properties,* Proceedingsof BIOPOL'2011 . International Conference on Biodegradable and Biobased Polymers, Strasbourg, France (2011)

[8] P.K. Bajpai, I. Singh, J. Madaan, *Comparative Studies of Mechanical and Morphological Properties of PLA and PP-based Natural Fiber Composites*, Journal of Reinforced Plastics and Composites, vol. 31, pp. 1712-1724 (2012)

[9] N. Suttiwijitpukdee, H. Sato, J. Zhang, T. Hashimoto, Y. Ozaki, *Intermolecular interactions and crystallization behaviors of biodegradable polymer blends between poly (3-hydroxybutyrate) and cellulose acetate butyrate studied by DSC, FT-IR, and WAXD*, Polymer, vol.52, pp. 461-471 (2011)

[10] S. Ghosh, J.C. Viana, R.L. Reis, J.F. Mano, *Effect of processing conditions on morphology and mechanical properties of injection-molded poly(L-lactic acid),*Polymer Engineering and Science, vol. 47, pp. 1141-1147 (2007)

[11] Y. Xie, D. Kohls, I. Noda, D. Schaefer, Y. Akpale, *Poly(3-hydroxybutyrate-co-3-hydroxyhexanoate) nanocomposites with optimal mechanical properties*, Polymer, vol. 50, pp. 4656-4670, (2009)

[12] T. Iwata, M. Fujita, Y. Aoyagi,Y. Doi, T. Fujisawa, *Time-Resolved X-ray Diffraction Study on Poly[(R)-3-hydroxybutyrate] Films during Two-Step-Drawing: Generation Mechanism of Planar Zigzag Structure,* Biomolecules, vol. 6, pp.1803-1809 (2005)

[13] C. Chen, J. Chueh, H. Tseng, H. Huang, S. Lee, Biomaterials, *Preparation and characterization of biodegradable PLA polymeric blends,*vol.24, pp.1167-1173 (2003)

[14] B.M.P. Ferreira, C.A.C. Zavaglia, E.A.R. Duek, *Films of PLLA/PHBV: Thermal, morphological, and mechanical characterization*, Journal of Applied Polymer Science, vol. 86, pp. 2898-2906 (2002)

[15] M.J. Jenkins, Y. Cao, L. Howell, G.A. Leeke, *Miscibility in blends of poly(3-hydroxybutyrate-*co*-3-hydroxyvalerate) and poly(ε-caprolactone) induced by melt blending in the presence of supercritical CO_2,* Polymer, vol. 48, pp.6304-6310 (2007)

[16] D. Haynes, N. K. Abayasinghe, G. M. Harrison, K.J. Burg, D. W. Smith Jr., *In Situ Copolyesters Containing Poly(L-lactide) andPoly(hydroxyalkanoate) Units*, Biomacromolecules, vol. 8, pp. 1131-1137 (2007)

Chapter 7.

Characterization of PHA/PLA – Cellulosic Fibers Composites[10]

This chapter presents an investigation to reach the fiber incorporation that will make a composite capable of fulfill the mechanical requirements for the interior door trims.

In the last two chapters is possible to conclude that the best matrix will be [30PHA:70PLA].

7.1 Introduction

Fiber-reinforced polymers have successfully proven their value in various applications due to their good properties. Commonly, petrol-based polymers are reinforced with glass or carbon fibers offering advantageous mechanical properties at low weight. To replace these petrol-based polymers and inorganic fiber reinforcements, natural fiber polymer composites technology is focused on creating more sustainable high performance and lightweight materials [1-4]. In fact, the growing of the environmental awareness and the creation of the new standards including “End of Life Vehicle” (ELV) regulations in the EU automotive sector forces the study and production of more environmental friendly and biodegradable materials. Composite materials based on raw materials derived from natural renewable resources are being studied, a new class of eco-composites.

The reinforcement with cellulosic fibers gives to the polymer composite relatively good mechanical properties (stiffness, strength, and toughness) as well as, a low cost substitute solutions and an ease of disposal. Several studies have been made using polymers reinforced with natural fibers such as, jute, flax, banana, sisal,

10 Adapted from N.C. Loureiro, J.L. Esteves, J.C. Viana, S. Ghosh Development of Polyhydroxyalkanoates/Poly(Lactic Acid) composites reinforced with cellulosic fibers, Composites part B: Engineering (submitted)

pineapple, coir and oil palm [7-9]. Cellulosic fibres made from wood have also being used, mainly those coming from paper pulp industry [10].

Lignocellulosic fibres present some advantageous: low density, high specific strength and modulus, nonabrasive character, acoustic insulation, and low cost. But also some disadvantages: high moisture absorption, inherent quality variations, hydrophilic character (and poor compatibility with the hydrophobic polymers), and odor development in application.

The behavior of any composite material depends directly on the fiber content, on the degree of dispersion and orientation of the fibers, on matrix properties and on the degree of interaction/adhesion between the matrix and reinforcing phase [11]. D. Guimarães [10] stated that for PLA/cellulosic fibers composites is not possible to incorporate more than 30% of fiber, otherwise the PLA matrix will not be able to accommodate all the fibers. Processing conditions play also an important role on the properties of these eco-composites. Investigations on the effect of processing techniques on the properties of composites [13-14] concluded that twin screw extrusion resulted in better fibre dispersion in a polymeric matrix, but a pre-processing stage before any moulding process (e.g., injection moulding) causes material degradation and reduction on the composite properties.

7.2 Mechanical properties prediction models

7.2.1 Modified Halpin-Tsai Equation (mHT)

The tensile properties of the composites (indicated by subscript c) can be predicted by the modified Halpin-Tsai equation, recurring to matrix (indicate by subscript m) and of fibers (indicate by subscript fib) properties. This model is used in determining the properties of composites that contain discontinuous fibers [15]. Latter, Nielson modified this equation including the maximum packaging fraction, Φ_{max}, of the reinforcement. The modified Halpin-Tsai equation gives the modulus, E_c, and the tensile stress, σ_c, of the composite, respectively, by [15]:

$$E_c = E_m \left(\frac{1 + A\eta_e V_f}{1 - \eta_e \psi V_f} \right) \quad (7.1)$$

$$\sigma_c = \sigma_m \left(\frac{1 + \xi\, \eta_t V_f}{1 - \eta_t \psi V_f} \right) \quad (7.2)$$

where, Ψ depends upon the particle packing fraction, ξ is determined from the Einstein coefficient ζ, and Φ_{max} is the maximum packing fraction and has a value of 0.82 for random packing of fibers [15]:

$$\psi = 1 + \left(\frac{1 - \phi_{max}}{\phi_{max}^2} \right) \quad (7.3)$$

$$\xi = \zeta - 1 \quad (7.4)$$

$$\zeta = 1 + \frac{2l}{d} \tag{7.5}$$

$$\eta_e = \frac{\frac{E_{fib}}{E_m} - 1}{\frac{E_{fib}}{E_m} + \xi} \tag{7.6}$$

$$\eta_t = \frac{\frac{\sigma_f}{\sigma_m} - 1}{\frac{\sigma_f}{\sigma_m} + \xi} \tag{7.7}$$

7.2.2 Ishai and Cohen model (ICm)

For an approximate solution, Ishai and Cohen [16] assumes that the constituents are in a state of macroscopically homogeneous stress. Adhesion is assumed to be maintained at the interface of a cubic inclusion embedded in a cubic matrix. When a uniform displacement is applied at the boundary the elastic modulus of the composite is given by the following equation:

$$E_c = E_m \left(1 + \frac{V_f}{m/(m-1) - V_f^{1/3}} \right) \tag{7.8}$$

$$m = \frac{E_{fib}}{E_m} \tag{7.9}$$

7.2.3 Rule of Mixtures (ROM)

The rule of mixtures (ROM) considers a perfect adhesion between the matrix (indicated by subscript m) and the dispersed phase (indicated by subscript d) and a perfect dispersion of the spherical inclusions in the matrix. This model can be used to predict the initial modulus and the flexural stress of the composite by, respectively:

$$E_c = \left(\left[\frac{E_{fib}}{E_m} - 1 \right] \times \emptyset_{fib} + 1 \right) \times E_m \tag{7.10}$$

$$\sigma_c = \left(\left[\frac{\sigma_{fib}}{\sigma_m} - 1 \right] \times \emptyset_{fib} + 1 \right) \times \sigma_m \tag{7.11}$$

where E_m is the initial modulus of the matrix, E_{fib} the initial modulus of the fibers, E_c the modulus of the composite, $\emptyset_{fib}$ the volume fraction of the fiber, σ_{fib} the maximum stress of the fiber, σ_m the maximum stress of the matrix, and σ_c is the maximum stress of the composite.

7.3 Results and Discussion

7.3.1 Tensile behavior

The results of the tensile tests of the composites are given in Table 7.1. An experimental stress-strain demonstrative curve for each specimen is shown into figure 7.1. The horizontal step represents the time of extensometer removal during the test.

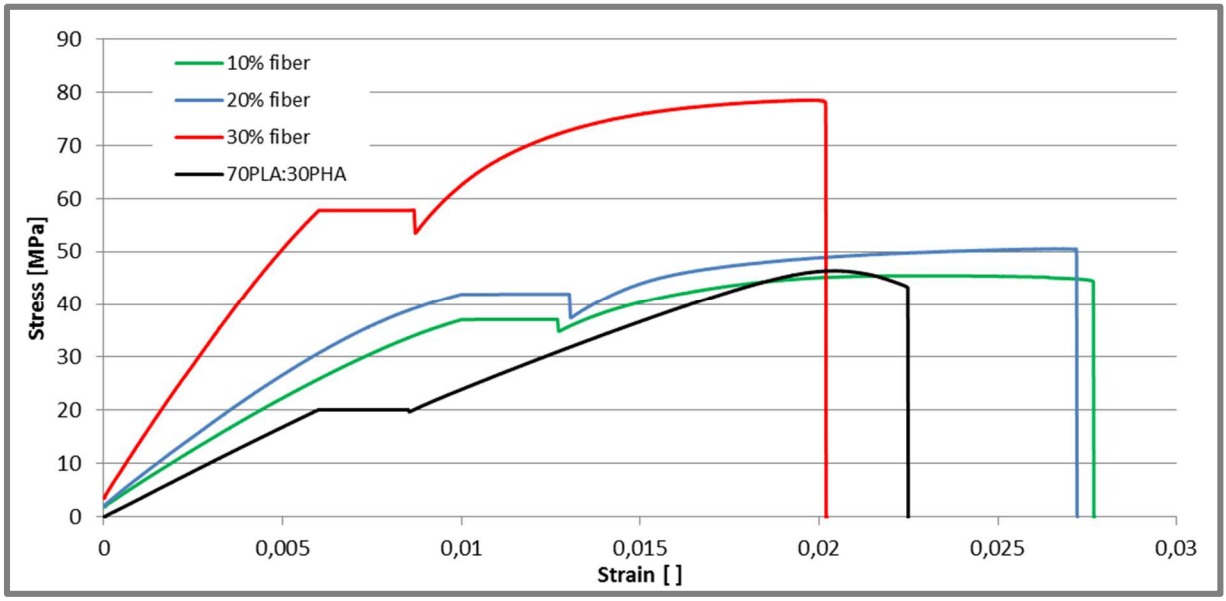

Figure 7.1 – Tensile Stress-Strain Curves obtained experimentally

Table 7.1 - Tensile Properties of PHA/PLA composites reinforced with cellulosic fiber

Fiber ratio [Mass Fraction]	Tensile modulus [GPa]	Maximum stress [MPa]	Strain at maximum stress [%]
0 %	3.36 ± 0.07	40.00 ± 1.5	2.0 ± 0.06
10 %	4.29 ± 0.37	44.21 ± 1.4	2.7 ± 0.33
20 %	5.14 ± 0.31	49.01 ± 1.6	2.4 ± 0.31
30 %	10.01 ± 0.34	79.72 ± 1.2	1.9 ± 0.18

Based on the predictive models, the estimated mechanical properties are presented in Table 7.2.

Table 7.2 – Predicted and Experimental tensile modulus

Reinforce Fiber [Mass Fraction]	Tensile Modulus [GPa]			
	experimental	ROM	mHT	ICm
0 %	3.36 ± 0.07	3.36	3.36	3.36
10%	4.29 ± 0.37	4.72	4.34	3.69
20%	5.14 ± 0.31	6.09	5.38	4.14
30%	10.01 ± 0.34	7.45	6.47	4.72

Fig. 7.2 shows the evolution of the modulus, E, with the reinforced fiber weight fraction.

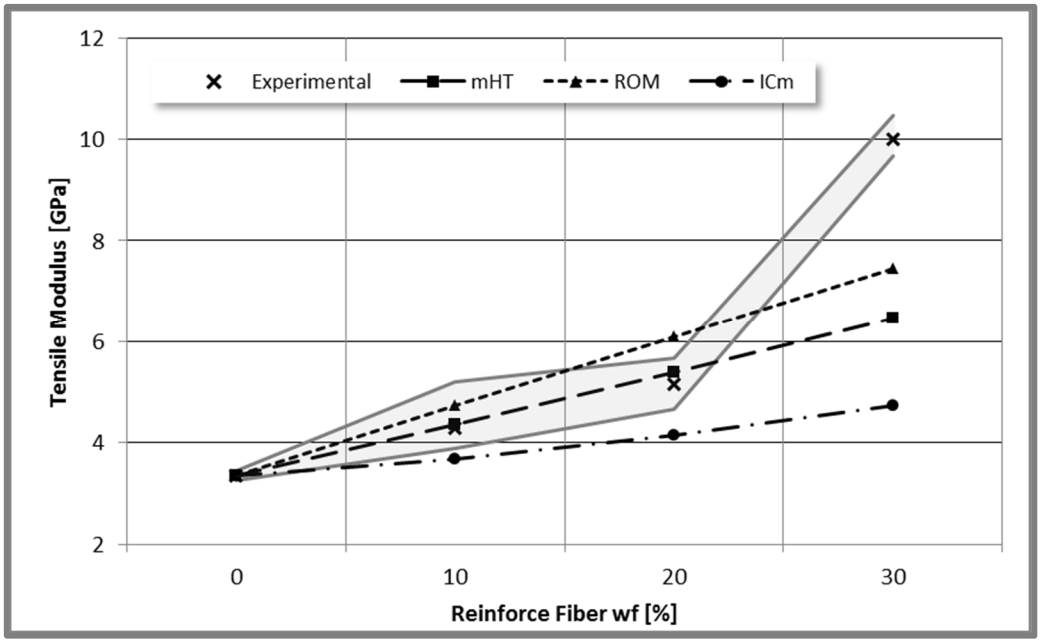

Figure 7.2 – Experimental tensile modulus, E, results and predicted values from the micromechanical models

The increase of fiber content results in a general increment on the initial tensile modulus of the composite. This is expected because the fiber contributes to the stiffness of the final composite. In Fig. 7.2 are also presented the predictions of E based on the above mentioned models: ROM, mHT and ICm.

ROM model supposes that the fiber and the matrix present a perfect adhesion.
The ICm is based in a cubic approximation. The results show that this model provides the lowest predication, meaning that the based hypothesis of the model is not suitable for this specific composite.
mHT equation supposes that the fiber presents a homogenous distribution through the matrix. The mHT equation gives an excellent prediction of E for incorporation until 20% (wf) of cellulosic fibers. Analyzing only until 20% (wf) of fiber incorporation, the maximum deviation between mHT equation and the experimental values is only about 3.5%, and for the ROM this deviation reaches 18%. This anticipates a homogenous dispersion of the fiber through the matrix. For 30 wt% of fibers, the models underpredict the experimental value. This may result from several factors including, not only the data obtain from the fibers, but also from the geometric assumptions from the adopted models.

In Table 7.3 are presented the experimental values and the predictions of the maximum tensile stress for ROM and mHT models for the various fiber incorporation ratios**.**

Table 7.3 – Experimental and Predicted tensile Stresses

Reinforce Fiber [Mass Fraction]	Tensile Stress [MPa]		
	Experimental	ROM	mHT
0 %	40.00 ± 1.5	40.00	40.00
10%	44.21 ± 1.4	49.54	44.83
20%	49.01 ± 1.6	59.52	49.91
30%	79.72 ± 1.2	69.97	52.24

Fig. 7.3 shows the variations of the maximum tensile stress with the wt% of fiber and respective models predictions.

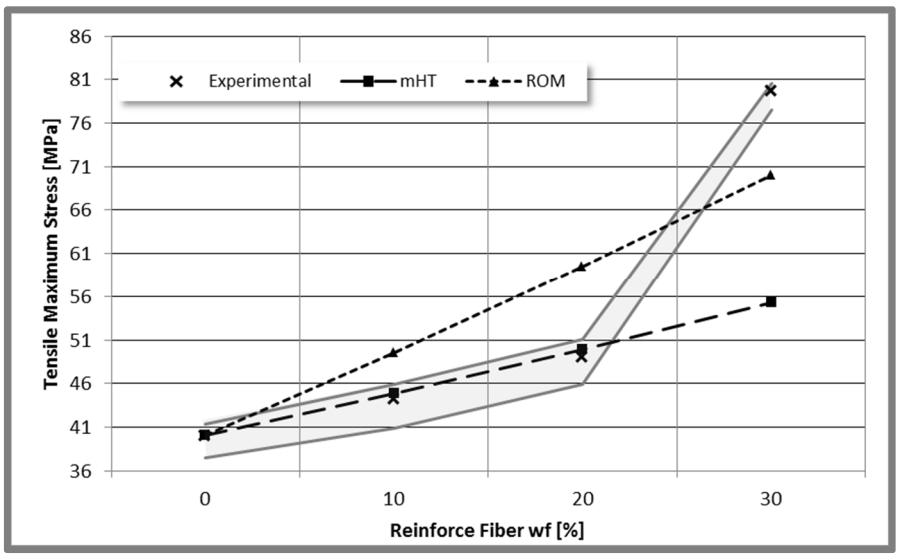

Figure 7.3– Tensile Maximum Stress Results and Predicted Values

The maximum stress of the composites can be also estimated with an excellent agreement from the above presented prediction models, namely the mHT equation. This equation gives very good predictions incorporation of fibers until 20 wt%. Until this percentage, the maximum deviation between mHT equation and the experimental values is about 1.3%, and for the ROM is about 20%. Again, for 30 wt% of fibers, the models under predict the experimental value.

7.3.2 Flexural behavior

The flexural test results of the blends are given in Table 7.4. An experimental stress-strain demonstrative curve for each specimen is depicted into figure 7.4.

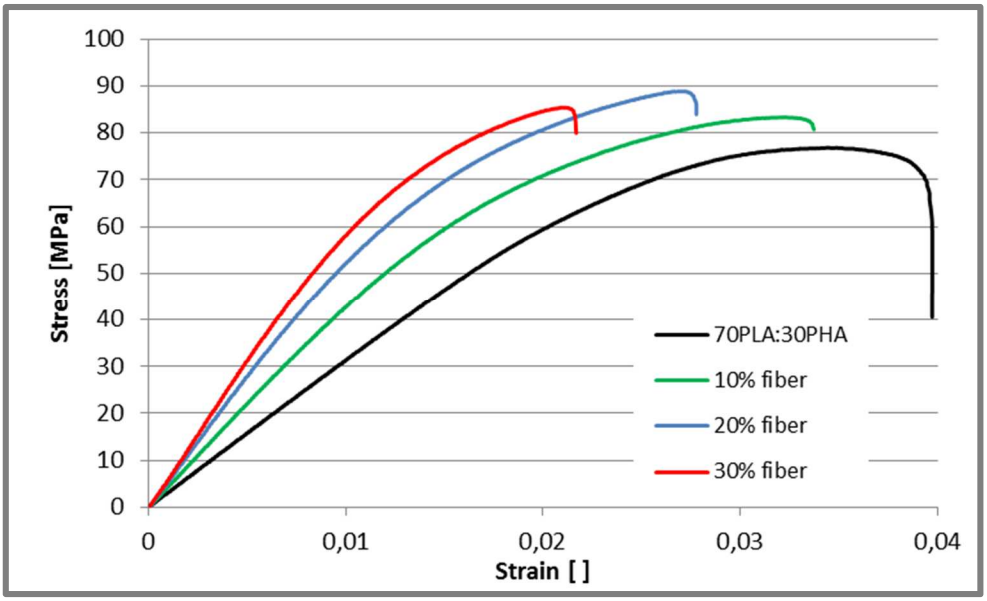

Figure 7.4 – Flexural Stress-Strain Curves obtained experimentally

Table 7.4 – Flexural Properties of PHA/PLA composites reinforced with cellulosic fiber

Fiber ratio [Mass Fraction]	Flexural Modulus [GPa]	Maximum Stress [MPa]	Strain at maximum Stress [%]
0 %	3.09 ± 0.13	77.49 ± 1.54	4.00 ± 0.29
10%	4.44 ± 0.07	82.51 ± 1.22	3.14 ± 0.22
20%	5.59 ± 0.09	89.02 ± 1.36	2.78 ± 0.12
30%	6.35 ± 0.19	85.36 ± 1.57	2.11 ± 0.04

Fig. 7.5 shows the variations of E_f with % of fiber and respective values of the prediction model (ROM). As for the tensile modulus, the ROM suggests that for fiber incorporation superior to 20% the fiber distribution is non-homogeneous.

Conversly, to the tensile modulus, the ROM models gives acceptable predictions up to 30% of incorporation of fibers.

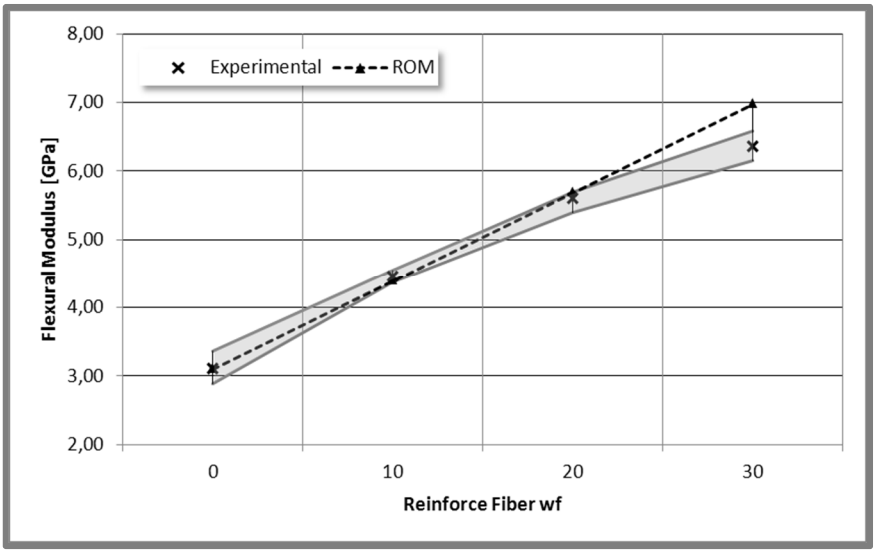

Figure 7.5 – Flexural Modulus, E_f, Results and Predicted Values from model

Fig. 7.6 shows the variations of maximum flexural stress with % fiber and respective models predictions. Again, the increment on the fiber content leads to a general increasing of the maximum flexural stress of the composite. However the incorporation of more than 20% of fiber results on a reduction on the maximum flexural stress, and a divergence from the theoretical predictive value. In general, the ROM gives very good predictions for fiber incorporation levels below 20%.

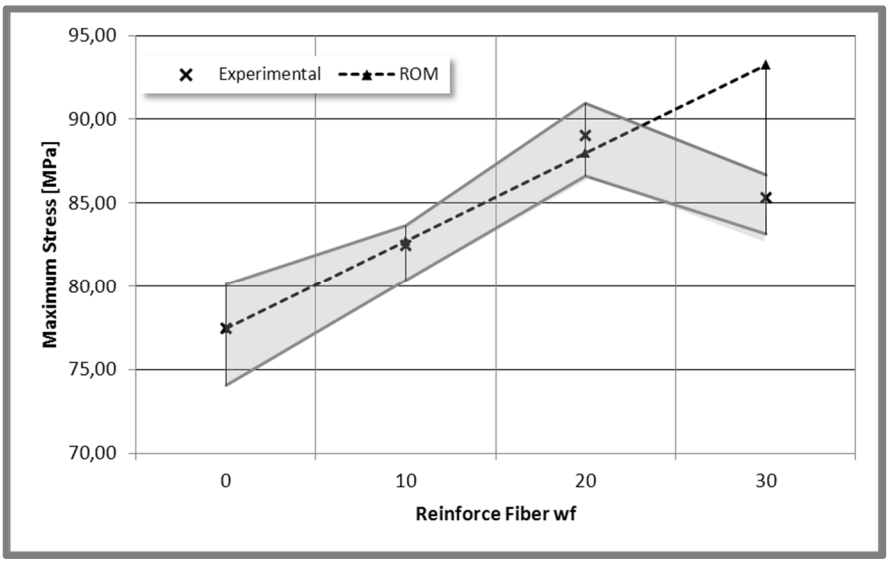

Figure 7.6 – Flexural Maximum Stress Results and Predicted Values

7.3.3 Impact behavior

Figure 7.7 presents the impact force over time during the impact test of the composites. The incorporation of fiber improves the energy absorption capabilities of the composites. However due to the non-homogeneous distribution of the fiber in the 30% fiber-composite, the impact toughness appears to decrease because the fiber bundles may act as stress concentrators, leading to fracture of the composite.

The impact results of the tested composites are given in Table 7.5. The impact energy (or toughness) establishes the amount of energy that the material can absorbed until it breaks.

Table 7.5 – Composite Impact properties

Fiber ratio [Mass Fraction]	Impact energy [J]	Deflection at break [mm]
0 %	1.7 ± 0.2	4.6 ± 1.4
10%	2.8 ± 0.5	4.8 ± 0.4
20%	2.8 ± 0.2	4.4 ± 0.8
30%	2.3 ± 0.3	3.2 ± 0.8

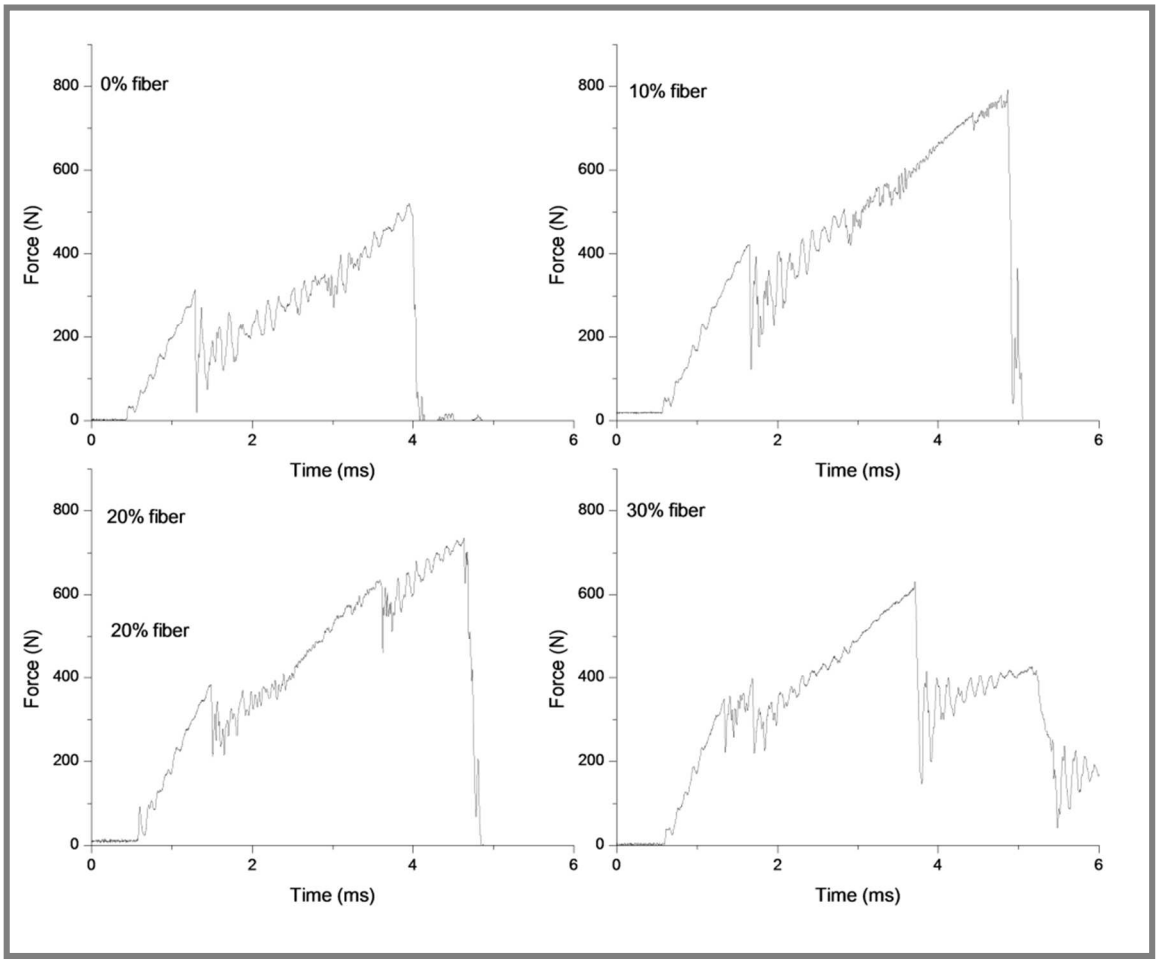

Figure 7.7 – Experimental impact force versus time for the instrumented impact tests

The variations of the impact toughness with fiber weight fraction are depicted in Fig. 7.8. The maximum toughness is found for composites with 10 and 20 wt% of fibers. The incorporation of 30% of fibers leads to a composite with a bad impact behavior with 18% less capability of absorbing energy considering the other fiber incorporations.

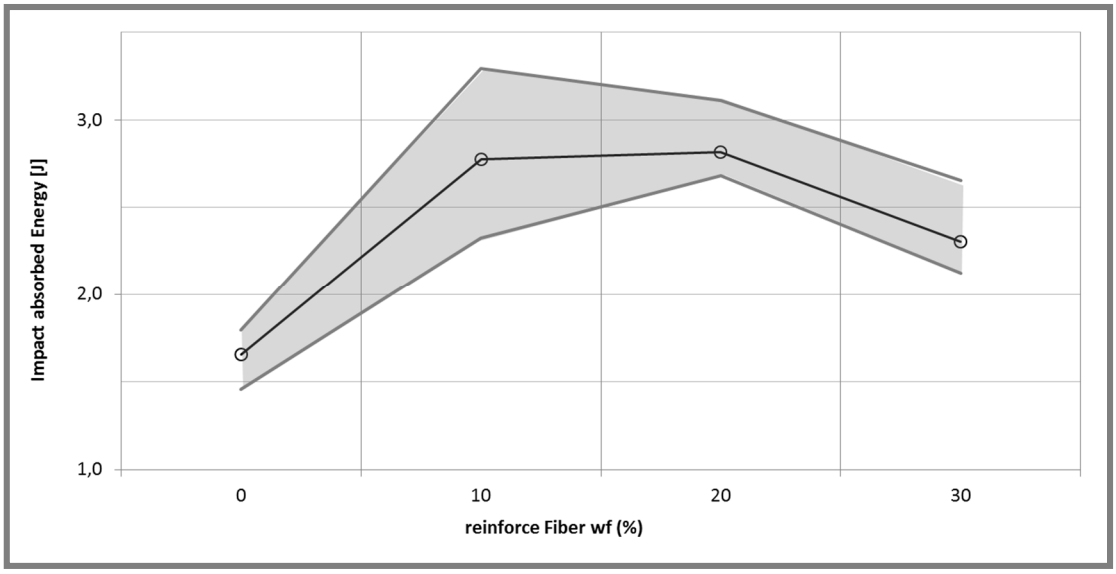

Figure 7.8 – Impact toughness.

The variations of the maximum deflection with fiber wf are depicted in Fig. 7.9. The addition of cellulosic fibers decreases the maximum deflection of the composites.

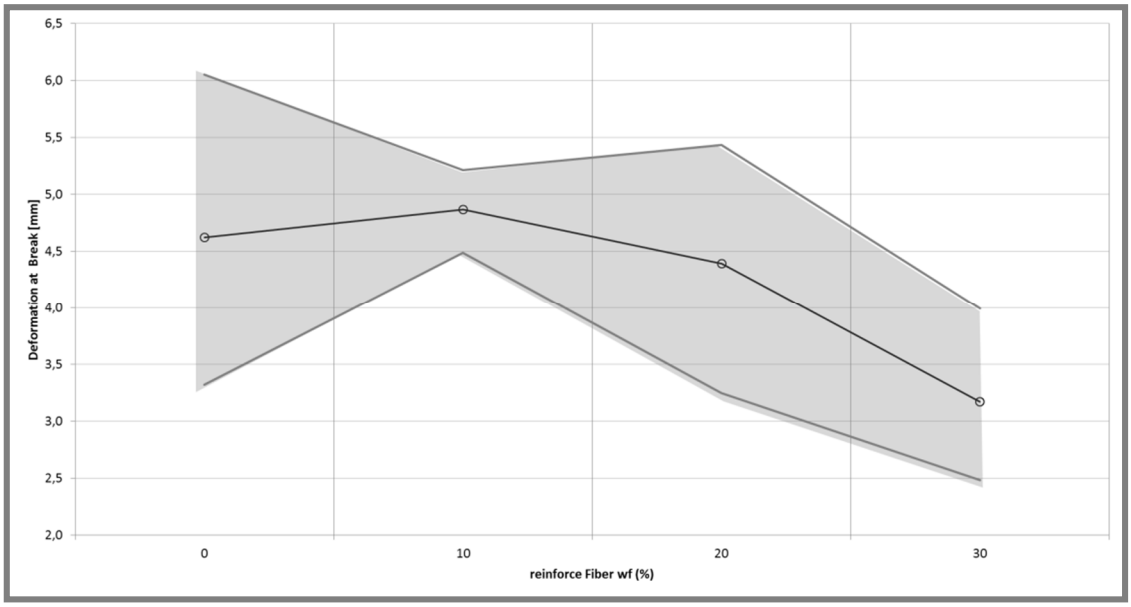

Figure 7.9 – Impact maximum deflection of various eco-composites.

The incorporation of 30% of fibers drives to a composite with decreasing on the deformation capabilities at break of around 33%.

7.3.4 Heat Deflection Temperature (HDT) measurement

The Heat Deflection Temperature (HDT) results are given in Table 7.6 and Fig. 7.10 for all fiber compositions.

Table 7.6 – Heat-Deflection Temperature of composites

Fiber ratio [Mass Fraction]	HDT [ºC]
0 %	48.5 ± 0.9
10%	49.2 ± 0.6
20%	56.0 ± 0.2
30%	51.7 ± 0.2

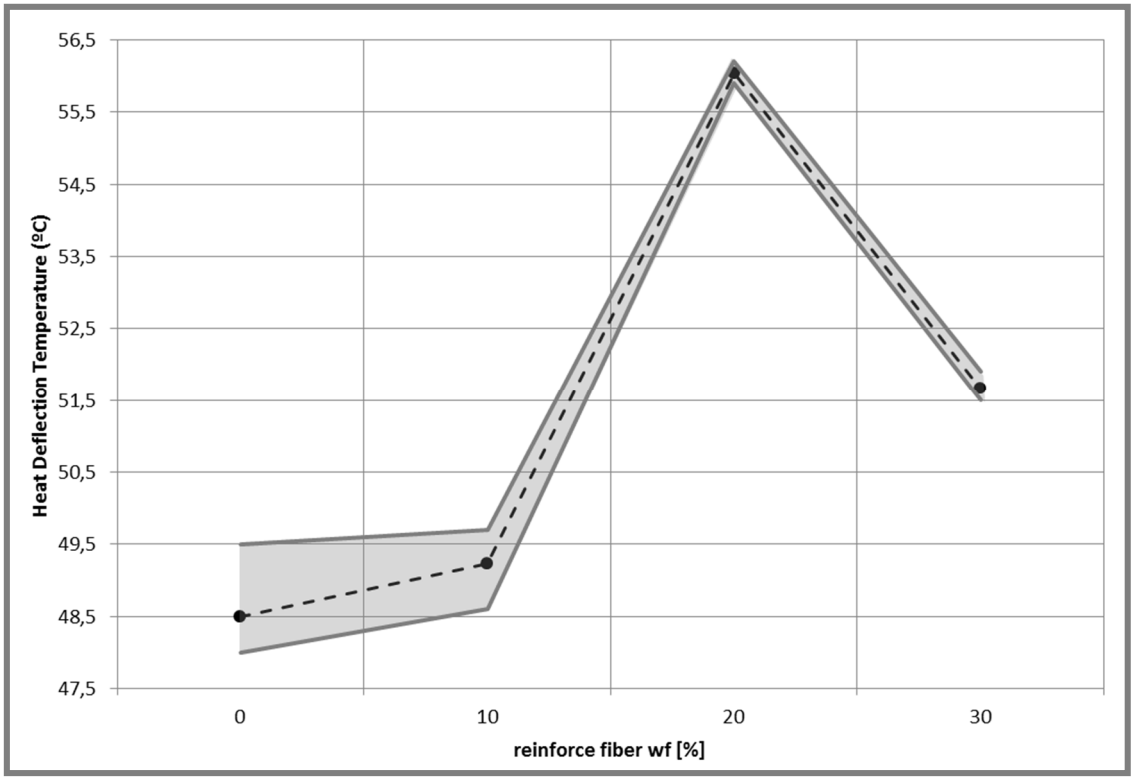

Figure 7.10 – Experimental HDT evolution over fiber composition

As expected the incorporation of fibers increases the HDT. The maximum synergetic effect is obtained with the incorporation of 20% of fibers leading to an increasing of 15% on the HDT value.

7.3.5 Microscopy analysis

The previous mechanical characterization highlights the effects of the adhesion between the polymeric matrix and the cellulosic fiber and of the dispersion of fibers.
The optical microscopy analysis images are shown in Figure 7.11 and SEM analysis in fig.7.12. The incorporation of 30% wf of fiber leads to a non-homogeneous composite and the incorporation until 20% wf drives to a homogeneous composite.

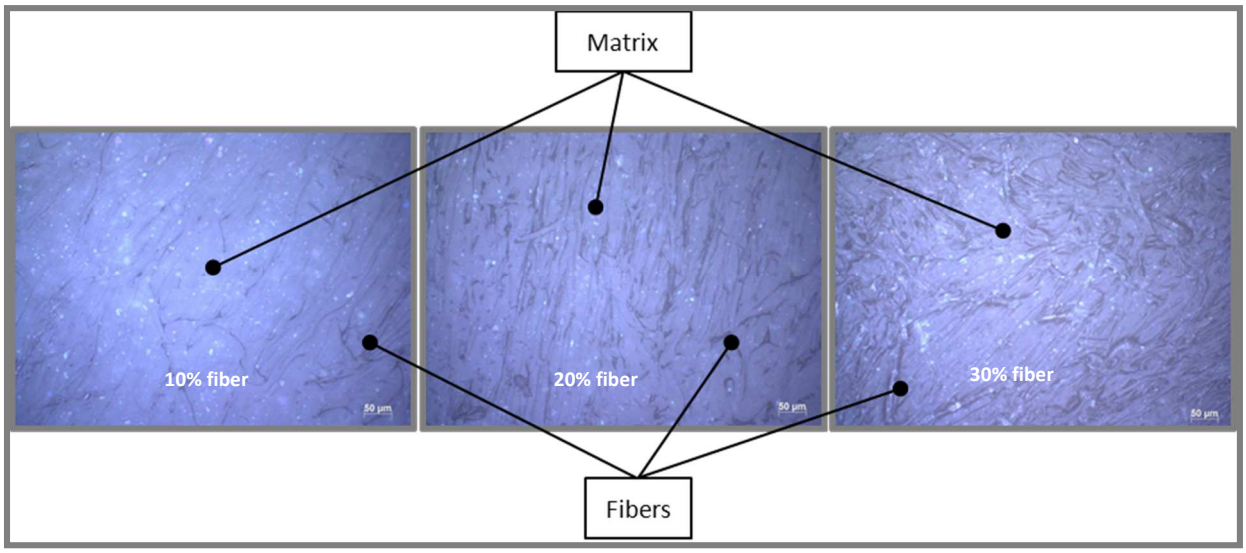

Figure 7.11 – Optical microscopy analysis (magnification 20x).

As possible to verify in figure 7.12, the matrix is a perfectly miscible one. Is not possible to identify a PLA or a PHA phase in the matrix.
The SEM analysis also corroborates that the fiber dispersion is homogenous until reach the 20% wf. After that the dispersion starts to random and lost the homogeneity.

As seen in fig. 7.13 the SEM analysis reveals that the fibers are deboned of the matrix inducing a lower interfacial adhesion. This interfacial behavior justifies the deviation of the experimental data and the predicated values based into perfect adhesion.

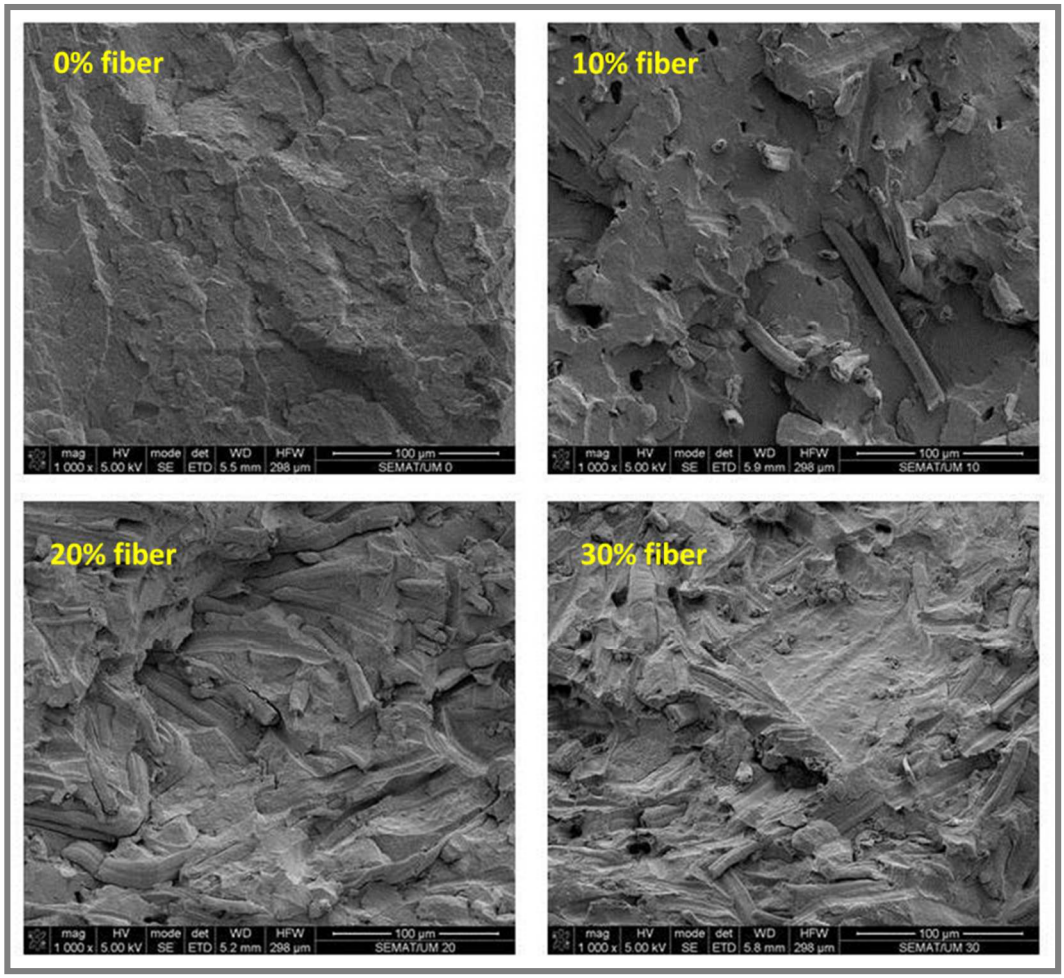

Figure 7.12 – SEM Analysis

.

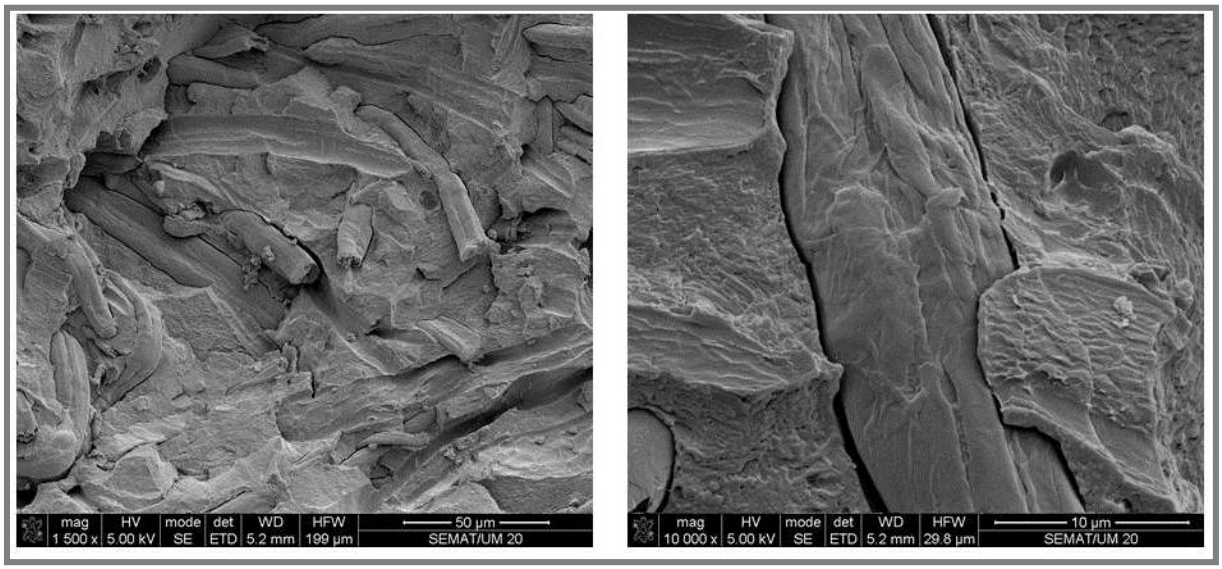

Figure 7.13 – Detail of the interface matrix-fiber obtain in SEM Analysis (20% fiber wf)

.

7.4 Conclusions

The properties of biodegradable composites can be tailored to achieve a given performance.

Composites with a [30:70] [PHA:PLA] matrix and with a fiber content of 10%, 20% and 30% (wf) were investigated in this work. The composites were injection molded, after being extruded and pelletized, and their mechanical (tensile, flexural and impact) and thermal (HDT) behaviors were assessed.

The increment of fiber amount increases the tensile and flexural moduli of the final composites. For the tensile modulus, a linear relationship is found, following the modified Halpin-Tsai equation (or the rules of mixtures) denoting a homogeneous dispersion of the fibers for fiber incorporation until 20% (wf).

The ROM validates the flexural behavior determined by the experimental tests. The experimental values allow us to concluded, again, that for fiber incorporation over than 20% (wf) the composite became non-homogeneous and therefore with reduced mechanical properties.

The moduli and maximum stress of the composites with fiber incorporation lower or equal to 20% (wf) can be estimated recurring to the presented prediction models.

The SEM analysis identifies a lower matrix/fiber interfacial adhesion that justifies the deviation of the experimental data and the predicated values.

The incorporation of 20% wf fiber improves the impact energy absorption and the Heat-Deflection Temperature.

Prediction models and material property characterization allowed unambiguous detection of a maximum of fiber incorporation.

Once that the composites are from renewable sources these data gives an indication of the potential use of these composites replacing the petrol-based matrix composites with synthetic reinforced fibers.

References

[1] J. Holbery, D. Houston, *Natural-fiber-reinforced polymer composites in automotive applications*, Journal of The Minerals, Metals & Materials Society, vol.58, pp.80-86 (2006)

[2] A.K. Mohanty, M. Misra, L.T. Drzal, *Sustainable Bio-Composites from Renewable Resources: Opportunities and Challenges in the Green Materials World,* Journal of Polymers and the Environment, vol.10, pp.19-26 (2002)

[3] A.K. Mohanty, M. Misra, G. Hinrichsen, *Biofibres, biodegradable polymers and biocomposites: An overview*, Macromolecuar Materials and Engineering, vol.276-277, pp.1-24 (2000)

[4] P.A. Fowler, J. Mark-Hughes, *Biocomposites: technology, environmental credentials and market forces*, Journal of the Science of Food and Agriculture, vol. 86, pp. 1781-1789 (2006)

[5] N. Pereira, M.L. Sousa, J.A.M. Agnelli, L.H.C. Mattoso, *Effect of Processing on the Properties of Polypropylene Reinforced with Short Sisal Fibers*; Proceedings of 4th International Conference on Wood Fiber Plastic Composites, Madison, United States of America (1997)

[6] M.A. Paul, M. Alexandre, P. Degee, C. Henrist, A. Rulmont, P. Dubois, *New nanocomposite materials based on plasticized poly(l-lactide) and organo-modified montmorillonites: thermal and morphological study*, Polymer, vol. 44, pp 443-450 (2003)

[7] A.P. Mathew, A. Dufresne, *Morphological Investigation of Nanocomposites from Sorbitol Plasticized Starch and Tunicin Whiskers*, Biomacromolecules, vol.3, pp. 609 – 617 (2002)

[8] L. Lundquist, B. Marque, P.-O. Hagstrand, Y. Leterrier, J.-A.E. Manson, *Novel pulp fibre reinforced thermoplastic composites*, Composites Science and Technology, vol. 63, pp. 137-152 (2003)

[9] A.P. Mathew, K. Oksman, M. Sain, *Mechanical properties of biodegradable composites from poly lactic acid (PLA) and microcrystalline cellulose (MCC)*, Journal of Applied Polymer Science, vol. 97, pp.2014-2025 (2005)

[10] D. Guimarães, *Efeito das condições de injecção nas propriedades de PLA reforçado com fibras celulósicas*, Master Thesis in Polymer Engineering, University of Minho, Portugal (2009)

[11] S. Mishra, S.S. Tripathy, M. Mishra, A.K. Mohanty, S.K. Nayak, *novel Eco-friendly Biocomposites: Biofiber Reinforced Biodegradable Polyester Amide Composites – Fabrication and Properties Evaluation,* Journal of Reinforced Plastics and Composites, vol. 21, pp. 55-70 (2002)

[12] N.C. Loureiro, J.L. Esteves, J.C. Viana, S. Ghosh, *Development and characterization of renewable source composites to replace petrol-based polymers into interior door trims*, Proceedings of ECCM15 – 15th European Conference on Composite Materials, Venice, Italy (2012)

[13] G. Kalaprasad, K. Joseph, S. Thomas, C. Pavithran, *Theroetical modeling of tensile properties of short sisal fibre-reinforced low-density polyethylene composites*, Journal of materials science, vol.32, pp.4261-4267 (1997)

[14] T. Gérard, T. Budtova, *PLA-PHA Blends: Morphology, thermal and mechanical Properties,* Proceedings of BIOPOL'2011 – International Conference on Biodegradable and Biobased Polymers, 2011.

[15] K.G. Sathyanarayana, K. Sukumaran,P.S. Mukherjee, C. Pavithran, S.G.K. Pillai, *Natural fibre-polymer composites*, Cement and Concrete Composites, vol. 12, pp. 117-136 (1990)

Chapter 8.

Application of Bio-composites into automotive interior Parts

8.1 Results compilation

The mechanical and morphological properties studies of PHA/PLA blends have been presented in previous chapters. As verify in those chapters the best matrix for interior door trims is the [PHA:PLA] [30:70] wf.

To tailor some properties, the study of cellulosic fibers incorporation was investigated in the previous chapter. In that chapter it was concluded that over than 20% of reinforced fiber the composite will not be homogeneous and for that reason is not possible to use it on engineering applications.

The study presented in chapter 7 drives to different values of the matrix behavior. When compared with the data obtain into chapter 5 all new values are lower than the first ones.
This is due to the previous extrusion used in chapter 7 study. The thermal cycle induced by the extrusion process provokes a different mechanical and thermal behavior of the composite at the end of the injection.

Since the automotive interior parts manufacturer only works in injection moulding processes this new composite will be produce recurring a similar process, namely the neat polymers will came from the supplier pelletized and in the injection process the fibers will be added.

Once that the main objective of this work is to replace the petrol-based polymers used into automotive interior parts with renewable-source composites is necessary that this green-composite presents equal or better properties than the actual used polymers.

The interior door trims are mainly injection molded into ABS or PP-copolymer, that's why is obligatory to compare the obtain results with the general ABS and PP properties.

Using online databases[11] it was possible to resume the main properties of ABS and PP. The results are expressed into table 8.1.

Table 8.1 –ABS and PP General Properties

Material	Tensile Modulus [GPa]	Maximum Tensile Stress [MPa]	Flexural Maximum Stress [MPa]	Impact Energy [J]	Heat Deflection Temperature [ºC]
ABS (injection Grade)	2,33	38,4	68,6	22,7	96
PP (injection Grade)	1,72	31,3	48,1	10,8	63

The compilation of the data related to the experimental part of this thesis showed, as express in table 8.2, that if the polymer blend suffers a previous extrusion, the mechanical and thermal behavior decreases about 10% with some exceptions that presents a bigger deviation.

Table 8.2 –Obtain Data Comparison and Estimated Deviation

	[70:30][PLA:PHA] injected (chap. 5)	[70:30][PLA:PHA] Extruded and injected (chap. 7)	Percentual Deviation
Tensile Modulus [GPa]	3,4	3,1	10%
Maximum Tensile Stress [MPa]	46,02	41,37	11%
Flexural Modulus [GPa]	3,5	3,4	3%
Maximum Flexural Stress (MPa]	62,30	40,00	56%
Absorved Energy [J]	6,4	1,7	274%
Heat Deflection Temperature [ºC]	62,1	48,5	28%

Since that the properties decreasing is due to the thermal needs of the extrusion process, is possible to estimate the properties of the composites if the extrusion doesn't take place.

That estimation is expressed into table 8.3.

Table 8.3 –Estimated composite properties

		Estimated Deviation	10% fiber	20% fiber	30% fiber
Tensile Modulus [GPa]	Real	10%	4,4	5,6	6,4
	Estimated		4,8	6,1	7,0
Maximum Tensile Stress [MPa]	Real	11%	77,49	82,51	85,36
	Estimated		86,20	91,78	94,95
Flexural Modulus [GPa]	Real	3%	4,3	5,1	10,0
	Estimated		4,4	5,3	10,3
Maximum Flexural Stress (MPa]	Real	56%	44,21	49,01	79,72
	Estimated		68,86	76,33	124,17
Absorved Energy [J]	Real	274%	2,8	2,8	2,3
	Estimated		10,5	10,5	8,6
Heat Deflection Temperature [ºC]	Real	28%	49,2	56,0	51,7
	Estimated		63,0	71,7	66,2

[11] *Source: www.matweb.com, consulted in November 2012 (more information in Appendixes)*

8.2 Production Technology

Is easy to conclude that the industrial process can't be and extrusion, pelletization and after an injection process. This sequence of processes will drive to a weaker composite that don't present the require behavior for an automotive interior part.

Therefore the part must be produce recurring to a process where a unique thermal cycle is applied to the materials.

Actually that process is the Compound Injection Moulding (CIM), where all materials needed are directly inserted into the fuse. The CIM machines warranty that all materials are inserted into the fuse at the right ratio and at the same time, driving to a homogeneous dispersion of all materials in the fuse and therefore into the part.

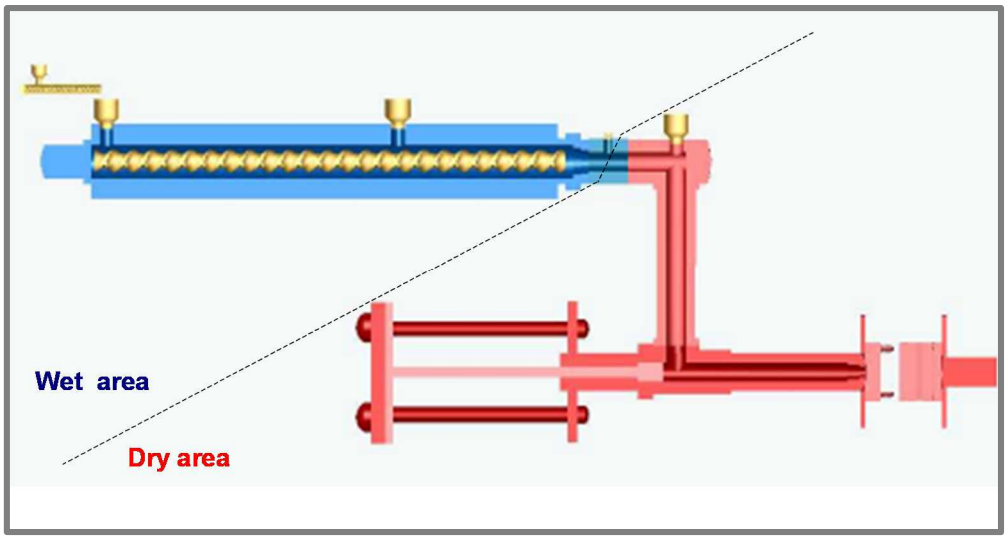

Figure 8.1 – CIM process (schematic)

As possible to verify in figure 8.1 the CIM process presents two different fuses. The first fuse is in the wet area. In that fuse the polymers are dosed by the hoppers system into the right ratio. It is called wet area because the polymers, due to the room conditions, can absorb some moisture that will be release during the traveling along the fuse.

The second fuse is on the dry area. In this area the fiber hopper deliver the right fiber quantity to establish the final ratio. This fuse is part of the injection system of the CIM equipment.

Is this last section, once that the polymers are without moisture and the fibers are well dried and isolated from the atmosphere the values of moisture content are very low. That's why it is called the dry area.

Figure 8.2 – CIM equipment

8.3 Composite Selection

Based in tables 8.1, 8.2 and 8.3 is possible to plot a 6 dimension radar chart (figure 8.3) that will emphasize the relation of all these parameters.

As seen in the figure, the values of the impact absorbed energy are quite different. That difference can have originated in the velocity of the test which is not indicated into the consulted database.

In this work it was used an impact velocity of 1m/s but is common into the generic polymer industry that this velocity rounds the 4,4 m/s.

Regarding the HDT, is possible to see that the ABS presents the highest value. However the value presented is an average of all ABS grades actually in the market.
It's possible to have an ABS with a HDT lower than the studied composites.

By analyzing the radar chart is possible to conclude that the composite with 20% fiber (light-gray shadow) is the one that present better or equal properties in all the dimensions.

For producing the automotive parts it's going to be used the composite that presents the equal or better properties in all dimensions.

By analyzing the 6D radar chart is possible to conclude that the composite with 20% fiber (gray shadow) is the one that fulfill the previous statement. The only dimension that this composite present a weaker behavior is on impact, but as have been said before these values needs some confirmation that outbound the aim of this thesis.

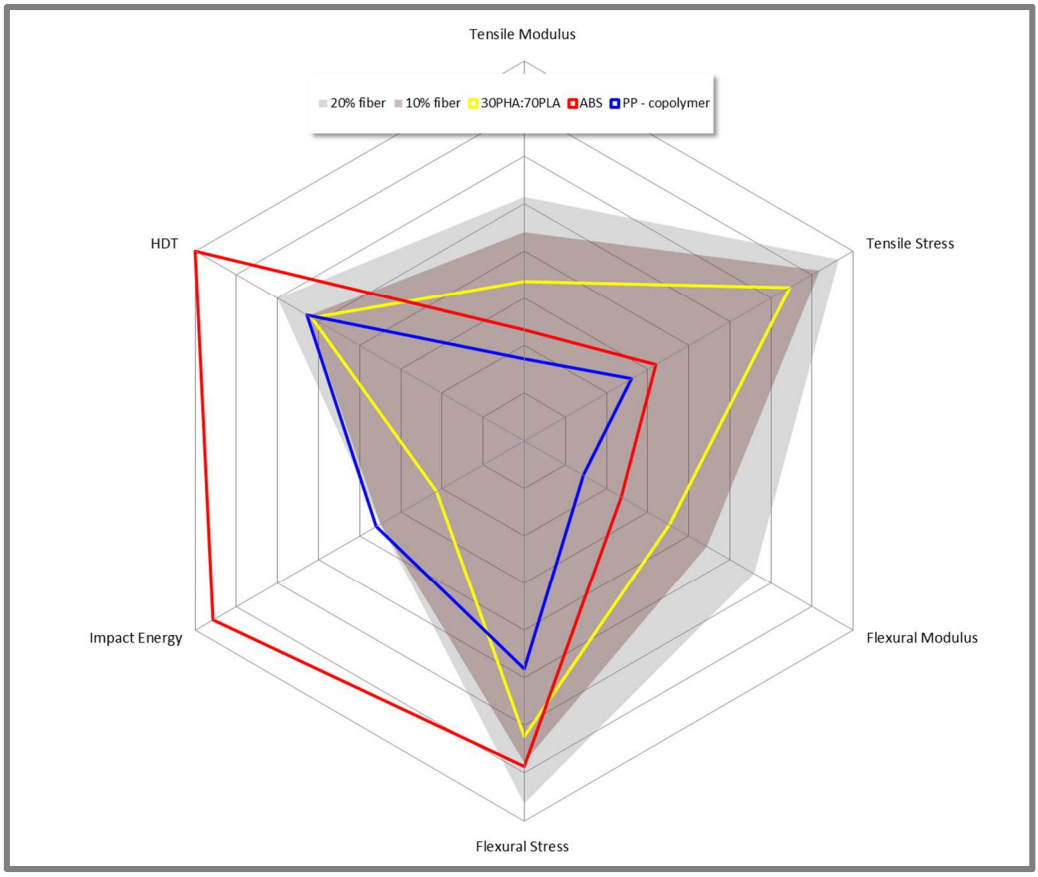

Figure 8.3 – 6 Dimension radar chart materials comparison

8.4 Automotive part

To demonstrate the possibility of using this composite and the CIM technology a part was injected.

It was chosen a cabin light support part from a well-known OEM from a 2008 model.

The original part is produced in an ABS/PA6 blend by injection moulding.

Figure 8.4 – Original Part

Using the injection parameters already optimized in the previous chapters on a CIM equipment with a composite material formed by a [PHA:PLA] [30:70] matrix and a ratio of 20% wf of cellulosic fiber is possible to obtain the same part but into bio-degradable composite.

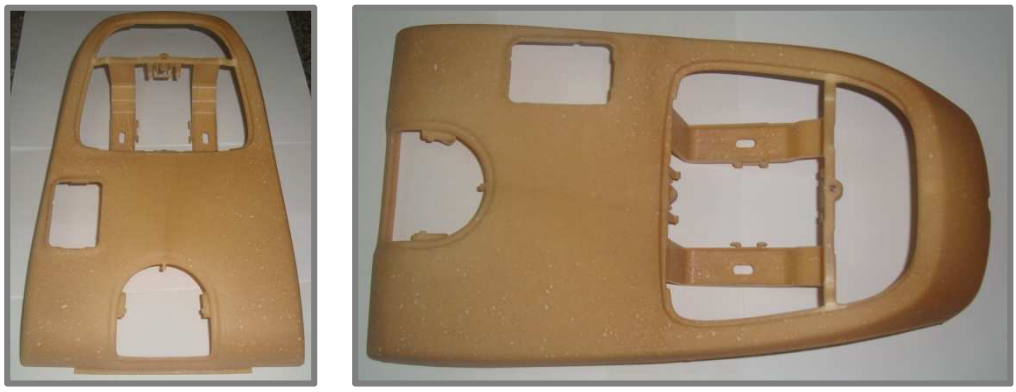

Figure 8.5 – eco-composite part

As can be seen by comparing figure 8.4 and 8.5 the part produce in eco-composite presents the same geometry. That allows the easy replacement of the actual part for this one and also allows the incorporation of the systems and parts that are integrated into the cabin interior light part.

Is possible to see, in fig. 8.6, that even the small details can be reproduced with this composite.

Figure 8.6 – eco-composite part detail

As happens nowadays the part color can be adjust with pigments.

8.5 Conclusions

The feasibility of producing interior parts on the studied eco-composites has been investigated.

Composites with a [30:70] [PHA:PLA] matrix and with a fiber content of 10% and 20% (wf) were compared with the most used petrol-based polymers for automotive interior parts (PP and ABS)

The incorporation of 20% wf fiber leads to an eco-composite that presents the best properties of all biopolymer blends and biocomposites studied.

When compared with ABS and PP, this eco-composite, normally, presents equal or better properties, excluding the impact absorbed energy.

Is possible to conclude that this composite can reveal himself an option for replace the petrol-based polymers in some cabin interior parts applications has demonstrated in this part case-study.

Chapter 9.

Final Remarks and Future Works

9.1 Final Remarks

The principals expected result of this thesis is focus on the development of a concept of an eco-efficient automotive door interior trim using 100 % of renewable sources materials, whilst meeting actual applicable crashworthiness standards and aesthetics requirements.

The work reported in this thesis proof that the properties of biodegradable composites can be tailored by a careful selection of the neat polymer or polymer blends that compose the matrix and the correct incorporation of reinforce fibers.

For the matrix a blend of PHA and PLA were chosen recurring to a study over the full ratio of compositions.

The mechanical and morphological behavior were study and the [PHA:PLA] [30:70] blend was chosen to be the matrix of the biodegradable composite that will be developed.

As mentioned before ([10], chapter 7), taking account previous works, the fiber incorporation can't be superior to 30% (wf).

To asset the best fiber fraction incorporation composites with a [PHA:PLA] [30:70] matrix and with a fiber content until 30% (wf) were investigated.

Comparing all the results is possible to conclude that for automotive interior parts, the best biodegradable composite that this work achieves is a composite with a matrix compose by [PHA:PLA] [30:70] (wf) and with a fiber incorporation of 20% (wf).

Using the actual production process is possible to process automotive interior parts with this composite as demonstrated in the case-study.

Therefore is possible to stat that the primary objective of this work has been achieved and the formulation of a 100% renewable-source composite capable of replace the petrol-based polymers use into interior door trims has been identified.

9.2 Future Works

For future works based in this thesis is possible to works in six different areas:

1st area – Directly connected with this work: Study the mechanical behavior of the injected composite into the CIM equipment. Study the influence of the Impact Velocity on the Absorbed Energy to compare with petrol-based polymers. Study the interface between fiber and matrix. Optimize the adhesion between the matrix and the fiber recurring to chemical and thermo-physical fibers treatments.

2nd area – Matrix: In this section is possible to study other renewable-source polymers, such as PHB, PGA, PBA, to replace PHA and/or PLA.

3rd area – Fibers: Study the incorporation of other fibers such as coconut, flax, cotton, hemp, jute, sisal among others. Is also possible to study the incorporation of woven and pre-impregnated fibers.

4th area – Other applications: Developed and test this composite for structural parts use it in moderate stress states. Study the incorporation of this composite into other transport systems and others industrial sectors.

5th area – Processing Technology: I suggest the study of processing this composites and composite parts, by other technologies such as compression moulding, Vacuum conformation, etc.

6th area – Long Term Composite Characterization: Study the long term behavior such as fatigue, creep, real degradation process, solar exposition, moisture degradation and chemical degradation occurring by the contact with lubricants and other environmental agents.

Appendixes

A.1

Datasheet of Polyhydroxyalkanoate

NaturePlast
L'évolution naturelle du plastique

TECHNICAL DATA SHEET **NATUREPLAST PHI 002**

Poly (hydroxyalkanoate) Injection

General properties

PHI 002 is a thermoplastic resin of Poly (hydroxyalkanoate) made from renewable vegetable resources (100%) and is specifically developed for injection moulding.

PHI 002 is an opaque grade. It could be used on conventional injection moulding equipments.

Physical Properties		**ISO**
Density	**1,25 (±0,05)**	1183
Melt Index (MI), g/10 min (190°C / 2,16Kg)	**15 – 30**	1133
Optical properties	**Opaque**	
Melt temperature (°C)	**145 - 155**	
Degradation temperature (°C)	**200**	
Mechanical Properties		**ISO**
Tensile strength at break, MPa	**35**	527
Tensile elongation at break, %	**2**	527
Tensile Modulus, MPa	**2950**	527
Charpy Impact (non notched) 4J, kJ/m²	**4.8**	179
Thermal Properties		**ISO**
HDT A (1,8 MPa), °C	**72.5**	75-2

Applications examples: cutlery, caps, technical pieces…

Processing information

PHI 002 can be easily processed on injection moulding grades conventional equipments, especially those used for PET or PS (smooth barrel are recommended). The material is stable in the molten state, provided that the drying procedures are followed. Mould flow is highly dependent on melt temperature. It is recommended to balance screw speed, back pressure and process temperature to control melt temperature.

NaturePlast
13 ROUTE DE TROUVILLE • 14000 CAEN • TEL : (+33) 2 31 93 60 87 • FAX : (+33) 2 31 86 70 98 • www.natureplast.eu
SAS au capital de 223 700 € • APE : 4690Z / SIRET : 493 447 281 00013 • TVA : FR 05 493 447 281

NaturePlast
L'évolution naturelle du plastique

Drying

Drying is necessary for PLA resins. A moisture content of less than 0.025% (250 ppm) is recommended to prevent the material degradation. Typical drying conditions **are 70°C, air dew point of -40°C, 4 hours**; or 4 **hours at 40°C in vacuum conditions**. The resin should not be exposed to atmospheric conditions after drying. Keep the package sealed until ready to use and promptly reseal any unused material. (If the resin is exposed to atmospheric condition for more than one hour, it should be dried according to above-mentioned method).

Purge and startup

PHI 002 is not compatible with a wide variety of polyolefin resins, and special purging sequences should be followed:

1. Clean extruder and bring temperatures to steady state with low-viscosity, general-purpose polystyrene or polypropylene.

2. Vacuum out hopper system to avoid contamination, and make sure that the humidity of the air is below -40°C air dew point.

3. Introduce PHA polymer into the extruder at the operating conditions used in the first step.

4. Once PHA polymer has purged, reduce barrel temperatures to desired set points.

5. At shutdown, purge machine with high-viscosity polystyrene or polypropylene.

Processing temperature	
Material temperature	**160°C**
Feed throat	**21°C**
Convey section	**160°C**
Compression section	**165°C**
Metering section	**170°C**
Nozzle	**170°C**
Mould	**20-25°C**
Screw speed	**50 rpm**
Back pressure (minimum)	**85 bars**

Notice: don't go higher than 190°C during processing in order to avoid the material degradation and the loss of mechanical and processing properties.

NaturePlast
13 ROUTE DE TROUVILLE • 14000 CAEN • TEL : (33) 2 31 93 60 87 • FAX : (33) 2 31 94 70 99 • www.natureplast.eu
SAS au capital de 223 700 € • APE : 4690Z / SIRET : 450 447 881 00013 • TVA : FR 05 45 364 2881

A.2

Datasheet of Poly(Lactic Acid)

NatureWorks LLC

Ingeo™ Biopolymer 3251D
Injection Molding Process Guide

Ingeo™ Biopolymer 3251D is designed for injection molding applications. This polymer grade has a higher melt flow capability than other Ingeo™ resins currently in the market place. The higher flow capability allows for easier molding of thin-walled parts.

It is designed for injection molding applications, both clear and opaque, requiring high gloss, UV resistance and stiffness.

Processing Temperature Profile		
Melt Temperature	370-410°F	188-210°C
Feed Throat	70°F	20°C
Feed Temperature	330-350°F	166-177°C
Compression Section	360-380°F	182-193°C
Metering Section	370-400°F	188-205°C
Nozzle	370-400°F	188-205°C
Mold	75°F	25°C
Screw Speed	100-200 rpm	
Back Pressure	50-100 psi	
Mold Shrinkage	.004 in/in. +/-.001	

Note: These are starting points and may need to be optimized.

Processing Information

Ingeo™ Biopolymer 3251D can be processed on conventional injection molding equipment. The material is stable in the molten state, provided that the drying procedures are followed. Mold flow is highly dependent on melt temperature. In order to control melt temperature, it is recommended to balance screw speed, back pressure, and process temperature. Injection speed should be medium to fast.

Process Details

Startup and Shutdown

Ingeo™ Biopolymer 3251D is not compatible with a wide variety of other resins, and special purging sequences should be followed:

1. Clean extruder and bring temperatures to steady state with low-viscosity, general-purpose polystyrene or polypropylene.
2. Vacuum out hopper system to avoid contamination.
3. Introduce Ingeo™ polymer into the extruder at the operating conditions used in Step one.
4. Once Ingeo™ polymer has purged, reduce barrel temperatures to desired set points.
5. At shutdown, purge machine with high-viscosity polystyrene or polypropylene.

Table 1 – Typical Material & Application Properties [1]		
	Ingeo 3251D (General Purpose)	ASTM Method
Physical Properties		
Specific Gravity	1.24	D792
Melt Index, g/10 min (210°C/2.16K) Melt Index, g/10 min (190°C/2.16K)	70-85 30-40	D1238
Relative Viscosity	2.5	
Crystalline Melt Temperature (°C)	160-170	D3418
Glass Transition Temperature (°C)	55-65	D3417
Clarity	Transparent	
Mechanical Properties		
Tensile Yield Strength, psi (MPa)	7,000 (48)	D638
Tensile Elongation, %	2.5	D638
Notched Izod Impact, ft-lb/in (J/m)	0.3 (16.0)	D256
Flexural Strength (MPa)	12,000 (83)	D790

Ingeo™ Biopolymer 3251D

Drying
In-line drying is recommended for Ingeo™ biopolymers. A moisture content of less than 0.010% (100 ppm) is recommended to prevent viscosity degradation. Polymer is supplied in foil-lined boxes or bags dried to<250 ppm.The resin should not be exposed to atmospheric conditions after drying. Keep the package sealed until ready to use and promptly dry and reseal any unused material. The drying curves for both amorphous and crystalline resins are shown to the right.

Note: Amorphous polymer must be dried below 120F (50C).

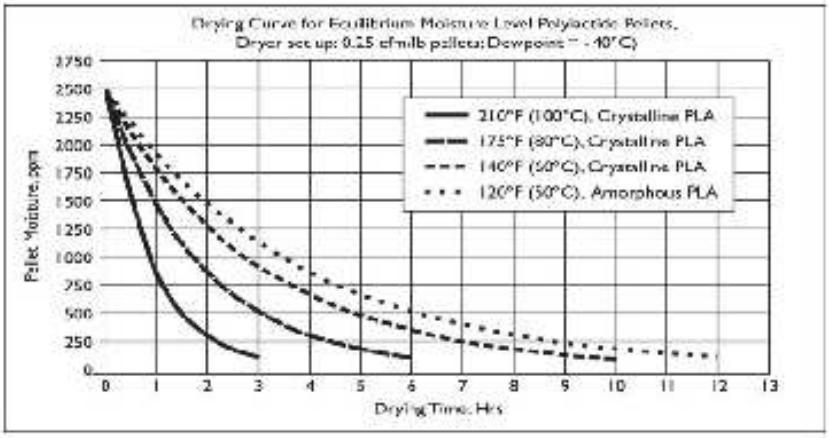

Compostability

Composting is a method of waste disposal that allows organic materials to be recycled into a product that can be used as a valuable soil amendment. Ingeo™ Biopolymer 3251D is made primarily of polylactic acid, a repeating chain of lactic acid, which undergoes a 2-step degradation process. First, the moisture and heat in the compost pile attack the polymer chains and split them apart, creating smaller polymers, and finally, lactic acid. Microorganisms in compost and soil consume the smaller polymer fragments and lactic acid as nutrients. Since lactic acid is widely found in nature, a large number of organisms metabolize lactic acid. At a minimum, fungi and bacteria are involved in polymer degradation. The end result of the process is carbon dioxide, water and also humus, a soil nutrient. This degradation process is temperature and humidity dependent. Regulatory guidelines and standards for composting revolve around four basic criteria: Material Characteristics, Biodegradation, Disintegration, and Eco-toxicity. Description of the requirements of these testing can be found in the appropriate geographical area: DIN V 54900-1 (Germany), EN 13432 (EU), ASTM D 6400 (USA), GreenPla (Japan).

This grade of NatureWorks® PLA meets the requirements of these four standards with limitation of maximum layer thickness of 1650 µm and for coating layers up to 37 µm thick

FDA Status

U.S. Status-
This is to advise you that on January 3, 2002 FCN 000178 submitted by NatureWorks® LLC to FDA became effective. This effective notification is part of list currently maintained on FDA's website at http://www.cfsan.fda.gov/~dms/opa-fcn.html. This grade of NatureWorks LLC Biopolymer may therefore be used in food packaging materials and, as such, is a permitted component of such materials pursuant to section 201(s) of the Federal, Drug, and Cosmetic Act, and Parts 182, 184, and 186 of the Food Additive Regulations. All additives and adjuncts contained in the referenced Ingeo™ Biopolymer formulation meet the applicable sections of the Federal Food, Drug, and Cosmetic Act. The finished polymer is approved for all food types and B-H use conditions. We urge all of our customers to perform GMP (Good Manufacturing Procedures) when constructing a package so that it is suitable for the end use. Again, for any application, should you need further clarification, please do not hesitate to contact NatureWorks LLC.

European Status
This grade of Ingeo™ Biopolymer complies with EU Plastics Directive 2002/72/EC, which applies to all EU member states. The Plastics Directive is a consolidated version of the "Monomers Directive (Commission Directive 90/128/EEC) and its first 7 amendments. This grade of Ingeo™ Biopolymer is also in compliance with "Bedarfgegenstände Gesetz", which is the German implementation of the EU Plastics Directive 2002/72/EC. Substances used in the manufacturing of this product which are not yet regulated by EU Plastics Directive 2002/72/EC, as amended, are in compliance with appropriate EU national regulations. NatureWorks® LLC would like to draw your attention to the fact that the EU-Directive 2002/72/EC, which applies to all EU-Member States, includes a limit of 10 mg/dm2 of the overall migration from finished plastic articles into food. In accordance with EU-Directive 2002/72/EC the mi-

gration should be measured on finished articles placed into contact with the foodstuff or appropriate food simulates for a period and at a temperature which are chosen by reference to the contact conditions in actual use, according to the rules laid down in EU-Directives 93/8/EEC (amending 82/711/EEC) and 85/572/EEC Please note that it is the responsibility of both the manufacturers of finished food contact articles as well as the industrial food packers to make sure that these articles in their actual use are in compliance with the imposed specific and overall migration requirements. Again, for any application, should you need further clarification, please do not hesitate to contact NatureWorks® LLC.

Safety and Handling Considerations
Material Safety Data (MSD) sheets for Ingeo™ Biopolymers are available from NatureWorks LLC. MSD sheets are provided to help customers satisfy their own handling, safety, and disposal needs, and those that may be required by locally applicable health and safety regulations, such as OSHA (U.S.A.), MAK (Germany), or WHMIS (Canada). MSD sheets are updated regularly; therefore, please request and review the most current MSD sheets before handling or using any product.

The following comments apply only to Ingeo™ Biopolymers; additives and processing aids used in fabrication and other materials used in finishing steps have their own safe-use profile and must be investigated separately.

Hazards and Handling Precautions
Ingeo™ Biopolymers have a very low degree of toxicity and, under normal conditions of use, should pose no unusual problems from incidental ingestion, or eye and skin contact. However, caution is advised when handling, storing, using, or disposing of these resins, and good housekeeping and controlling of dusts are necessary for safe handling of product. Workers should be protected from the possibility of contact with molten resin during fabrication. Handling and fabrication of resins can result in the generation of vapors and dusts that may cause irritation to eyes and the upper respiratory tract. In dusty atmospheres, use an approved dust respirator. Pellets or beads may present a slipping hazard. Good general ventilation of the polymer processing area is recommended. At temperatures exceeding the polymer melt temperature (typically 170ºC), polymer can release fumes, which may contain fragments of the polymer, creating a potential to irritate eyes and mucous membranes. Good general ventilation should be sufficient for most conditions. Local exhaust ventilation is recommended for melt operations. Use safety glasses if there is a potential for exposure to particles which could cause mechanical injury to the eye. If vapor exposure causes eye discomfort, use a full-face respirator. No other precautions other than clean, body-covering clothing should be needed for handling Ingeo™ Biopolymers. Use gloves with insulation for thermal protection when exposure to the melt is localized.

Combustibility
Ingeo™ Biopolymers will burn. Clear to white smoke is produced when product burns. Toxic fumes are released under conditions of incomplete combustion. Do not permit dust
to accumulate. Dust layers can be ignited by spontaneous combustion or other ignition sources. When suspended in air, dust can pose an explosion hazard. Firefighters should wear positive-pressure, self-contained breathing apparatuses and full protective equipment. Water or water fog is the preferred extinguishing medium. Foam, alcohol-resistant foam, carbon dioxide or dry chemicals may also be used. Soak thoroughly with water to cool and prevent re-ignition.

Disposal
DO NOT DUMP INTO ANY SEWERS, ON THE GROUND, OR INTO ANY BODY OF WATER. For unused or uncontaminated material, the preferred options include recycling into the process or sending to an industrial composting facility, if available; otherwise, send to an incinerator or other thermal destruction device. For used or contaminated material, the disposal options remain the same, although additional evaluation is required. (For example, in the U.S.A., see 40 CFR, Part 261, "Identification and Listing of Hazardous Waste.") All disposal methods must be in compliance with Federal, State/Provincial, and local laws and regulations.

NOTICE: No freedom from any patent owned by NatureWorks LLC or others is to be inferred. Because use conditions and applicable laws may differ from one location to another and may change with time, Customer is responsible for determining whether products and the information in this document are appropriate for Customer's use and for ensuring that Customer's workplace and disposal practices are in compliance with applicable laws and other governmental enactments. NatureWorks LLC assumes no obligation or liability for the information in
this document. **NO WARRANTIES ARE GIVEN; ALL IMPLIED WARRANTIES OF MERCHANTABILITY OR FITNESS FOR A PARTICULAR USE ARE EXPRESSLY EXCLUDED.**

Environmental Concerns
Generally speaking, lost pellets are not a problem in the environment except under unusual circumstances when they enter the marine environment. They are benign in terms of their physical environmental impact, but if ingested by waterfowl or aquatic life, they may mechanically cause adverse effects. Spills should be minimized, and they should be cleaned up when they happen. Plastics should not be discarded into the ocean or any other body of water.

Product Stewardship
NatureWorks LLC has a fundamental duty to all those that make and use our products, and for the environment in which we live. This duty is the basis for our Product Stewardship philosophy, by which we assess the health and environmental information on our products and their intended use, then take appropriate steps to protect the environment and the health of our employees and the public.

Customer Notice
NatureWorks LLC encourages its customers and potential users of its products to review their applications for such products from the standpoint of human health and environmental quality. To help ensure our products are not used in ways for which they were not intended or tested, our personnel will assist customers in dealing with ecological and product safety considerations. Your sales representative can arrange the proper contacts. NatureWorks LLC literature, including Material Safety Data sheets, should be consulted prior to the use of the company's products. These are available from your NatureWorks LLC representative.

NOTICE REGARDING PROHIBITED USE RESTRICTIONS: NatureWorks LLC does not recommend any of its products, including samples, for use as: Components of, or packaging for, tobacco products; Components of products where the end product is intended for human or animal consumption; In any application that is intended for any internal contact with human body fluids or body tissues; As a critical component in any medical device that supports or sustains human life; In any product that is designed specifically for ingestion or internal use by pregnant women; and in any application designed specifically to promote or interfere with human reproduction.

NatureWorks LLC

15305 Minnetonka Blvd., Minnetonka, MN 55345

For additional information in the U.S. and Canada,
call toll-free 1-877-423-7659
In Europe, call 31-(0)35-699-1344
In Japan, call 81-33-285-0824

A.3

Datasheet of Acylonitrile Butadiene Styrene

Overview of materials for Acrylonitrile Butadiene Styrene (ABS), Molded

Categories: Polymer; Thermoplastic; ABS Polymer; Acrylonitrile Butadiene Styrene (ABS), Molded

Material Notes: This property data is a summary of similar materials in the MatWeb database for the category "Acrylonitrile Butadiene Styrene (ABS), Molded". Each property range of values reported is minimum and maximum values of appropriate MatWeb entries. The comments report the average value, and number of data points used to calculate the average. The values are not necessarily typical of any specific grade, especially less common values and those that can be most affected by additives or processing methods.

Vendors: Click here to view all available suppliers for this material.

Please click here if you are a supplier and would like information on how to add your listing to this material.

Physical Properties	Metric	English	Comments
Density	0.350 - 3.50 g/cc	0.0126 - 0.126 lb/in³	Average value: 1.06 g/cc Grade Count:295
Water Absorption	0.0250 - 2.30 %	0.0250 - 2.30 %	Average value: 0.422 % Grade Count:75
Moisture Absorption at Equilibrium	0.150 - 0.220 %	0.150 - 0.220 %	Average value: 0.197 % Grade Count:25
Water Absorption at Saturation	0.300 - 1.00 %	0.300 - 1.00 %	Average value: 0.736 % Grade Count:22
Viscosity	155000 - 255000 cP @Temperature 240 - 260 °C	155000 - 255000 cP @Temperature 464 - 500 °F	Average value: 195000 cP Grade Count:7
Maximum Moisture Content	0.150	0.150	Average value: 0.150 Grade Count:9
Linear Mold Shrinkage	0.00150 - 0.00800 cm/cm	0.00150 - 0.00800 in/in	Average value: 0.00525 cm/cm Grade Count:191
Linear Mold Shrinkage, Transverse	0.00250 - 0.00800 cm/cm	0.00250 - 0.00800 in/in	Average value: 0.00522 cm/cm Grade Count:18
Melt Flow	0.0800 - 80.0 g/10 min	0.0800 - 80.0 g/10 min	Average value: 12.3 g/10 min Grade Count:299
Spiral Flow	73.66 - 86.36 cm @Temperature 260 - 260 °C	29.00 - 34.00 in @Temperature 500 - 500 °F	Average value: 80.0 cm Grade Count:2

Chemical Properties	Metric	English	Comments
Styrene Content	0.0500 %	0.0500 %	Average value: 0.0500 % Grade Count:6

Mechanical Properties	Metric	English	Comments
Hardness, Rockwell R	95.0 - 119	95.0 - 119	Average value: 108 Grade Count:131
Hardness, H358/30	85.0 - 104 MPa	12300 - 15100 psi	Average value: 93.6 MPa Grade Count:10
Ball	86.0 - 115 MPa	12500 - 16700 psi	Average value: 98.2 MPa Grade

Indentation Hardness			Count:18
Tensile Strength, Ultimate	24.1 - 73.1 MPa	3500 - 10600 psi	Average value: 38.4 MPa Grade Count:131
	20.0 - 52.0 MPa @Temperature -18.0 - 90.0 °C	2900 - 7540 psi @Temperature -0.400 - 194 °F	Average value: 35.8 MPa Grade Count:3
Tensile Strength, Yield	20.0 - 73.1 MPa	2900 - 10600 psi	Average value: 43.3 MPa Grade Count:256
	64.0 - 64.0 MPa @Temperature -18.0 - -18.0 °C	9280 - 9280 psi @Temperature -0.400 - -0.400 °F	Average value: 64.0 MPa Grade Count:1
Elongation at Break	2.40 - 110 %	2.40 - 110 %	Average value: 26.1 % Grade Count:194
	15.0 - 15.0 % @Temperature -18.0 - -18.0 °C	15.0 - 15.0 % @Temperature -0.400 - -0.400 °F	Average value: 15.0 % Grade Count:1
Elongation at Yield	1.70 - 20.0 %	1.70 - 20.0 %	Average value: 3.19 % Grade Count:116
Modulus of Elasticity	0.778 - 6.10 GPa	113 - 885 ksi	Average value: 2.33 GPa Grade Count:184
	2.81 - 2.81 GPa @Temperature -18.0 - -18.0 °C	408 - 408 ksi @Temperature -0.400 - -0.400 °F	Average value: 2.81 GPa Grade Count:1
Flexural Modulus	0.0241 - 6.89 GPa	3.50 - 1000 ksi	Average value: 2.36 GPa Grade Count:228
	1.50 - 4.00 GPa @Temperature 60.0 - 90.0 °C	218 - 580 ksi @Temperature 140 - 194 °F	Average value: 2.84 GPa Grade Count:2
Flexural Yield Strength	10.3 - 111 MPa	1500 - 16100 psi	Average value: 68.6 MPa Grade Count:181
Izod Impact, Unnotched	0.981 J/cm - NB	1.84 ft-lb/in - NB	Average value: 6.11 J/cm Grade Count:16
	0.600 - 2.00 J/cm @Temperature -30.0 - 0.000 °C	1.12 - 3.75 ft-lb/in @Temperature -22.0 - 32.0 °F	Average value: 1.28 J/cm Grade Count:3
Izod Impact, Unnotched (ISO)	39.2 kJ/m² - NB	18.7 ft-lb/in² - NB	Average value: 69.7 kJ/m² Grade Count:20
	NB - NB @Temperature -20.0 - -20.0 °C	NB - NB @Temperature -4.00 - -4.00 °F	Grade Count:1
	NB - NB @Thickness 4.00 - 4.00 mm	NB - NB @Thickness 0.157 - 0.157 in	Grade Count:1
Charpy Impact Unnotched	2.00 J/cm² - NB	9.52 ft-lb/in² - NB	Average value: 11.7 J/cm² Grade Count:82
	0.300 J/cm² - NB @Temperature -40.0 - -20.0 °C	1.43 ft-lb/in² - NB @Temperature -40.0 - -4.00 °F	Average value: 5.98 J/cm² Grade Count:54
Charpy Impact, Notched	0.500 - 14.0 J/cm²	2.38 - 66.6 ft-lb/in²	Average value: 1.90 J/cm² Grade Count:115
	0.300 - 1.60 J/cm² @Temperature -30.0 - -30.0 °C	1.43 - 7.61 ft-lb/in² @Temperature -22.0 - -22.0 °F	Average value: 0.802 J/cm² Grade Count:53
Gardner Impact	1.80 - 22.6 J	1.33 - 16.7 ft-lb	Average value: 15.5 J Grade Count:5
Falling Dart Impact	2.82 - 37.6 J	2.08 - 27.7 ft-lb	Average value: 22.7 J Grade Count:6
Tensile Creep Modulus, 1 hour	2200 - 2500 MPa	319000 - 363000 psi	Average value: 2370 MPa Grade Count:3

Tensile Creep Modulus, 1000 hours	1500 - 1900 MPa	218000 - 276000 psi	Average value: 1770 MPa Grade Count:3
Taber Abrasion, mg/1000 Cycles	50.0 - 115	50.0 - 115	Average value: 99.4 Grade Count:10
Izod Impact, Notched	0.100 - 6.40 J/cm	0.187 - 12.0 ft-lb/in	Average value: 2.29 J/cm Grade Count:221
	0.350 - 2.14 J/cm @Temperature -50.0 - -20.0 °C	0.656 - 4.01 ft-lb/in @Temperature -58.0 - -4.00 °F	Average value: 0.827 J/cm Grade Count:10
	0.480 - 1.87 J/cm @Temperature -40.0 - 0.000 °C	0.899 - 3.50 ft-lb/in @Temperature -40.0 - 32.0 °F	Average value: 0.827 J/cm Grade Count:8
	0.480 - 1.87 J/cm @Thickness 3.17 - 3.20 mm	0.899 - 3.50 ft-lb/in @Thickness 0.125 - 0.126 in	Average value: 0.827 J/cm Grade Count:8
Izod Impact, Notched (ISO)	2.00 - 48.0 kJ/m²	0.952 - 22.8 ft-lb/in²	Average value: 17.4 kJ/m² Grade Count:71
	4.00 - 16.0 kJ/m² @Temperature -30.0 - 0.000 °C	1.90 - 7.61 ft-lb/in² @Temperature -22.0 - 32.0 °F	Average value: 8.81 kJ/m² Grade Count:36
	6.00 - 13.0 kJ/m² @Temperature -40.0 - -20.0 °C	2.86 - 6.19 ft-lb/in² @Temperature -40.0 - -4.00 °F	Average value: 8.81 kJ/m² Grade Count:3
	6.00 - 13.0 kJ/m² @Thickness 4.00 - 4.00 mm	2.86 - 6.19 ft-lb/in² @Thickness 0.157 - 0.157 in	Average value: 8.81 kJ/m² Grade Count:3

Electrical Properties	**Metric**	**English**	**Comments**
Electrical Resistivity	1.00e+9 - 1.00e+18 ohm-cm	1.00e+9 - 1.00e+18 ohm-cm	Average value: 1.55e+16 ohm-cm Grade Count:76
Surface Resistance	1000 - 2.00e+17 ohm	1000 - 2.00e+17 ohm	Average value: 3.51e+15 ohm Grade Count:71
Static Decay	0.300 - 3.00 sec	0.300 - 3.00 sec	Average value: 1.56 sec Grade Count:5
Dielectric Constant	2.00 - 3.50	2.00 - 3.50	Average value: 2.90 Grade Count:45
Dielectric Strength	15.7 - 53.0 kV/mm	400 - 1350 kV/in	Average value: 30.1 kV/mm Grade Count:58
Dissipation Factor	0.00400 - 0.0150	0.00400 - 0.0150	Average value: 0.00771 Grade Count:42
Arc Resistance	60.0 - 120 sec	60.0 - 120 sec	Average value: 87.9 sec Grade Count:7
Comparative Tracking Index	92.0 - 600 V	92.0 - 600 V	Average value: 560 V Grade Count:63
Hot Wire Ignition, HWI	7.00 - 30.0 sec	7.00 - 30.0 sec	Average value: 19.2 sec Grade Count:7
High Amp Arc Ignition, HAI	15.0 - 120 arcs	15.0 - 120 arcs	Average value: 106 arcs Grade Count:7
High Voltage Arc-Tracking Rate, HVTR	25.4 - 150 mm/min	1.00 - 5.91 in/min	Average value: 83.8 mm/min Grade Count:6

Thermal Properties	**Metric**	**English**	**Comments**
CTE, linear	0.800 - 155 µm/m-°C	0.444 - 86.1 µin/in-°F	Average value: 79.9 µm/m-°C Grade Count:128
CTE, linear,	73.8 - 100 µm/m-°C	41.0 - 55.6 µin/in-°F	Average value: 86.9 µm/m-°C Grade

Transverse to Flow			Count:33
Specific Heat Capacity	1.96 - 2.13 J/g-°C	0.468 - 0.509 BTU/lb-°F	Average value: 2.05 J/g-°C Grade Count:6
Thermal Conductivity	0.128 - 0.200 W/m-K	0.888 - 1.39 BTU-in/hr-ft²-°F	Average value: 0.179 W/m-K Grade Count:19
Maximum Service Temperature, Air	77.0 - 109 °C	171 - 228 °F	Average value: 93.6 °C Grade Count:12
Hot Ball Pressure Test	75.0 - 90.0 °C	167 - 194 °F	Average value: 82.5 °C Grade Count:6
Deflection Temperature at 0.46 MPa (66 psi)	68.0 - 140 °C	154 - 284 °F	Average value: 96.0 °C Grade Count:157
Deflection Temperature at 1.8 MPa (264 psi)	65.0 - 220 °C	149 - 428 °F	Average value: 90.0 °C Grade Count:282
	96.0 - 96.0 °C @Temperature 120 - 120 °C	205 - 205 °F @Temperature 248 - 248 °F	Average value: 94.7 °C Grade Count:1
	94.0 - 94.0 °C @Temperature 80.0 - 80.0 °C	201 - 201 °F @Temperature 176 - 176 °F	Average value: 94.7 °C Grade Count:1
	94.0 - 94.0 °C @Time 14400 - 14400 sec	201 - 201 °F @Time 4.00 - 4.00 hour	Average value: 94.7 °C Grade Count:1
Vicat Softening Point	45.0 - 135 °C	113 - 275 °F	Average value: 101 °C Grade Count:213
Heat Distortion Temperature	85.0 - 86.1 °C	185 - 187 °F	Average value: 85.4 °C Grade Count:3
Glass Transition Temp, Tg	105 - 109 °C	221 - 228 °F	Average value: 107 °C Grade Count:9
UL RTI, Electrical	50.0 - 80.0 °C	122 - 176 °F	Average value: 63.2 °C Grade Count:22
UL RTI, Mechanical with Impact	50.0 - 80.0 °C	122 - 176 °F	Average value: 65.9 °C Grade Count:22
UL RTI, Mechanical without Impact	50.0 - 80.0 °C	122 - 176 °F	Average value: 63.2 °C Grade Count:22
Flammability, UL94	HB - 5VA	HB - 5VA	Grade Count:210
Oxygen Index	19.0 - 30.0 %	19.0 - 30.0 %	Average value: 21.6 % Grade Count:5
Glow Wire Test	650 - 960 °C	1200 - 1760 °F	Average value: 714 °C Grade Count:18

Optical Properties	**Metric**	**English**	**Comments**
Gloss	25.0 - 96.7 %	25.0 - 96.7 %	Average value: 77.9 % Grade Count:33
Transmission, Visible	0.000 - 88.0 %	0.000 - 88.0 %	Average value: 46.9 % Grade Count:11

Processing Properties	Metric	English	Comments
Processing Temperature	160 - 274 °C	320 - 525 °F	Average value: 232 °C Grade Count:93
Rear Barrel Temperature	149 - 250 °C	300 - 482 °F	Average value: 201 °C Grade Count:44
Middle Barrel Temperature	177 - 255 °C	350 - 491 °F	Average value: 217 °C Grade Count:53
Front Barrel Temperature	191 - 260 °C	375 - 500 °F	Average value: 228 °C Grade Count:44
Nozzle Temperature	191 - 274 °C	375 - 525 °F	Average value: 231 °C Grade Count:34
Mold Temperature	10.0 - 85.0 °C	50.0 - 185 °F	Average value: 57.5 °C Grade Count:99
Injection Velocity	200 - 240 mm/sec	7.87 - 9.45 in/sec	Average value: 206 mm/sec Grade Count:13
Drying Temperature	70.0 - 93.3 °C	158 - 200 °F	Average value: 82.1 °C Grade Count:83
Dry Time	2.00 - 24.0 hour	2.00 - 24.0 hour	Average value: 4.08 hour Grade Count:73
Moisture Content	0.0100 - 0.150 %	0.0100 - 0.150 %	Average value: 0.0714 % Grade Count:29
Dew Point	-29.0 - -17.8 °C	-20.2 - 0.000 °F	Average value: -26.2 °C Grade Count:12
Injection Pressure	4.14 - 130 MPa	600 - 18900 psi	Average value: 54.7 MPa Grade Count:49
Back Pressure	0.000 - 2.00 MPa	0.000 - 290 psi	Average value: 0.623 MPa Grade Count:44
Clamp Pressure	30.8 - 69.0 MPa	4470 - 10000 psi	Average value: 48.7 MPa Grade Count:7
Shot Size	30.0 - 80.0 %	30.0 - 80.0 %	Average value: 57.7 % Grade Count:13
Vent Depth	0.00380 - 0.00760 cm	0.00150 - 0.00299 in	Average value: 0.00487 cm Grade Count:6
Cushion	0.317 - 0.635 cm	0.125 - 0.250 in	Average value: 0.544 cm Grade Count:7
Screw Speed	25.0 - 100 rpm	25.0 - 100 rpm	Average value: 63.5 rpm Grade Count:34

Some of the values displayed above may have been converted from their original units and/or rounded in order to display the information in a consistent format. Users requiring more precise data for scientific or engineering calculations can click on the property value to see the original value as well as other conversions to equivalent units. We advise that you only use the original value or one of the new conversions in your calculations to minimize rounding error. We also ask that you refer to MatWeb's terms of use regarding this information. Click here to view all the property values for this datasheet as they were originally entered into MatWeb.

A.4

Datasheet of PolyPropylene

Overview of materials for Polypropylene, Molded

Categories: Polymer; Thermoplastic; Polypropylene (PP); Polypropylene, Molded

Material Notes: This property data is a summary of similar materials in the MatWeb database for the category "Polypropylene, Molded". Each property range of values reported is minimum and maximum values of appropriate MatWeb entries. The comments report the average value, and number of data points used to calculate the average. The values are not necessarily typical of any specific grade, especially less common values and those that can be most affected by additives or processing methods.

Vendors: Click here to view all available suppliers for this material.

Please click here if you are a supplier and would like information on how to add your listing to this material.

Physical Properties	Metric	English	Comments
Bulk Density	0.525 g/cc	0.0190 lb/in³	Average value: 0.525 g/cc Grade Count:33
Density	0.886 - 1.70 g/cc	0.0320 - 0.0614 lb/in³	Average value: 0.933 g/cc Grade Count:729
Filler Content	20.0 - 70.0 %	20.0 - 70.0 %	Average value: 36.7 % Grade Count:3
Water Absorption	0.000 - 1.00 %	0.000 - 1.00 %	Average value: 0.0714 % Grade Count:121
Moisture Absorption at Equilibrium	0.100 %	0.100 %	Average value: 0.100 % Grade Count:58
Water Absorption at Saturation	0.0100 %	0.0100 %	Average value: 0.0100 % Grade Count:5
Particle Size	5.00 - 2500 µm	5.00 - 2500 µm	Average value: 741 µm Grade Count:11
Viscosity Measurement	80.0 - 500000 @Temperature 180 - 180 °C	80.0 - 500000 @Temperature 356 - 356 °F	Average value: 171000 Grade Count:3
Thickness	25.4 - 102 microns	1.00 - 4.00 mil	Average value: 88.9 microns Grade Count:6
Linear Mold Shrinkage	0.000 - 0.0250 cm/cm	0.000 - 0.0250 in/in	Average value: 0.0132 cm/cm Grade Count:203
Linear Mold Shrinkage, 6.35 mm section	0.0250 cm/cm	0.0250 in/in	Average value: 0.0250 cm/cm Grade Count:5
Linear Mold Shrinkage, Transverse	0.0100 - 0.0155 cm/cm	0.0100 - 0.0155 in/in	Average value: 0.0134 cm/cm Grade Count:5
Melt Flow	0.200 - 2000 g/10 min	0.200 - 2000 g/10 min	Average value: 27.1 g/10 min Grade Count:829
Base Resin Melt Index	0.500 - 50.0 g/10 min	0.500 - 50.0 g/10 min	Average value: 15.1 g/10 min Grade Count:17
Ash	0.00800 - 26.0 %	0.00800 - 26.0 %	Average value: 1.16 % Grade Count:23
Collected Volatile Condensable Material	0.0500 - 3.00 %	0.0500 - 3.00 %	Average value: 0.391 % Grade Count:29

Mechanical	Metric	English	Comments

Properties			
Hardness, Rockwell R	20.0 - 117	20.0 - 117	Average value: 95.8 Grade Count:414
Hardness, Shore D	40.0 - 83.0	40.0 - 83.0	Average value: 68.6 Grade Count:69
Ball Indentation Hardness	62.0 - 106 MPa	8990 - 15400 psi	Average value: 85.5 MPa Grade Count:15
Tensile Strength, Ultimate	9.00 - 80.0 MPa	1310 - 11600 psi	Average value: 31.1 MPa Grade Count:155
	10.0 - 23.0 MPa @Temperature 60.0 - 120 °C	1450 - 3340 psi @Temperature 140 - 248 °F	Average value: 16.0 MPa Grade Count:1
Film Elongation at Break, MD	93.0 - 530 %	93.0 - 530 %	Average value: 258 % Grade Count:3
Tenacity	0.203 - 0.441 N/tex	2.30 - 5.00 g/denier	Average value: 0.308 N/tex Grade Count:8
Tensile Strength, Yield	12.0 - 369 MPa	1740 - 53500 psi	Average value: 32.3 MPa Grade Count:766
Elongation at Break	3.00 - 900 %	3.00 - 900 %	Average value: 156 % Grade Count:288
Elongation at Yield	3.50 - 100 %	3.50 - 100 %	Average value: 9.65 % Grade Count:554
Modulus of Elasticity	0.00800 - 8.25 GPa	1.16 - 1200 ksi	Average value: 1.72 GPa Grade Count:213
Flexural Modulus	0.0260 - 6.89 GPa	3.77 - 999 ksi	Average value: 1.44 GPa Grade Count:721
	0.350 - 0.680 GPa @Temperature 60.0 - 120 °C	50.8 - 98.6 ksi @Temperature 140 - 248 °F	Average value: 0.472 GPa Grade Count:2
Flexural Yield Strength	20.0 - 180 MPa	2900 - 26100 psi	Average value: 48.1 MPa Grade Count:53
Compressive Yield Strength	34.5 - 55.2 MPa	5000 - 8000 psi	Average value: 39.0 MPa Grade Count:8
Compressive Modulus	1.38 GPa	200 ksi	Average value: 1.38 GPa Grade Count:6
Shear Modulus	0.680 - 0.920 GPa	98.6 - 133 ksi	Average value: 0.757 GPa Grade Count:10
Secant Modulus	1.03 - 2.20 GPa	150 - 319 ksi	Average value: 1.39 GPa Grade Count:6
Izod Impact, Unnotched	0.196 J/cm - NB	0.367 ft-lb/in - NB	Average value: 8.39 J/cm Grade Count:57
	2.1356 - 5338.47 J/cm @Temperature -18.0 - -18.0 °C	4.0009 - 10001.1 ft-lb/in @Temperature -0.400 - -0.400 °F	Average value: 10.9 J/cm Grade Count:12
Izod Impact, Unnotched (ISO)	NB	NB	Grade Count:6
Charpy Impact Unnotched	0.300 J/cm² - NB	1.43 ft-lb/in² - NB	Average value: 8.29 J/cm² Grade Count:100
	0.700 J/cm² - NB @Temperature -50.0 - -20.0 °C	3.33 ft-lb/in² - NB @Temperature -58.0 - -4.00 °F	Average value: 4.06 J/cm² Grade Count:94
Charpy Impact, Notched	0.200 - 9.50 J/cm²	0.952 - 45.2 ft-lb/in²	Average value: 1.24 J/cm² Grade Count:104

	0.130 - 1.70 J/cm² @Temperature -30.0 - 10.0 °C	0.619 - 8.09 ft-lb/in² @Temperature -22.0 - 50.0 °F	Average value: 0.367 J/cm² Grade Count:85
Gardner Impact	0.904 - 40.7 J	0.667 - 30.0 ft-lb	Average value: 10.3 J Grade Count:59
	1.99983 - 36.1552 J @Temperature -30.0 - -18.0 °C	1.47500 - 26.6667 ft-lb @Temperature -22.0 - -0.400 °F	Average value: 20.2 J Grade Count:27
	15.0225 - 23.9528 J @Temperature -30.0 - -30.0 °C	11.0800 - 17.6667 ft-lb @Temperature -22.0 - -22.0 °F	Average value: 20.2 J Grade Count:8
	15.0225 - 23.9528 J @Thickness 3.17 - 3.20 mm	11.0800 - 17.6667 ft-lb @Thickness 0.125 - 0.126 in	Average value: 20.2 J Grade Count:8
Falling Dart Impact	4.98 - 28.0 J	3.67 - 20.7 ft-lb	Average value: 10.8 J Grade Count:5
Coefficient of Friction	0.250	0.250	Average value: 0.250 Grade Count:6
Tensile Creep Modulus, 1 hour	550 - 700 MPa	79800 - 102000 psi	Average value: 657 MPa Grade Count:7
Tensile Creep Modulus, 1000 hours	220 - 440 MPa	31900 - 63800 psi	Average value: 349 MPa Grade Count:7
Tear Strength	20.2 - 226 kN/m	115 - 1290 pli	Average value: 115 kN/m Grade Count:8
Compression Set	16.0 - 65.0 %	16.0 - 65.0 %	Average value: 31.0 % Grade Count:5
Film Tensile Strength at Break, MD	3.10 - 152 MPa	450 - 22000 psi	Average value: 70.1 MPa Grade Count:3
Tangent Modulus	1290 - 3260 MPa	187000 - 472000 psi	Average value: 1910 MPa Grade Count:8
Izod Impact, Notched	0.160 J/cm - NB	0.300 ft-lb/in - NB	Average value: 0.784 J/cm Grade Count:655
	0.0400 - 0.90763 J/cm @Temperature -40.0 - 0.000 °C	0.0749 - 1.7004 ft-lb/in @Temperature -40.0 - 32.0 °F	Average value: 0.447 J/cm Grade Count:52
	1.00 - 1.35 J/cm @Temperature -20.0 - -20.0 °C	1.87 - 2.53 ft-lb/in @Temperature -4.00 - -4.00 °F	Average value: 0.447 J/cm Grade Count:2
	1.00 - 1.35 J/cm @Diameter 3.17 - 3.17 mm	1.87 - 2.53 ft-lb/in @Diameter 0.125 - 0.125 in	Average value: 0.447 J/cm Grade Count:2
Izod Impact, Notched (ISO)	2.00 - 56.0 kJ/m²	0.952 - 26.6 ft-lb/in²	Average value: 8.99 kJ/m² Grade Count:49
	1.10 - 8.00 kJ/m² @Temperature -40.0 - 2.00 °C	0.523 - 3.81 ft-lb/in² @Temperature -40.0 - 35.6 °F	Average value: 4.02 kJ/m² Grade Count:26

Electrical Properties	**Metric**	**English**	**Comments**
Electrical Resistivity	1000 - 1.00e+18 ohm-cm	1000 - 1.00e+18 ohm-cm	Average value: 1.46e+17 ohm-cm Grade Count:88
Surface Resistance	100 - 1.00e+15 ohm	100 - 1.00e+15 ohm	Average value: 1.35e+14 ohm Grade Count:79
Static Decay	0.0100 - 20.0 sec	0.0100 - 20.0 sec	Average value: 2.03 sec Grade Count:10
Dielectric Constant	2.20 - 2.38	2.20 - 2.38	Average value: 2.30 Grade Count:63
Dielectric Strength	19.7 - 140 kV/mm	500 - 3560 kV/in	Average value: 128 kV/mm Grade Count:65
Dissipation Factor	0.0000700 - 0.00300	0.0000700 - 0.00300	Average value: 0.000410 Grade Count:61
Arc	88.0 - 136 sec	88.0 - 136 sec	Average value: 104 sec Grade Count:3

Resistance			
Comparative Tracking Index	600 V	600 V	Average value: 600 V Grade Count:60

Thermal Properties	Metric	English	Comments
CTE, linear	18.0 - 185 µm/m-°C	10.0 - 103 µin/in-°F	Average value: 113 µm/m-°C Grade Count:109
Melting Point	61.0 - 180 °C	142 - 356 °F	Average value: 159 °C Grade Count:185
Crystallization Temperature	110 - 115 °C	230 - 239 °F	Average value: 111 °C Grade Count:5
Maximum Service Temperature, Air	65.0 - 125 °C	149 - 257 °F	Average value: 78.3 °C Grade Count:26
Deflection Temperature at 0.46 MPa (66 psi)	55.0 - 238 °C	131 - 460 °F	Average value: 102 °C Grade Count:663
Deflection Temperature at 1.8 MPa (264 psi)	37.0 - 172 °C	98.6 - 341 °F	Average value: 63.4 °C Grade Count:242
Vicat Softening Point	35.0 - 158 °C	95.0 - 316 °F	Average value: 119 °C Grade Count:272
Minimum Service Temperature, Air	-30.0 °C	-22.0 °F	Average value: -30.0 °C Grade Count:5
Brittleness Temperature	-20.0 - 21.0 °C	-4.00 - 69.8 °F	Average value: -15.4 °C Grade Count:18
UL RTI, Electrical	65.0 - 221 °C	149 - 430 °F	Average value: 140 °C Grade Count:6
UL RTI, Mechanical with Impact	65.0 - 221 °C	149 - 430 °F	Average value: 140 °C Grade Count:6
UL RTI, Mechanical without Impact	65.0 - 221 °C	149 - 430 °F	Average value: 140 °C Grade Count:6
Flammability, UL94	HB - V-0	HB - V-0	Grade Count:79
Oxygen Index	24.0 - 30.0 %	24.0 - 30.0 %	Average value: 26.3 % Grade Count:6
Shrinkage	1.05 - 2.00 %	1.05 - 2.00 %	Average value: 1.36 % Grade Count:23

Optical Properties	Metric	English	Comments
Haze	0.200 - 91.0 %	0.200 - 91.0 %	Average value: 37.8 % Grade Count:59
Gloss	30.0 - 160 %	30.0 - 160 %	Average value: 65.3 % Grade Count:20
Yellow Index	0.000300 - 2.44 %	0.000300 - 2.44 %	Average value: 0.426 % Grade Count:10

Processing Properties	Metric	English	Comments

Processing Temperature	87.8 - 320 °C	190 - 608 °F	Average value: 209 °C Grade Count:111
Feed Temperature	180 - 210 °C	356 - 410 °F	Average value: 195 °C Grade Count:5
Rear Barrel Temperature	177 - 274 °C	350 - 525 °F	Average value: 207 °C Grade Count:23
Middle Barrel Temperature	191 - 274 °C	375 - 525 °F	Average value: 212 °C Grade Count:27
Front Barrel Temperature	199 - 274 °C	390 - 525 °F	Average value: 221 °C Grade Count:23
Nozzle Temperature	204 - 243 °C	400 - 470 °F	Average value: 225 °C Grade Count:17
Head Temperature	210 °C	410 °F	Average value: 210 °C Grade Count:5
Mold Temperature	5.00 - 80.0 °C	41.0 - 176 °F	Average value: 40.3 °C Grade Count:73
Ejection Temperature	26.7 - 54.4 °C	80.0 - 130 °F	Average value: 40.6 °C Grade Count:4
Roll Temperature	40.0 - 50.0 °C	104 - 122 °F	Average value: 43.3 °C Grade Count:5
Drying Temperature	60.0 - 100 °C	140 - 212 °F	Average value: 76.9 °C Grade Count:24
Dry Time	1.00 - 4.00 hour	1.00 - 4.00 hour	Average value: 2.55 hour Grade Count:30
Moisture Content	0.0500 - 1.00 %	0.0500 - 1.00 %	Average value: 0.620 % Grade Count:15
Injection Pressure	2.76 - 103 MPa	400 - 15000 psi	Average value: 58.9 MPa Grade Count:32
Hold Pressure	2.07 - 8.27 MPa	300 - 1200 psi	Average value: 5.17 MPa Grade Count:6
Back Pressure	0.172 - 1.03 MPa	24.9 - 150 psi	Average value: 0.603 MPa Grade Count:10

A.5

General References

In addition to the references already listed in the thesis it also was consulted the following:

Papers in Peered Journals

[1] G.E. Luckachan, C.K.S. Pillai, *Biodegradable Polymers – A Review on Recent Trends and Emerging Perspectives*, Journal of Polymers and the Environment, vol.19, pp. 637-676 (2011)

[2] R.M. Rasal, A.V. Janorkar, D.E. Hirt, *Poly(lactic acid) modifications*, Progress in Polymer Science, vol. 35, pp.338-356 (2010)

[3] Z. Wang, Y. Li, J. Yang, Q. Gou, Y. Wu, X. Wu, P. Liu, Q. Gu, *Twisting of Lamellar Crystalls in Poly(3-hydroxybutyrate-co-3-hydroxyvalerate) Ring-Banded Spherulites*, Macromolecules, vol. 43, pp. 4441-4444 (2010)

[4] M. Cheng, Y. Sun, *Relationship between free volume properties and structure of poly(3-hydroxybutyrate-co-3-hydroxyvalerate) membranes via various crystallization conditions,* Polymer, vol. 50, pp. 5298-5307 (2009)

[5] A.U.B. Queiroz, F. P. C.-Queiroz, *Innovation and Industrial Trends in Bioplastics*, Journal of Macromolecular Science: Part C: Polymer Reviews, vol.49, pp. 65-78 (2009)

[6] K. Numata, H. Abe, T. Iwata, *Biodegradability of Poly(hydroxyalkanoate) Materials*, Materials, vol.2, pp. 1104-1126 (2009)

[7] L. Miao, Z. Qiu, W. Yang, T. Ikehara, *Fully biodegradable poly(3-hydroxybutyrate-co-hydroxyvalerate)/Poly(ethylene succinate) blends: Phase behavior, crystallization and mechanical properties,* Reactive & Functional Polymers, vol.68, pp. 446 – 457 (2008)

[8] S. Ghosh, R.L. Reis, J. Mano, *Bio-inspired Mineral Growth on Porous Spherulitic Textured Poly(L-lactic Acid)/ Bioactive Glass Composite Scaffolds*, Advanced Engineering Materials, pp.B18-B22 (2008)

[9] S. Ghosh, J.C. Viana, R.L Reis, J.F. Mano, *Development of porous lamelar poly(L- lactic acid) scaffolds by conventional injection molding process*¸ Acta Biomaterilia, vol.4, pp. 887-896 (2008)

[10] S. Singh, A.K. Mohanty, T. Sugie, Y. Takai, H. Hamada, *Renewable resource based biocomposites from natural fiber and polyhydroxy-co—valerate (PHBV) bioplastics*, Composites: Part A, vol. 39, pp. 875-886 (2008)

[11] Y. Xie, I. Noda, Y.A. Akpalu, *Influence of Cooling Rate on Thermal Behavior and Solid-State Morphologies of Polyhydrxyalkanoates*, Journal of Applied Polymer Science, vol. 109, pp. 2259-2268 (2008)

[12] E.B. Hermida, V.I. Mega, *Transcrystallization kinetics at the poly(3-hydroxybutyrate-co-3-hydroxyvalerate)/hemp fibre interface*, Composites: Part A, vol.38, pp. 1387–1394 (2007)

[13] S. Ghosh, J.C. Viana, R.L. Reis, J.F. Mano, *The double porogen approach as a new technique for the fabrication of interconnected poly(L-lactic acid) and starch based biodegradable scaffolds*¸ Journal of Material Science: Materials in Medicine, vol.18, pp. 185-193 (2007)

[14] E.M. Antipov, V.A. Dubinsky, A.V. Rebrov, Y.P. Nekrasov, S.A. Gordeev, G. Ungar, *Strain-induced mesophase and hard-elastic behavior of biodegradable polyhydroxyalkanoates fibers*, Polymer, vol. 47, pp. 5678 – 5690 (2006)

[15] L. Yu, K. Dean, L. Li, *Polymer blends and composites from renewable resources,* Progress in Polymer Science, vol.31, pp. 576-602 (2006)

[16] M.A.T. Duarte, R.G. Hugen, E.S. Martins, A.P.T. Pezzin, S.H. Pezzin, *Thermal and Mechanical Behavior of Injection Molded Poly(3-hydroxybutyrate/Poly(ε-caprolactone) Blends*, Materials Research, vol.9, pp.25-27 (2006)

[17] M.S. Huda, L.T. Drzal. A.K. Mohanty, M. Misra, *Chopped glass and recycled newspaper as reinforcement fibers in injection molded poly(lactic acid) (PLA) composites: A comparative study*, Composites Science and Technology, vol. 66, pp. 1813 – 1824 (2006)

[18] L. Sharma, Y. Ogino, T. Kanaya, *Shish Kebab Morphology induced in Polyhydroxybutyrate under shear flow*, Macromolecular Materials and Engineering, vol. 289, pp. 1059 – 1067 (2004)

[19] A.K. Mohanty, M.Misra, L.T. Drzal, *Sustainable Bio-Composites from Renewable Resources: Opportunities and Challenges in the Green Materials World*, Journal of Polymers and the Environment, vol.10, pp.19-26 (2002)

[20] S. J. Eichhorn, C. A. Baillie, N. Zafeiropoulos, L. Y. Mwaikambo, M. P. Ansell, A. Dufresne, K. M. Entwistle, P. J. Herrera-Franco, G. C. Escamilla and L. Groom, M. Hughes, C. Hill, T.G. Rials, P.M. Wild, *Review: Current international research into cellulosic fibers and composites*, Journal of Materials Science, vol.36, pp. 2107-2131 (2001)

[21] M.A. Osman, A. Atallah, M. Müller, U.W. Suter, *Reinforcement of poly(dimethylsiloxane) networks by mica* flakes, Polymer, vol. 42, pp.6545-6556 (2001)

[22] Magurno, *Vegetable fibres in automotive interior components* , Die Angewandte Makromolekulare Chemie, vol. 272, pp-99-107, (1999)

[23] M. Scandola, M.L. Focarete, G. Adamus, W. Sikorska, I. Baranowska, S.Swierczek, M. Gnatowski, M. Kowalczuk, Z. Jedlinski, *Polymer Blends of Natural Poly(3-hydroxybutyrate-co-3-hydroxyvalerate) and Synthetic Atactic Poly(3-hydroxybutyrate). Characterization and Biodegradation Studies*, Macromolecules, vol. 30, pp. 2568 – 2574 (1997)

[24] L.H.C Mattoso, F.C. Ferreira, A.A.S. Curvelo, *Lignocellulosic-PlasticComposites*, SINC do Brazil, São Paulo, Brazil (1997)

[25] K. Oksman, *Improved interaction between wood and synthetic polymers in wood/polymer composites*, Wood Science and Technology, vol.30, pp.197-205 (1996)

[26] S. Ahmed, F.R. Jones, *A review of particulate reinforcement theories for polymer composites*, Journal of Materials Science, vol. 25, pp. 4933-4942 (1990)

Papers in Conferences

[27] T. Gérard, T. Budtova, *Preparation and characterization of Polyhydroxyalkanoates (PHA) and Polylactide (PLA) blends*, Proceeding of 27th World Congress of the Polymer Processing Society, Marrakech, Morocco (2011)

[28] V. Ventosinos, *Perspectivas de los materiales ecológicos en el automóvil. Plataforma GreenMotion*, GreenMotion Day, Pontevedra, Spain (2011)

[29] A.C. Anunciação, E.S.F. Irokawa, M.M.R. Cunha, J.J.D. Câmara, *The application of natural fibers and wood's lresidues in the automobile industry and its advantages*, Proceedings of 4th International Conference on Design Research, Rio de Janeiro, Brazil (2007)

[30] N. Pereira, M.L. Sousa, J.A.M. Agnelli, L.H.C. Mattoso, *Effect of Processing on the Properties of Polypropylene Reinforced with Short Sisal Fibers*; Proceedings of 4th International Conference on Wood Fiber Plastic Composites, Madison, United States of America (1997)

Books

[31] P. Tesinová, *Advances in Composite Materials – Analysis of natural and man-made materials*, InTech, Rijeka, Croatia (2011)

[32] D. Gay, S. Hoa, S. Tsai, *Composite Materials: Design and Applications,* CRC Press, New York, USA (2003)

[33] C.A. Harper, *Handbook of Plastics, Elastomers and Composites*, McGraw-Hill, New York, USA (2002)

A.6

Publications due to this work

Peered Journals

N.C. Loureiro, J.L. Esteves, J.C. Viana, S. Ghosh, *Mechanical Characterization of Polyhydroxyalcanoate and Poly(Lactic Acid) Blends,* Journal of Thermoplastic Composite Materials (2011 Impact Factor: 0,810) (accepted)

N.C. Loureiro, J.L. Esteves, J.C. Viana, S. Ghosh, *Morphological study on Polyhydroxyalkanoates and Poly(Lactic Acid) blends obtained by injection moulding*, Journal of Macromolecular Science, Part B - Physics (2011 Impact Factor: 0,739) (submitted)

N.C. Loureiro, J.L. Esteves, J.C. Viana, S. Ghosh, *Development of Polyhydroxyalkanoates/Poly(Lactic Acid) composites reinforced with cellulosic fibers for automotive applications*, Composites part B: Engineering (2011 Impact Factor: 1,731) (submitted)

International Conferences

N.C. Loureiro, J.L. Esteves, J.C. Viana, S. Ghosh, *Mechanical characterization of composites of PLA/PHA matrix reinforced with cellulosic fibers*, ICCS17 - 17th International Conference on Composite Structures, Porto, Portugal (2013) (oral presentation)

A.T. Marques, J.L. Esteves, J.C. Viana, H. Faria, N.C. Loureiro, A. Arteiro, *Design for sustainability with composite systems*, ICEM15 – 15th International Conference on Experimental Mechanics, Porto, Portugal (2012) (oral presentation)

N.C. Loureiro, J.L.Esteves, J.C. Viana, S. Ghosh, *Development and characterization of renewable source composites to replace petrol-based polymers into interior door trims,* ECCM15 - 15th European Conference on Composite Materials, Venice, Italy (2012) (oral presentation)

N.C. Loureiro, J.L. Esteves, J.C. Viana, *Mechanical Characterization of PLA/PHA Blends,* ICCS16 - 16th International Conference on Composite Structures, Porto, Portugal (2011) (oral presentation)

National Conferences

N.C. Loureiro, J.L. Esteves, J.C. Viana, *Sustainable Automotive Components for interior door trims,* 3ª Conferência Anual do Programa MIT-Portugal, Guimarães, Portugal, 2012 (poster presentation)

N.C. Loureiro, J.L. Esteves, J.C. Viana, *Sustainable Automotive Components for interior door trims,* 2ª Conferência Anual do Programa MIT-Portugal, Porto, Portugal, 2010 (poster presentation)

N.C. Loureiro, J.L. Esteves, J.C. Viana, *Sustainable Automotive Components for interior door trims,* Ciência 2010 – Encontro com a Ciência em Portugal, Lisbon, Portugal, 2010 (poster presentation)

N.C. Loureiro, J.L. Esteves, J.C. Viana, *Caracterização Mecânica de Misturas de PLA/ABS*, ENMEC2010 – Encontro Nacional de Materiais e Estruturas Compósitas, Porto, Portugal (2010) (oral presentation)

Invited Talks

N.C. Loureiro, *Desenvolvimento de produto: Metodologias de minimização do impacto ambiental*, Ciclo de Seminários da Unidade Curricular de Introdução à Engenharia 1 da Licenciatura em Engenharia Mecânica do Instituto Superior de Engenharia do Porto, Porto, Portugal (2012)

N.C. Loureiro, *Materiais Sustentáveis: A engenharia ao serviço do ambiente*, Semana Europeia da Mobilidade, Câmara Municipal de Gaia – Divisão do Ambiente, Instituto Superior Politécnico Gaya, V.N. Gaia, Portugal (2012)

N.C. Loureiro, *Materiais e Desenvolvimento Sustentável: Oportunidades e mitos*, Ciclo de Tertúlias "Sextas Culturais", Centro Universitário do Minho, Braga, Portugal (2012)

N.C. Loureiro: *Desenvolvimento de produto: Da matriz de decisão à matriz de impacto ambiental*, Ciclo de Seminários da Unidade Curricular de Introdução à Engenharia 1 da Licenciatura em Engenharia Mecânica do Instituto Superior de Engenharia do Porto, Porto, Portugal (2011)

N.C. Loureiro, *Materiais Sustentáveis: Verdades, Mentiras e Ideias Portuguesas,* Encontros de Investigação do CID_ISPGaya, FNAC- Gaiashopping, V.N. Gaia, Portugal (2011)